UNIVERSITÀ DI SIENA 1240

**DEPARTMENT OF BIOTECHNOLOGY, CHEMISTRY AND PHARMACY**

**PhD in Chemical and Pharmaceutical Sciences**

**XXVIII cycle**

**Coordinator: Prof. Stefano Mangani**

# Development of liposome-based drug delivery system to improve drug-like properties and anticancer activity of tyrosine kinase inhibitors with pyrazolo [3,4-*d*] pyrimidine structure

**SSD: CHIM/08**

**Tutor: Prof. Maurizio Botta**

**Co-tutor: Dr. Mario Chiariello**

**PhD student: Dr. Pierpaolo Calandro**

**Academic Year 2015-2016**

**Abstract**

Cancer is a multifactorial disease whose causes are still unknown. Frequently, mutations in several genes play an important role in cellular growth processes and, based on their specific roles, they are usually distinguished in proto-oncogenes and oncosuppressors. One of the most studied oncogenes is c-Src, encoding for a non-receptor tyrosine kinase protein that plays a multitude of roles in cell signalling. The activation of c-Src is involved in the control of many functions, including cell adhesion, growth, movement, and differentiation by a different set of cell surface receptors. c-Src is found to be over-expressed and mutationally activated in a wide variety of human cancers. Moreover, c-Src may have an influence on the development of the metastatic phenotype.

Significant progresses in the understanding of cancer biology have prompted extensive research within novel classes of anticancer drugs. A number of tyrosine kinase inhibitors targeting the c-Src tyrosine kinase (as well as related tyrosine kinases) have been developed for therapeutic use.

4-aminopyrazolo [3,4-d] pyrimidines compounds were firstly used as c-Src family kinases (SFKs) inhibitors in 1996 but later demonstrated to inhibit all SFKs members with IC50 values in the low nanomolar range. These compounds have been extensively used for studying the biological pathways of SFKs and, even though they are a class of promising anti-tumor compounds because of their good activity against several cancer cell lines, these molecules showed a poor aqueous solubility, limiting them as clinical drug candidates. In the continuing effort to find new anticancer agents, our group conducted large studies on a series of new c-Src inhibitors with a pyrazolo [3,4-d] pyrimidine scaffold.

The aim of this thesis was to improve the solubility profile and the pharmacokinetic properties of selected compounds, chosen on the base of their inhibitory activity on c-Src. To overcome the poor water solubility of these molecules, pyrazolo [3,4-d] pyrimidines compounds were encapsulated in liposomes formulations. Liposomes were prepared and characterized for size, ζ potential distribution and polydispersity index (PDI) by dynamic light scattering in order to obtain a homogeneous population of small unilamellar vesicles (SUV); subsequently, fluorescent liposomes were prepared to assess the ability of liposomes to interact with neuroblastoma (SH-SY5Y) and glioblastoma (U87) cells by confocal microscopy; finally, encapsulation efficiency and activity by cellular assays were studied to determine cytotoxicity, showing that

liposomes loaded with pyrazolo [3,4-d] pyrimidine compounds determine a cytotoxic effect in SH-SY5Y (Neuroblastoma) or U87 (Glioblastoma) cell line equal to or higher than the free compound solubilised in DMSO. Moreover, biodistribution of liposomes loaded with pyrazolo [3,4-d] pyrimidine was evaluated in male Sprague Dawley rats after 24h of treatment. Altogether, the obtained data strongly indicate that the encapsulation of pyrazolo [3,4-d] pyrimidine compounds in liposomes represent an effective method to improve the biodistribution of pyrazolo [3,4-d] pyrimidines and attribute a therapeutic efficacy to this novel formulation.

During my Ph.D. period, I also focused on the study of active targeting of liposomes against tumor areas that overexpress plasmin. The plasminogen/plasmin system plays a key role in tumor development and, in particular, in progression and metastasis. The aim of my project was to functionalize the surface of stealth liposomes encapsulating pyrazolo [3,4-d] pyrimidines with a peptide able to bind plasmin. Since plasmin is overexpressed in tumor areas, the bond between plasmin and the peptide in liposomes surface would lead to a destabilization of the liposomes and consequently to a greater drug release in the tumor site. The obtained liposomes were characterized after purification evaluating the size, the ζ potential distribution, the polydispersity index (PDI) and the encapsulation efficiency (EE). Furthermore, several tests to quantify the peptide bound to liposomes were performed, unfortunately with poor results. Moreover, peptide-bearing fluorescent liposomes were also prepared and tested on hepatocarcinoma cell line HepG2 to investigate any change in the cellular uptake. In addition, cytotoxicity assays on HepG2 cells were performed to test the efficacy of liposomes conjugated with the peptide with respect to non-conjugated liposomes, both encapsulating the selected compounds. Liposomes functionalized with the peptide resulted more stable and with better physicochemical properties than non-functionalized liposomes. Furthermore, confocal microscopy of fluorescent liposomes highlighted the ability of liposomes with the peptide to penetrate in hepatocarcinoma cells after 1h of treatment with respect to non-functionalized liposomes, not able to be internalized after the same time. Finally, cytotoxicity data showed that liposomes with the peptide have lower IC50 values than non-functionalized liposomes.

In conclusion, data obtained showed that it was obtained a good functionalized liposomal formulation able to be recognized by hepatocarcinoma cells secreting

plasmin. Further in vivo tests will be performed to study the ability of these liposomes to release the compound in tumor areas over-expressing plasmin.

# Chapter 1

## Preparation and characterization of stealth liposomes for the delivery and release of tyrosine kinase inhibitors with pyrazolo [3,4-*d*] pyrimidine structure.

## 1. Introduction

The term “neoplasia” term in pathology indicates a mass of tissue that displays an uncontrolled growth compared to a normal tissue and persists in this state after the cessation of the stimuli which led to the process (Kumar et al., 2007).

Cancer cells result mutated in several genes that frequently play an important role in the growth processes or DNA repair. Two classes of genes have been identified as the main responsible for cancer development and progression: proto-oncogenes and oncosuppressors. (Spandidos DA and Anderson ML, 1989).

Proto-oncogenes are genes regulating cellular growth and differentiation. Activation of proto-oncogenes by genetic alteration such as mutations, translocations, overexpression, or fusion lead to the formation of oncogenes promoting uncontrolled cellular proliferation. A mutation into a single allele of a proto-oncogene is sufficient to set off a neoplastic phenotype and for this reason they are called dominant (Covelli I and Veneziani BM, 2000). One of the most studied oncogene is c-Src, first discovered in 1970 by J. Michael Bishop and Harold E. Varmus. Other oncogenes frequently found overexpressed into many type of tumors are Myc, Abl, Fos and Ras. On the contrary, oncosuppressors, are genes limiting cellular growth and, as both alleles must be altered in order to set off the neoplastic phenotype, they are called recessive as opposed to proto-oncogenes. The most studied tumor suppressors are Rb, p53, BRCA1, BRCA-2 and NF-1.

### 1.1 Src Family Kinases (SFKs) and the tyrosine kinase c-Src

c-Src is a non-receptor tyrosine kinase protein encoded by the Src gene and belonging to the homonymous family of Src kinases (SFKs). SFKs is composed by nine members grouped into three subfamilies: Src, Yes, Fyn and Fgr belong to the Src-A subfamily, Lck, Hck, Blk and Lyn belong to the Src-B subfamily, Yrk form its own subfamily.

J. Michael Bishop and Harold E. Varmus were awarded with the Nobel Prize in Physiology or Medicine in 1989 for the discovery of c-Src.

c-Src can interact with EGFR, PDGFR or other RTKs and activate the phosphatidylinositol 3-kinase (PI3K)-Akt, the Ras-Raf-mitogen activated protein kinase (MAPKs), Jak-signal transducers and activators of transcription (STAT) cascades as well as FAK-Paxillinp130-Crk-associated substrate (Cas) cascades, crucial for cell

cycle progression, proliferation, motility, adhesion, and survival (Figure 1) (Reynolds AB et al., 2014). In normal cells, c-Src is mostly in an inactive state, being only transiently activated during the cellular events in which it is involved. By contrast, c-Src is overexpressed and/or hyperactivated in several tumour types and its expression correlates with increased tumour malignancy and poor prognosis (Sen B and Johnson FM, 2011). c-Src has roles in the progression of both *in vitro* and *in vivo* preclinical models of many solid tumours, such as colon, breast, liver, prostate and pancreatic cancers, neuroblastoma, and haematological tumours such as chronic myeloid leukaemia (CML) and lymphomas (Parsons SJ and Parsons JT, 2004). Moreover, c-Src is a strong promoting factor for the development of metastatic cancer phenotypes (Irby RB and Yeatman TJ, 2000; Finn RS, 2008). In addition, c-Src exhibits downstream activity in both angiogenesis and bone resorption pathways, indicating functions in tumor cell maintenance and survival (Parsons SJ and Parsons JT, 2004). Given its prominent role in tumor progression, c-Src has become a promising target to achieve a broad therapeutic benefit in patients with c-Src-dependent cancers (Creedon H and Brunton VG, 2012).

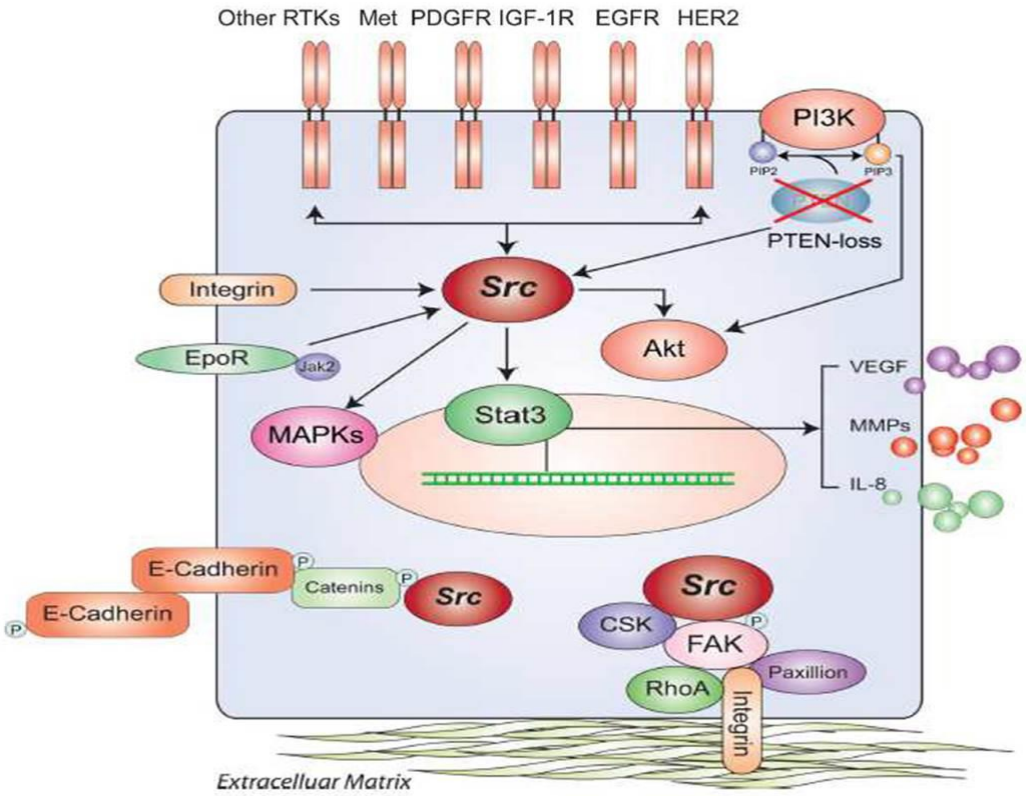


**Figure 1. Canonical c-Src signaling.** (Zhang S and Yu D, 2012).

Src and the other members of the family are highly homologous proteins and share a structural domain organization that comprises from the N-terminal end (Figure 2):

- a SH4 domain (Src Homology 4) which includes the first 16 amino acid residues and it is responsible for the interaction of the SFKs to cell membranes. The anchoring of SFKs to the membranes is favoured by the acylation of two amino acid residues of the consensus sequence Met-Gly-Cys of the N-terminal region. All the Src tyrosine kinases are myristoylated at Gly in position +2 or palmitoylated at Cys at position +3;
- a Unique domain, different among all members, whose function is not known yet;
- a SH3 domain (Src Homology 3), consisting of 50-60 amino acid residues with a non-catalytic function, which mediate intra- and inter-molecular protein-protein interactions involved in the control of the enzymatic activity, interactions with the substrates and the sub-cellular localization;
- a SH2 domain (Src Homology 2), consisting of about 100 amino acid residues, with no catalytic function, which modulate the catalytic activity or the substrates recognition via protein-protein interaction. Crystallographic studies have shown that a highly conserved Arg residue ($Arg^{175}$) in c-Src, is important for electrostatic interactions with phosphorylated $Tyr^{517}$ when c-Src is in the inactivated form;
- a SH1 domain (Src Homology 1) or catalytic domain consisting of about 260 amino acids, responsible for the enzymatic activity. Structurally it can be distinguished a small lobe and a large lobe. The small lobe is primarily involved in the anchoring and the orientation of ATP. The large lobe is involved in the binding with the substrate and contains the activation site where the $Tyr^{416}$ is localized (in c-Src) and whose phosphorylation determines the full activation of the enzyme. The catalytic site, where the transfer of phosphate from ATP to the substrate takes place, is in the cleft between the two lobes;
- a C-terminal region of about 15-17 amino acid residues, which contains a highly-conserved Tyr in 527 position (in c-Src) in all the kinases of the family. The $Tyr^{527}$ is an important regulatory site since its phosphorylation causes conformational changes, due to the intramolecular interaction of $pTyr^{527}$ with SH2 domain, such as to inactivate the kinase. The phosphorylation of $Tyr^{527}$ is

mediated by the action of two tyrosine kinases, C-terminal Src kinase (Csk) and its homologue Csk-homologous kinase (Chk) (Chong YP et al., 2005). *In vivo*, in basal conditions, the $Tyr^{527}$ is phosphorylated in the 90-95% of c-Src proteins.

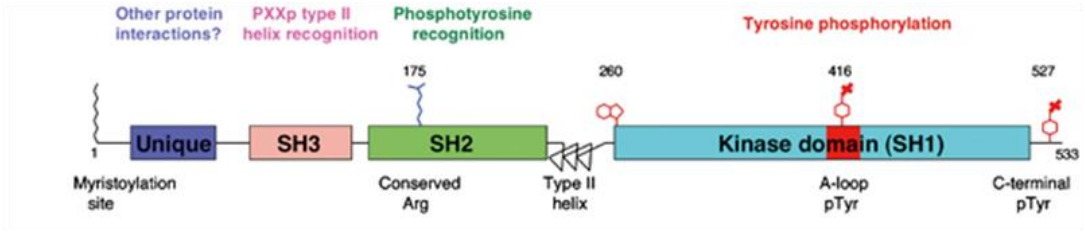


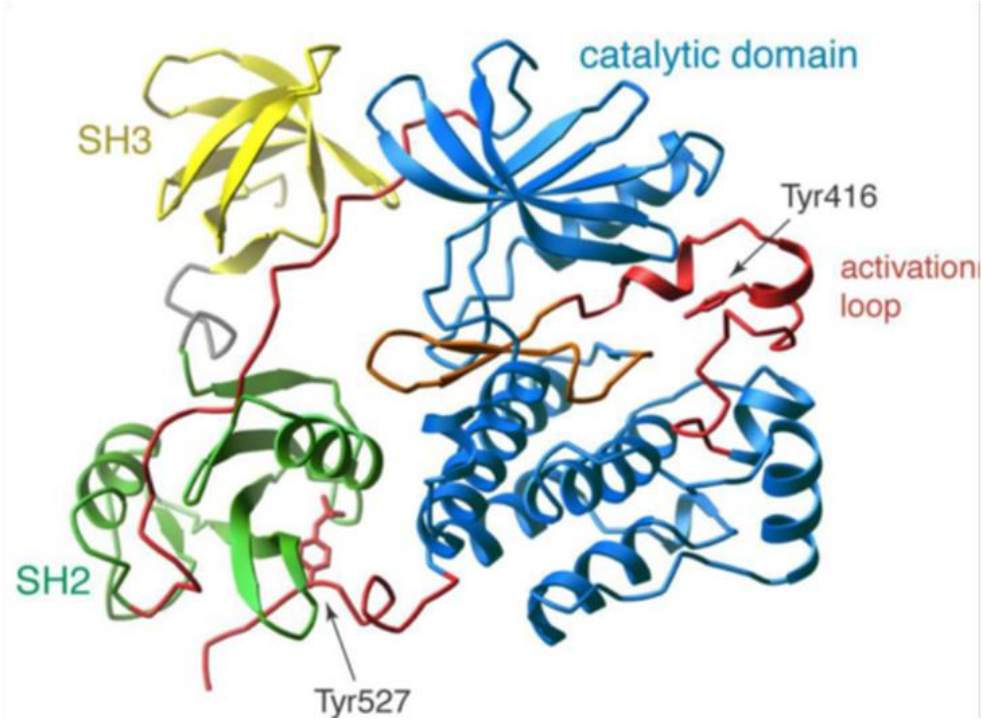


**Figure 2. Structural domains of the c-Src tyrosine kinase** (Miller WT, 2003).

Since the activity of c-Src tyrosine kinase is finely regulated in normal cell conditions, a modification of this mechanism may result in constitutive activation of the kinase.

In literature, four tyrosine phosphatases involved in the de-phosphorylation mechanism of $Tyr^{527}$ of SFKs in various cellular systems are described: the tyrosine phosphatase-1B (PTP1B) (Bjorge JD et al., 2000), the transmembrane tyrosine phosphatase CD45 (Wang D et al., 2002) and the tyrosine phosphatase SHP-1 and SHP-2 (Poole AW and Jones ML, 2005).

Furthermore, the binding with external ligands allows the SFKs autophosphorylation that can remain active despite the presence of $Tyr^{527}$ phosphorylation. This indicates

that the phosphorylation of inhibitory tyrosine and the intramolecular interaction resulting are not sufficient to maintain the SFKs activities in a state completely inhibited.

Also, the breaking of the intramolecular bound between $pTyr^{527}$ and SH2 domain is responsible for the activation of the kinase. After the dissociation of the $pTyr^{527}$-SH2 interaction, the inhibitory tyrosine is accessible to the phosphatase. The de-phosphorylation of $pTyr^{527}$ coincides with the destruction of all intramolecular interactions and is followed by phosphorylation of the activating site which induces a complete kinase activation.

### 1.2 Synthetic inhibitors of SFKs

SFKs are involved in receptors-mediated signal transduction and are structurally characterized by the presence of SH domains (SH1-SH4) involved in the modulation of its activity. Each domain represents a possible target of inhibition of c-Src. Deregulation of protein kinase has been shown to be implicated in the pathogenesis of many diseases, including cancer. Then the inhibition of the involved kinases has been proposed as a promising pharmacological approach of human diseases. SFKs are largely studied as possible pharmaceutical target. Several types of inhibitor have been developed, (i) direct inhibitors of the catalytic domain; (ii) inhibitors against the SH3 and SH2 domains; (iii) inhibitors of the acylation. A molecule that must be used as inhibitor / modulator of c-Src must have some characteristics: small size, cell permeability, high specificity or selectivity, sufficient strength to compete with the excess of endogenous ligands. The specificity of the inhibitors derives from the degree of sequence homology among family members (in SFKs the homology among members is about 70-80%, while decreases to 20% for members of different families (Hanke JH et al., 1996).

### 1.3 Pyrazolo [3,4-*d*] pyrimidines as potent c-Src inhibitors

The 4-aminopyrazolo [3,4-*d*] pyrimidines PP1 and PP2 (Figure 3) were the first SFKs inhibitors and were reported by Pfizer in 1996 (Hanke JH et al., 1996). These compounds inhibit all SFKs members with $IC_{50}$ values in the low nanomolar range in an ATP-competitive manner, as demonstrated by crystal structures of different SFKs members in presence of the 4-aminopyrazolo [3,4-*d*] pyrimidines, including the PP1:Hck176 and PP2: Lyn complexes (Williams NK et al., 2009).

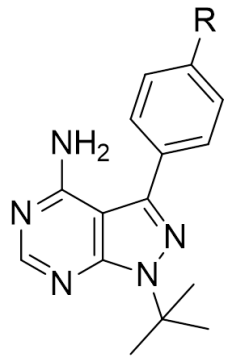


**1 PP1** R = CH3
**2 PP2** R = Cl

**Figure 3. Molecular structure of first pyrazolo [3,4-*d*] pyrimidine PP1 and PP2**

In the continuing effort to find new anticancer agents, our group conducted large studies on a series of new c-Src/Abl inhibitors a pyrazolo [3,4-*d*] pyrimidine scaffold (Carraro F et al., 2004, 2006; Angelucci A et al., 2006; Manetti F et al., 2007). Several members of this family were found to induce apoptosis and to reduce cell proliferation in different solid tumor cell lines like A431(epidermoid carcinoma), 8701-BC (breast cancer), Saos-2 (osteosarcoma), and PC3 (prostate adenocarcinoma).

To better understand the mechanism of inhibition towards c-Src, the crystal structure of a domain of c-Src (aa 256−533) and Si192 compound with pyrazolo [3,4-*d*] pyrimidines structure has been obtained (Figure 4). Results confirmed previously docking studies, showing binding of the compound in the ATP site of c-Src. (Radi M et al., 2011; Tintori C et al., 2015).

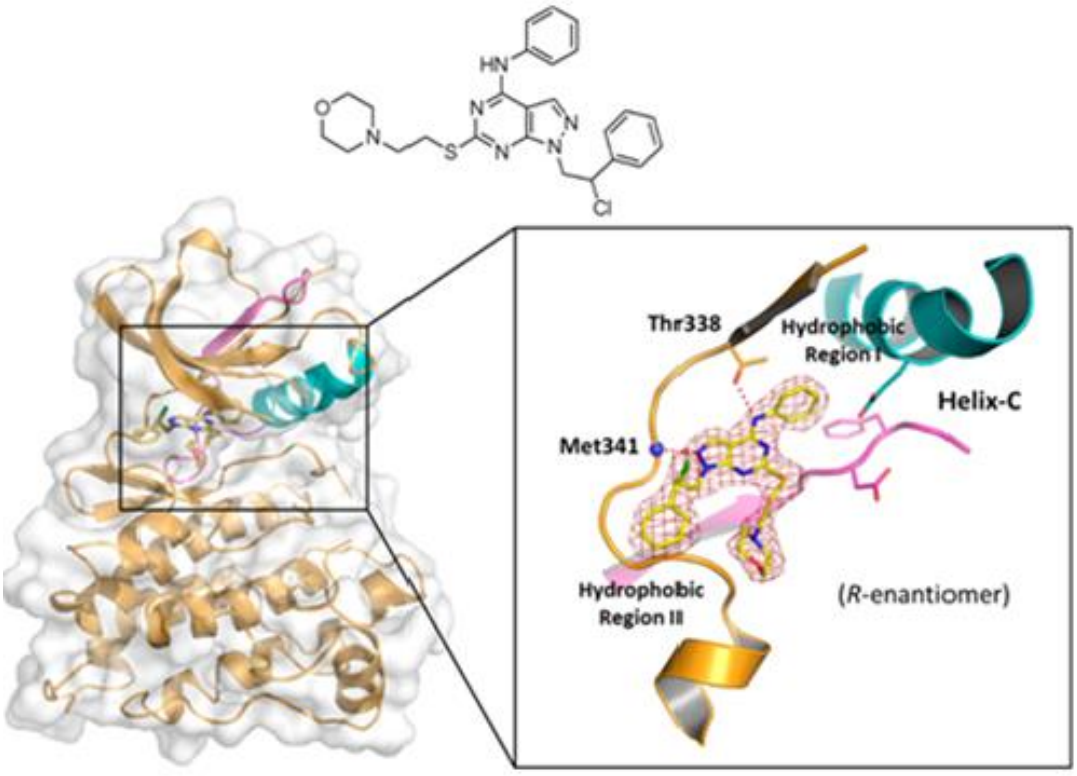


**Figure 4. Crystal structure of a domain of c-Src (aa 256−533) and the Si306 compound** (modified from Tintori C et al., 2015)**.**

## 1.4 Cancer and nanotechnology

Cancer treatment includes surgery, radiation, and chemotherapeutics but these treatments cannot eradicate metastatic tumours. Cancer mortality is indeed mainly related to the appearance end effects of metastasis.

In the last 20 years, large investments to help the search for new strategies in the treatment of cancer have been done. In this way, huge progresses in the synthesis of anti-cancer drugs have been done. Several drugs, i.e. imatinib and dasatinib against some blood cancers (e.g. chronic myeloid leukemia), may be employed for treatment, obtaining a longer survival or in some cases the remission of the disease.

The main problem of the traditional chemotherapeutic agents is the relative lack of specificity versus cancer cells (Alexis Fcet al.2008; Bawarski WE et al. 2008). Chemotherapeutic drugs are administered mainly intravenously, thereby distributing to the whole human body, resulting in a low therapeutic index with high level of toxicity to healthy tissues and a low efficacy against tumor. Side effects may be severe and often lead to a poor quality of life (Ganta S et al. 2008). Furthermore, the efficacy of therapies may be affected by the pathophysiological properties of the tumor. Tumor can be

located in physically hard-to-reach areas, such as the brain, or protected by local environment due to increased tissue hydrostatic pressure (Drummond DC et al. 1999; Klein CA, 2009; Szakács et al. 2006). Thus, there is a need to develop new agents that can specifically reach the tumor tissue without dangerous side effects. To improve the efficacy of drug delivery, nanotechnology-based drug delivery systems are gaining considerable attention as they have the potential to reduce side effects, minimize toxicity and improve anticancer efficacy (Suri SS et al., 2007). Nanotechnology consist in the engineering and manufacturing of nano-sized molecules using atomic or molecular components, which can be expected to benefit all fields of medicine (Alexis F et al. 2008). It is an emerging technology that will have a significant impact on the advancement of tumor therapies (Kim KY, 2007). Several nanotechnology platforms, such as dendrimers, liposomes, polymeric micelles and solid nanoparticles, are being developed (Bawarski WE et al., 2008; Surendiran A et al., 2009). The use of nanoparticles as carriers of conventional chemotherapeutic agents has been shown to experimentally improve cancer treatment efficacy (Ma P et al., 2009). Interestingly, some nano-formulations of traditional anticancer agents have already been approved for the clinical use. For example, Doxil® and Abraxane® are two nanoformulations approved by the US FDA for cancer treatment. Doxil® is a long circulating formulation of doxorubicin (DOX), which has been well known for significant improvements over free DOX. Abraxane® is an albumin-bound nanoparticle formulation of paclitaxel for the treatment of metastatic breast cancer, reducing the hypersensitivity reaction associated with the traditionally used solvent for paclitaxel (Bharali DJ et al., 2009). In Table 1 are listed some nano-formulation approved for the treatment of various disease.

| PRODUCT | COMPOSITION | INDICATION | APPROVED |
|---|---|---|---|
| | **Lipid-Based Nanoparticles** | | |
| Abelcet | Lipid complex formulation of amphotericin B | Invasive fungal infections | 1995 |
| AmBisome | Liposomal preparation of amphotericin B | Fungal and protozoal infections | 1997 |
| DaunoXome | Liposomal preparation of daunorubicin | HIV-related Kaposi's sarcoma | 1996 |
| DepoCyt | Liposomal formulation of cytarabine | Lymphomatous meningitis | 1999 |
| DepoDur | Liposomal formulation of morphine sulfate | Relief of postsurgical pain | 2004 |
| Doxil/Caelyx | PEGylated liposomal formulation of doxorubicin | Various cancers | 1995 |
| Inflexal V | Liposomal influenza vaccine | Influenza | 1997 |
| Visudyne | Liposomal formulation of verteporfin | Wet age-related macular degeneration | 2000 |
| | **Polymer-Based Nanoparticles** | | |
| Adagen | PEGylated adenosine deaminase enzyme | Severe combined immunodeficiency disease | 1990 |
| Cimzia | PEGlyated Fab' fragment of a humanized anti-TNF-alpha antibody | Crohn's disease, rheumatoid arthritis | 2008 |
| Copaxone | Polymer composed of L-glutamic acid, L-alanine, L-lysine, and L-tyrosine | Multiple sclerosis | 1996 |
| Eligard | Leuprolide acetate and PLGH polymer formulation | Advanced prostate cancer | 2002 |
| Macugen | PEG-anti-VEGF aptamer | Neovascular age-related macular degeneration | 2004 |
| Mircera | Chemically synthesized ESA, methoxy PEG-epoetin beta | Symptomatic anemia associated with chronic kidney disease | 2007 |
| Neulasta | Conjugate of PEG and filgrastim | Chemotherapy-induced neutropenia | 2002 |
| Oncaspar | PEGylated formulation of L-asparaginase | Acute lymphoblastic leukemia | 1994 |
| Pegasys | PEGylated interferon alfa-2a | Hepatitis C | 2002 |
| PegIntron | PEGylated interferon alfa-2b | Hepatitis C | 2001 |
| Renagel | Polyamine (polymer loaded with amine groups) | Chronic kidney disease | 2000 |
| Somavert | PEGylated human growth hormone receptor antagonist | Acromegaly | 2003 |
| | **Protein-Based Nanoparticles** | | |
| Abraxane | Albumin-bound paclitaxel (*nab*-paclitaxel) | Breast cancer | 2005 |

**Table 1. Select FDA-approved agents utilizing nanomedicine** (Emerging Therapeutics for the 21st Century, 2012)

### 1.4.1 Nanoparticle targeting

Several studies indicate that nanoparticles used in cancer chemotherapeutic treatments possess more specific targeting ability to tumor cells. The enhanced drug absorption and bioavailability of anticancer agents results in an improved anticancer efficacy and decreased side effects (Davis ME et al., 2008; Li SD and Huang L, 2008).

The enhanced anticancer effects and improved safety compared with their free-drug counterparts are due to the size and surface properties of the nanoparticles. Anticancer nanoparticles should bypass biological barriers to reach their target and, to the end, it is widely accepted that the diameter of nanoparticles for cancer treatment should be in the range of 10 to 100 nm (Davis ME et al., 2008; Gullotti E and Yeo Y, 2009). Moreover, the study of nanoparticle surface properties is essential to control their behaviour (Davis ME et al., 2008).

Two mechanism of targeting, passive and active, can be distinguished. Passive targeting strategies rely on the passive accumulation of nanoparticles according to the properties of the delivery system and/or the pathophysiology of target tissues. Nanoparticles action makes use of the differences in several aspects between tumor and healthy tissues. Most nanoparticles are expected to accumulate in tumors due to the pathophysiologic characteristics of tumor blood vessels. Tumor cells requires the formation of new blood vessels to supply nutrients and oxygen requests. In this stage, cells may have an "angiogenetic switch" which determines an increase of the secretion of signals that intensely stimulate angiogenesis processes. Still, tumor vasculature is often incomplete and vessels have enlarged gap junction with respect to the normal endothelium, so macromolecules easily access the tumor interstitium (Hobbs SK et al., 1998). Furthermore, tumours are characterised by an irregular lymphatic system. Consequently, the clearance of macromolecules from the tumour interstitium is delayed (Brigger I et al., 2002). Moreover, in many solid tumours, such as rectal and breast tumours, there is an elevated interstitial fluid pressure in comparison to normal tissues. Thus, unlike normal tissues, where clearance of macromolecules proceeds rapidly and steadily via the lymphatic system, clearance of macromolecules from the tumour lymphatic system is impaired and they can remain in the tumour interstitium for a long period (Maeda H, 2001). This well-established phenomenon that leads to a spontaneous accumulation of nanoparticles in tumor microenvironment is known as "Enhanced Permeability and Retention effect" (EPR) (Figure 5).

Another example of passive targeting is based on pH-sensitive nanoparticles. During tumor growth, regions far from new formed vessels show slow cellular growth, cell death and necrosis due to insufficient oxygen and nutrient supply. Moreover, lack of oxygen leads to the production of $CO_2$, carbonic acid and lactic acid, resulting in low interstitial pH, that represent another characteristic of the tumour microenvironment (Schornack PA and Gillies RJ, 2003). The pH values surrounding tumour tissues are usually in the 5.5 to 6.5 range (Ganta S et al., 2008). pH-responsive nanocarriers have significant enhanced stability in circulation at physiological pH of 7.4, but can release their payload (chemotherapy drugs) in the tumour in presence of lower pH values which destabilize the nanoparticles structure. For example, a 5-fluorouracil-loaded pH-responsive dendrimer nanocarrier showed a significant faster release rate at pH 6.5 than

at pH 7.4, resulting in a longer half-life after i.v. administration and high tumour targeting in mice (Jin et al., 2011).

Still, passive targeting approaches suffer from several limitations. The targeting of cancer cells using the EPR effect is not feasible in all tumors because the degree of tumor vascularization and porosity of tumor vessels, which must have specific characteristic, can vary with the tumor type and status (Peer D et al., 2007). In addition, cancer cells can display a reduced number of specific interactions leading to internalization of nanoparticles. Functionalising the surface of nanoparticles with ligands such as antibodies, aptamers, peptides or small molecules, recognizing tumour-specific or tumour-associated markers, can promote the active targeting of nanoparticles to tumours (Alexis F et al., 2008). Recently, targeted therapies in cancer have been developed (Malinowsky K et al., 2010). Monoclonal antibodies (mAbs) and small inhibitors molecules are two major types of targeted therapy that can lead to the selective inhibition of proliferation of cancer cells rather than normal dividing cells. The FDA has already approved several mAbs for cancer treatment. For example, Alemtuzumab, targeting CD52, was successfully approved for chronic lymphocytic leukemia (Gerber DE, 2008). Tumor signaling pathways, often based on kinases, are the focus of the development of targeted anticancer therapies. For example, cetuximab, which targets the epidermal growth factor receptor (EGFR), has been used for the treatment of metastatic colorectal cancer in clinic (Dietel M and Sers C, 2006). Combining nanoparticles with small molecules, which could target cancer cells or cancer stem cells (CSCs), could improve the targeting property of nanoparticles as they can recognise and bind to target cells via ligand-receptor interactions. Importantly, to maximise specificity in the binding, the antigen or receptor on the target cells should be overexpressed in cancer. (Goren D et al., 2000). For example, immunoliposomes with an internalizing anti-CD19 ligand had a significantly improved therapeutic efficacy than their counterpart with a noninternalizing anti-CD20 ligand (Sapra P and Allen TM, 2002).

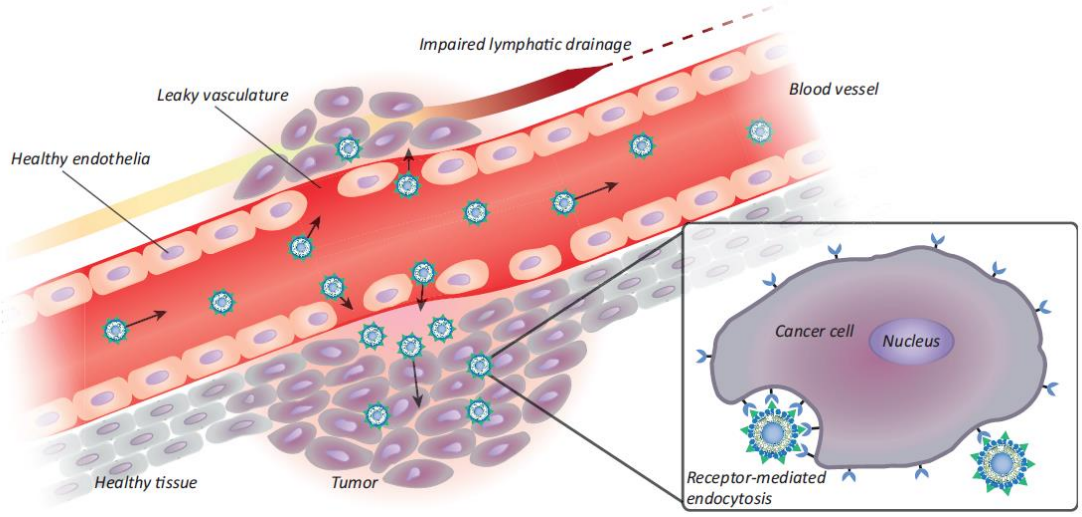


**Figure 5. Active and passive targeting**. Passive targeting of nanoparticles to tumors through the enhanced permeability and retention (EPR) effect. Angiogenic vessels in rapidly growing tumors are abnormally constructed with large vascular fenestrae and impaired lymphatic drainage. As a result, particles <200 nm preferentially accumulate in the tumor interstitium. Post-extravasation, intracellular uptake of ligand-targeted liposomes is facilitated by receptor-mediated endocytosis (inset) (Noble GT et al., 2014).

## 1.5 Liposomes as drug delivery system

Liposomes were first discovered and described by a British haematologist in 1961, when he and his colleagues observed that phospholipids upon dispersion in water spontaneously formed spherical, self-closed vesicles consisting of concentric lipid bilayers (Bangham AD et al., 1965). The phospholipid reorganisation in aqueous solution is mainly driven by the hydrophobic effect that organizes amphiphilic molecules (phospholipids) to minimize entropically unfavourable interactions between hydrophobic acyl-chains and surrounding aqueous medium (Lasic DD, 1998). Various intermolecular forces, such as electrostatic interactions, hydrogen bonding, as well as van der Waals and dispersion forces further settle this effect (Israelachvili J et al., 1980). Liposomes were defined as an artificial microscopic vesicle consisting of a central aqueous compartment surrounded by one or more concentric phospholipid layers (lamellas) with a diameter ranging from the nanometre to the micrometre scale. Furthermore, drugs with different lipophilicities can be encapsulated into liposomes: strongly lipophilic drugs are entrapped almost totally in the lipid bilayer, while intensely hydrophilic drugs are located entirely in the aqueous compartment and drugs with intermediary LogP coefficient effortlessly distribute between the lipid and aqueous phases, both in the bilayer and in the aqueous core (Figure 6) (Maria Laura I et al., 2006).

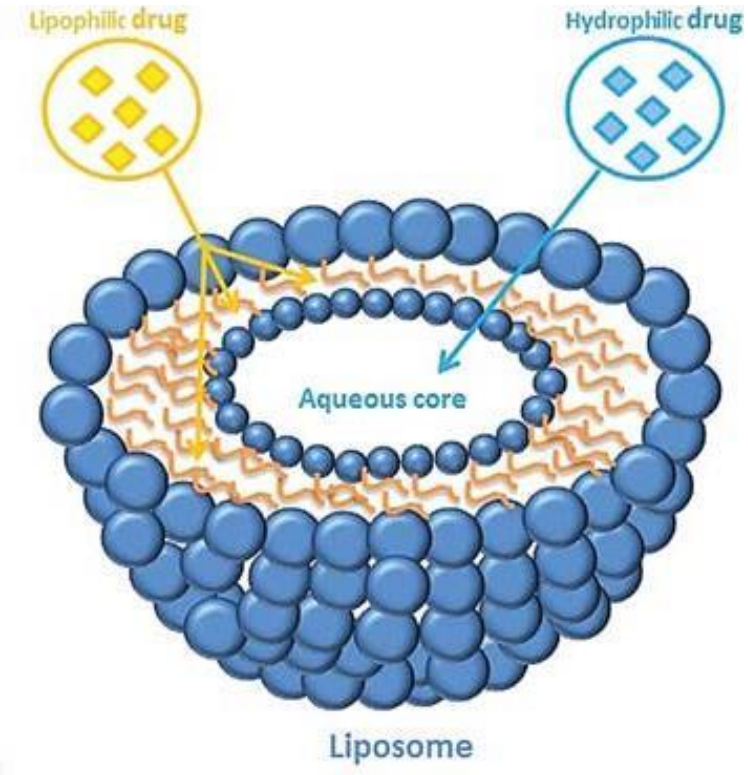


**Figure 6. Lipophilic or hydrophilic drug entrapment models in liposomes structure** (Laouini A et al., 2012)

Since most of the pharmacologically active molecules are lipophilic, and therefore not soluble in water, nanocarriers with moderate or high lipophilicity are needed to effectively encapsulate these compounds. Nanocarriers based on lipids or phospholipids are, therefore, good candidates for this purpose. For this reason, liposomes are developing large potential applications. At first, they were used to study biological membranes; nevertheless, drug-delivery applications are now the most widely investigated area of their practical applications because of their biocompatibility, biodegradability, low toxicity, aptitude to trap both hydrophilic and lipophilic drugs (Johnston MJ et al., 2007) and ability to simplify site-specific drug delivery to tumor tissues (Hofheinz RD et al., 2005). Liposomes were introduced as drug-delivery vehicles in the 1970s. However, early results were rather disappointing, owing mainly to their colloidal and biological instability and their inefficient and unstable encapsulation of drug molecules. Their utility was improved following basic research that increased our understanding of their stability and interaction characteristics (Lasic

DD and Papahadjopoulos D, 1995). In parallel, several pharmaceutical enterprises in the 1980s and early 1990s put several commercial products on the market. At present, these include antifungal, anticancer and cosmetics preparations that compare favourably to existing treatments, but a recent renaissance in liposome research is promising many more products to come (Table 2). Many studies have been conducted on liposomes with the goal of decreasing drug toxicity and/or improve targeting to specific cells (Omri A et al., 2002; Schiffelers RM et al., 2001; Stano P et al., 2004).

| Approved products | Drug | Lipid composition | Indications | Year approved |
|---|---|---|---|---|
| AmBisome (Gilead) | Amphotericin B | HSPC, DSPG and cholesterol | Fungal infections, leishmaniasis | 1990 (Europe), 1997 (USA), 2000 |
| Doxil/Caelyx (Johnson & Johnson) | Doxorubicin | HSPC, cholesterol and DSPE-PEG(2k) | Kaposi's sarcoma, ovarian cancer, breast cancer, multiple myeloma + velcade | 1995 1999 2003 2007 (Europe, Canada) |
| Abelcet (Enzon) | Amphotericin B | Sodium cholesteryl sulfate | Aspergillosis | 1995 |
| DaunoXome (Galen) | Daunorubicin | DSPC and cholesterol | Kaposi's sarcoma | 1996 (Europe), 1996 (USA) |
| Amphotec (Intermune) | Amphotericin B | Sodium cholesteryl sulfate | Invasive aspergillosis | 1996 |
| DepoCyt (Pacira) | Cytosine arabinoside | DOPC, DPPG, cholesterol and triolein | Lymphomatous meningitis, neoplastic | 1999 |
| Myocet (Cephalon) | Doxorubicin | $^{E}$gg phosphatidylcholine and cholesterol | Breast cancer + cyclophosphamide | 2000 (Europe) |
| Visudyne (QLT) | Verteporphin | EPC and DMPC | Wet macular degeneration | 2000 (USA), 2003 (Japan) |
| Lipo-Dox (Taiwan Liposome) | Doxorubicin | DSPC, cholesterol and DSPE-PEG(2 k) | Kaposi's sarcoma breast and ovarian cancer | 2001 (Taiwan) |
| DepoDur (Pacira) | Morphine sulfate | DOPC, DPPG, cholesterol, tricaprylin and triolein | Pain following surgery | 2004 |
| Marqibo (Talon) | Vincristine | Egg sphyngomielin and cholesterol | Acute lymphoblastic leukemia | 2012 (USA) |

**Table 2. Liposomes on market**

### 1.5.1 Liposomes composition

Liposomes are mainly composed of phospholipids with different amounts of cholesterol (Figure 7). These molecules are biologically inert and feebly immunogenic and they have low inherent toxicity.

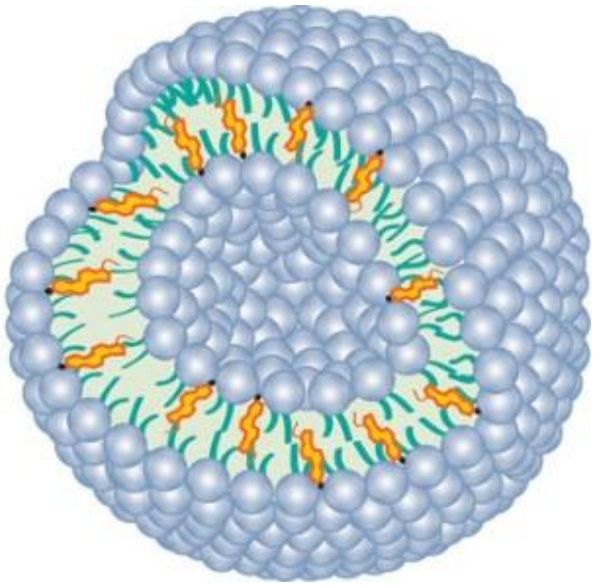

**Figure 7. Liposome structure** (Monteiro N et al., 2014)

Phospholipids are amphiphilic molecules that have a hydrophilic head and two hydrophobic chains. When phospholipids are dispersed in aqueous solutions, they have a strong tendency to form membranes because of their amphipathic nature (Papahadjopoulos D and Kimelberg HK, 1974). On one hand, their polar heads prefer to interact with the aqueous environment, while their long apolar aliphatic chains promote interaction with one another. In aqueous solution, these properties favour the formation of two lipid layers. The hydrophobic chains of each layer face each other and constitute to form a lipophilic inner compartment that acts as a permeability barrier, both inward and outward. Hydrophobic interactions ensure the formation of these lipid bilayers and van der Waals forces keep the long hydrocarbon tails together, thus strengthening this architecture. Lastly, hydrogen bonds and polar interactions between water molecules of the aqueous environment and the polar heads of lipids stabilize this organization. The final organization of lipids depends on their nature, concentration, temperature and geometric form (Frolov VA et al., 2011). If ions or molecules are present during the formulation process, they can be encapsulated inside these membranes.

*Phospholipids*

The glycerophospholipids, or phosphoglycerides, are constituted by a molecule of glycerol esterified in position 3 by the ortho phosphoric acid ($H_3PO_4$), while the other two hydroxyl groups are generally esterified from long-chain fatty acids, unbranched, which usually present a number of carbon atoms from 14 to 24. Considering the number

of carbon atoms, the fatty acid can be named as lauric (C12), myristic (C14), palmitic (C16) and stearic (C18). Finally, the phosphoric acid group binds to the hydroxyl group of an alcohol completing the polar head. Depending on the type of the alcohol molecule, phospholipids can present or not a net charge leading to the formation of various types of phospholipids, with different characteristics (Figure 8). The nature of the phospholipid is also related to the length of the fatty acid chains. Fatty acids chains differ in the number of carbon atoms and the degree of unsaturation (Vemuri S and Rhodes CT, 1995).

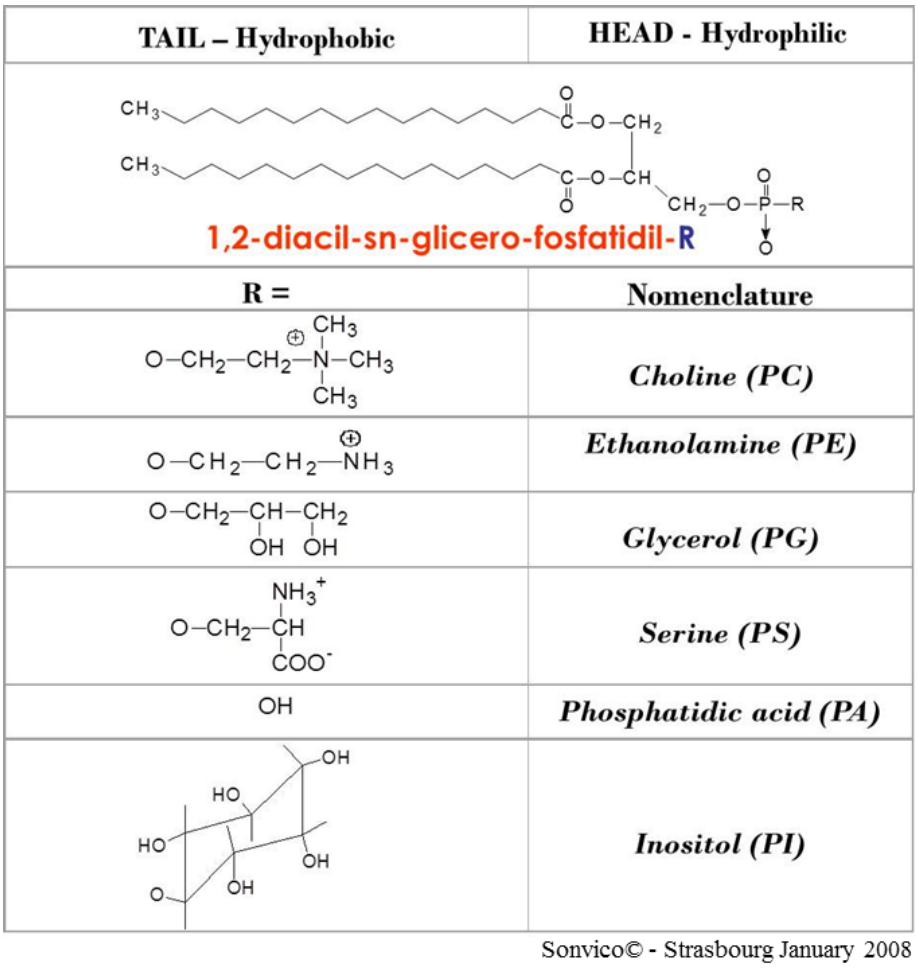


**Figure 8. Phospholipids structure.**

The chains can be unsatured, when a double bond exists between two carbon atoms (C = C) in a hydrocarbon chain or saturated, when hydrocarbon chains have no double

bonds (i.e. C – C). Most of the unsatured fatty acid chains have a *cis* configuration (Figure 9).

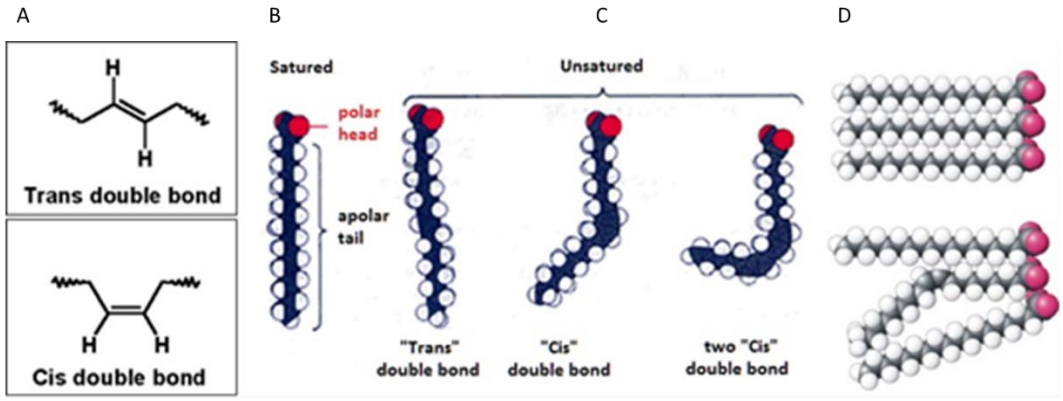


**Figure 9. Fatty acid structure.** (A) *Trans* and *cis* double bonds. (B) Saturated phospholipids. (C) Unsatured *trans*, *cis* and two *cis* phospholipids. (D) Bilayer structure with saturated phospholipids (up) or in presence of unsaturated phospholipids (down).

The *cis* configuration forces phospholipids to assume an angular structure, of approximately thirty degrees hampering the achievement of an ordered packing of the phospholipid layer, that will occur with the only presence of phospholipids with saturated fatty acids chains or unsatured chains in *trans* configuration.

Lipids varieties may give rise to different structures in an aqueous environment (Figure 10).

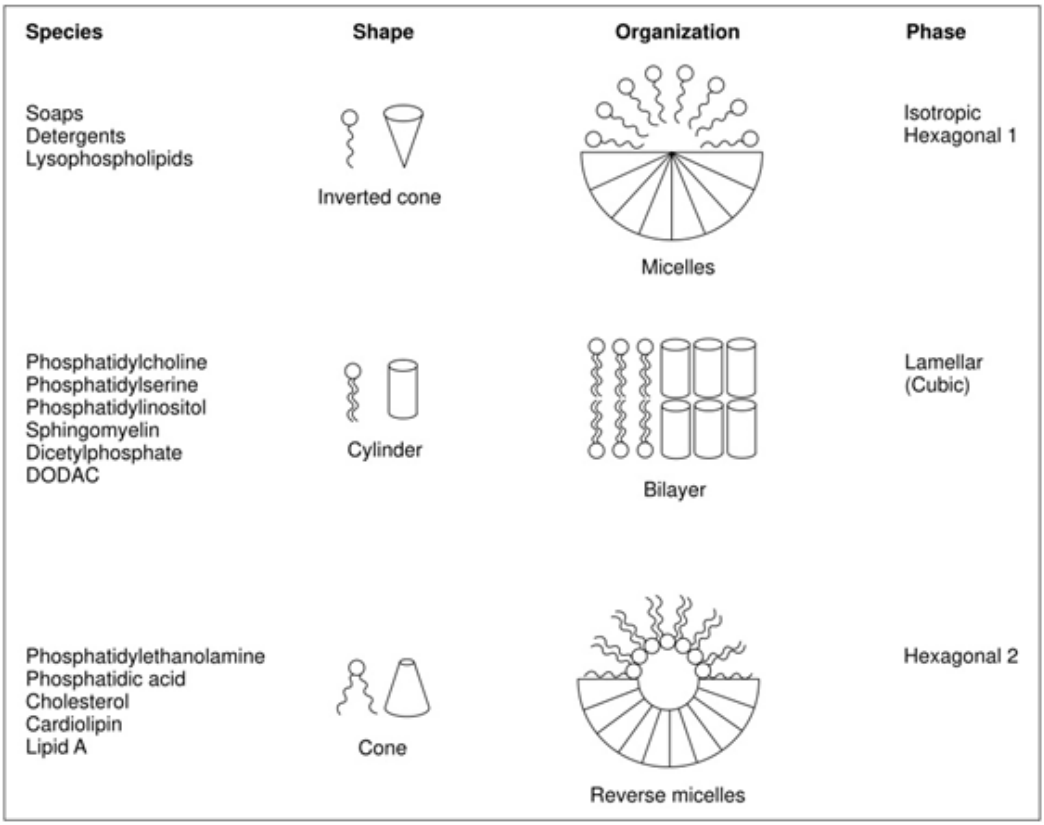


**Figure 10. Main packing lipid structures** (Lasic DD, 1998)**.**

Phospholipids self-assembly may depend on the curvatures existing at hydrocarbon-water interfaces. Then the nascent structure is regulated by the Surface Packing Parameter (P), obtained from the following formula:

$$P = \frac{V}{a \times Lc}$$

where $V$ is the volume of the hydrophobic portion, $a$ is the surface area of the polar portion at the air / water interface and $Lc$ is the length of the hydrophobic chains (Figure 11).

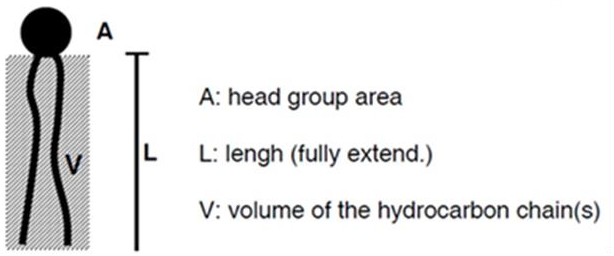


**Figure 11. Packing paramenter (P) factors.**

For A > V structures with high curvature (such as micelles) are formed. When the areas are comparable, a bilayer configuration is the most stable form, while for V > A, reverse micelles (with negative surface curvature) are formed.

A fundamental characteristic of all membranes is the phospholipids phase transition (T*c*), which consist in the ability of phospholipids to change their state from solid–ordered phase to a fluid–disordered phase known also as liquid crystals. The transition is closely dependent on the temperature, called melting transition temperature (T*c*). T*c* values are influenced by the length and the degree of saturation of the lipid chains: the greater is the lipid chain, the greater is the T*c*. Instead, if more double bonds are present, the T*c* will be lower (Table 3).

| phospholipid | acyl chain length, no. unsaturation | $T_c$ (°C) |
|---|---|---|
| DSPC | 18 : 0, 18 : 0 | 55 |
| HSPC | 16–18 (mixture) | 52 |
| DPPC | 16 : 0, 16 : 0 | 42 |
| POPC | 16 : 0, 18 : 1 | −7 |
| SLPC | 18 : 0, 18 : 2 | −16.7 |
| DOPC | 18 : 1, 18 : 1 | −21 |
| DSPG | 18 : 0, 18 : 0 | 53 |
| DPPG | 16 : 0, 16 : 0 | 41.1 |
| DSPA | 18 : 0, 18 : 0 | 58 |

**Table 3. Crystalline phase transition (T*c*) in °C of some phospholipids** (adapted from Drummond DC et al., 1999).

*Cholesterol*

Cholesterol is a molecule of a sterols family with an amphipathic structure and is most abundant sterol in mammalian membranes (Figure 12). In membranes, cholesterol arranged with the hydroxyl group oriented towards the aqueous phase to form hydrogen bonds with the polar heads of the phospholipids and the steroid group, with the alkyl chain, oriented towards the fatty acids chains of the phospholipids. The planar steroidal group fits the first ten carbon atoms of the fatty acid chains and, being relatively rigid, reduces the movement and, at the same time, confers more space for movements to the carbon atoms that are located towards the terminal end of the chain.

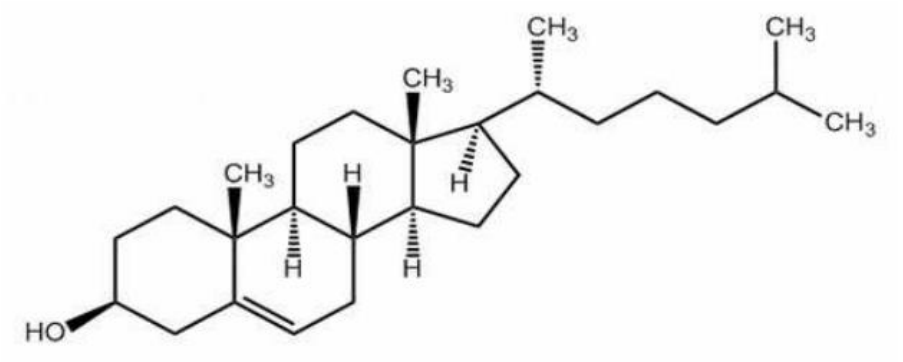


**Figure 12. Cholesterol structure**

This interaction with phospholipids determine two opposite effects of the cholesterol on the membrane, according to the temperature (Figure 13):

- Condensing effect: at higher temperature than T*c*, cholesterol reduces the motility of the chains, and then the fluidity of the phospholipid bilayer.
- Fluidifying effect: at a lower temperature of T*c*, cholesterol prevents the strong intermolecular bonds between phospholipids, giving to the system more fluidity and permeability than it would have without cholesterol.

Cholesterol is used to improve the characteristics of the liposomal membranes, since it decreases the influence of temperature on the permeability parameter, modulating membrane fluidity, and increases their stability in the presence of biological fluids such as blood or plasma (Smallbonea K et al., 2005).

In fact, cholesterol-free liposomes tend to react more with plasma proteins such as albumin, transferrin, and macroglobulin. This situation, destabilizing the liposomal structures, reduces their utility as drug delivery systems.

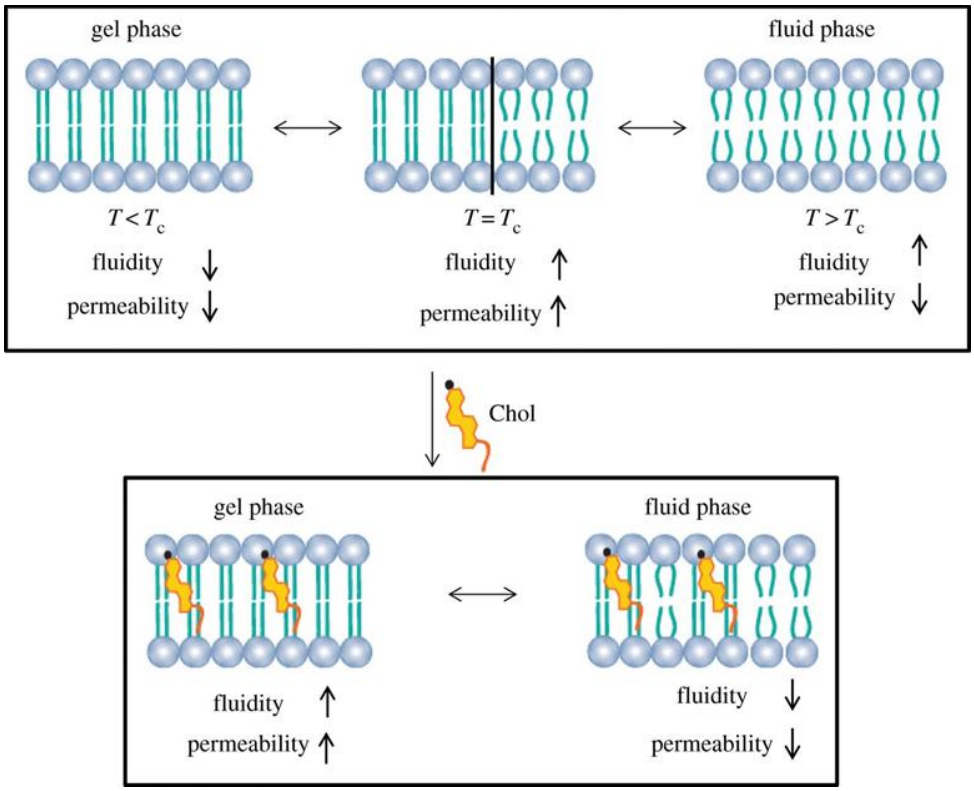


**Figure 13. Effect of temperature and cholesterol on phospholipid bilayer permeability.** Cholesterol eliminates the transition phase of the lipid bilayer, increases the lipid bilayer permeability in the gel phase and decreases it in the fluid phase. (adapted from Monteiro N et al., 2014).

### 1.5.2 Liposomes classification

Liposomes can be classified into several categories according to their size and lamellarity (number of lipid layers) as well as to their composition, which is closely linked to the type of application for which must be used.

*Size and Lamellarity*

The size and lamellarity of the liposomal vesicles represent a critical parameter in determining the liposomes average lifetime of circulation in the blood as well as affect the degree of encapsulation of a drug (Figure 14). Liposomes are divided into:

- ✓ Multilamellar Large Vesicles (MLV) with a diameter greater than 500 nm consisting of more layers. MLV ensure a high incorporation of lipophilic drugs and are stable for long periods of time. Since the RES quickly catches them, MLV are the ideal system for the targeting to these cells.
- ✓ OligoLamellar Vesicles (OLV) with a diameter between 100 and 500 nm, present more layers;

- ✓ Multivesicular Vesicles (MVV): with a diameter, greater than 1000 nm, incorporate other smaller liposomes;
- ✓ Giant Unilamellar Vesicles (GUV): with a diameter, greater than 1000 nm, consist of one single bilayer;
- ✓ Large Unilamellar Vesicles (LUV): with a diameter between 200 and 1000 nm, present only one slat. LUV are particularly useful for the transport of hydrophilic drugs, especially macromolecules;
- ✓ Small Unilamellar Vesicles (SUVs) with a diameter between 20 and 200 nm, consist of a single bilayer. SUVs are thermodynamically unstable and susceptible to aggregation and fusion if uncharged. However, they have the longer half-life time in the circulation and are the most use as drug delivery system.

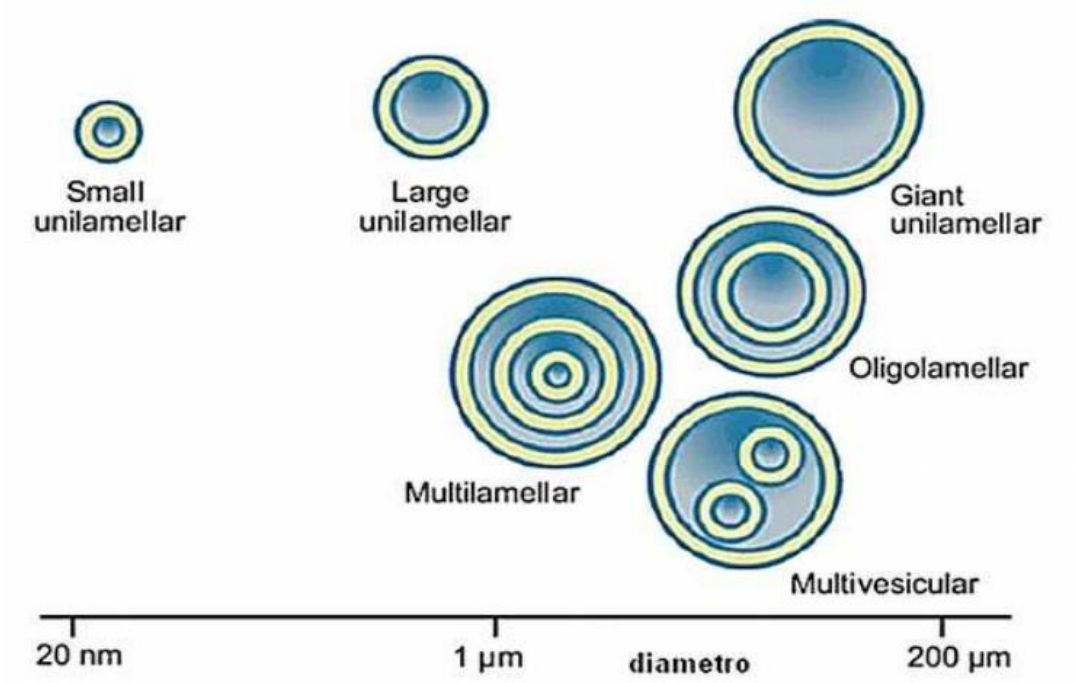


**Figure 14. Size and lamellarity of liposomes.**

*Composition*

Depending on the changes made to the structure of the liposomal particles, these assume features according to which they are classified as:

- ✓ pH-sensitive liposomes: are affected by changes in pH because of their structure. In particular, at pH 6.5 lipids which they are made of, are protonated favouring the release

of the drug. This is an extremely advantageous feature because in the tumor microenvironment, because of the necrotic tissue that is formed with the growth of the tumor, occurs a considerable lowering of the pH compared to the physiological conditions (Millis JK and Needham D, 2004).

- ✓ Thermosensitive liposomes: at a critical temperature (usually around 38-39°C) these liposomes become permeable to the drug, releasing it. This behaviour can be useful when the area in which the tumor mass resides is heated after the administration, so as to obtain the best release of the drug. This leads to concentrate the drug in the area concerned, necessitating lower doses and reducing the toxicity in other body districts (Park JW et al., 2004).
- ✓ Immunoliposomes: are created to be able to release the drug to a cell that presents a specific antigen. This is possible by integrating in the phospholipid membrane of the liposome a monoclonal antibody specific for tumor antigens. The bond between the antigen and the antibody directs the liposome to the target cell and the release of the drug preferentially in this cell (Moghassemi S and Hadjizadeh A, 2014).
- ✓ Niosomes: non-ionic liposomes with a phospholipidic membrane consisting of non-ionic amphiphilic lipid of synthesis, usually with added of cholesterol. Niosomes are smaller than 200 nanometres and are much more stable and less toxic than those with a phospholipid amphoteric nature. They are an evolution of the liposomes, with similar chemical properties (Moghimi SM and Szebeni J, 2003).
- ✓ Stealth liposomes (long circulation): to increase the plasma half-life is possible to modify the liposomes surface with hydrophilic polymers, flexible and not ionic such as polyethylene glycol (PEG). In this way, the pegylated liposomes can circulate longer, escape from the immune system without being destroyed and reach the tumor tissue gradually releasing the drug (Laouini A et al., 2012).

### 1.5.3 Preparation methods

Numerous methods for the preparation of liposomes are available today and they differ for the techniques used to disperse phospholipids. The following are the most popular methods in the preparation of liposomes:

- ✓ Thin-film hydration (Bangham method): lipids are solubilized with the use of an organic solvent (usually a chloroform:methanol 3:1 mixture) which then evaporates forming a thin lipid film on the wall of a glass container. The film is then hydrated by

stirring at temperature above the T*c* of the phospholipid that has the highest T*c* (Figure 15). With this process, MLV are obtained. MLV will have a wide size distribution, depending on the hydration time, the re-suspension method, the lipid concentration and composition and the volume of suspending of the aqueous phase (Antimisiaris SG et al., 2007). MLV can then be restricted to low-pressure extrusion or by means of ultrasound passing from MLVs to SUVs.

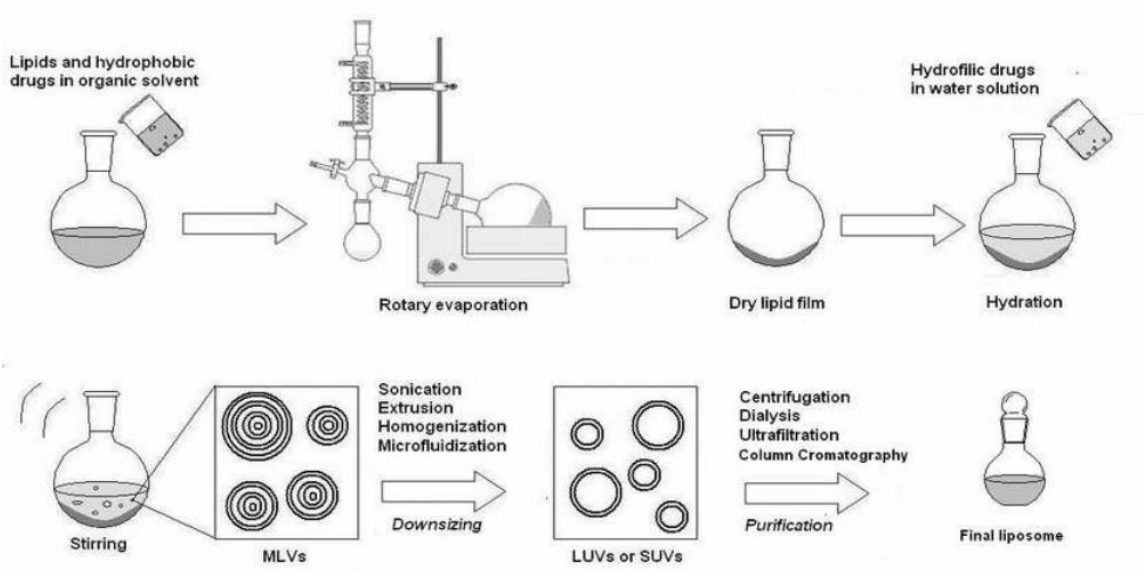


**Figure 15. Thin-film hydration technique (Rangel L., 2013)**

- ✓ Reverse-phase Evaporation Vesicles (REV): liposomes are formed from water-in-oil emulsions of phospholipids and buffer, in the excess of an organic phase. Phospholipids are firstly dissolved in organic solvents to form a film, then solvents are removed by evaporation. The thin film is re-suspended in diethyl ether, followed by the addition of water. The preparation is then sonicated for a short time, forming a homogeneous emulsion. The organic solvents are removed under reduced pressure by continued rotary evaporation, resulting in the formation of a viscous gel-like intermediate phase characterized by a LUV dispersion. This method can encapsulate large macromolecules. The main disadvantage of this method is the exposure of the macromolecules to organic solvents and to sonication conditions, which may result in the denaturation of sensitive molecules (Szoka F and Papahadjopoulos D, 1980).
- ✓ Solvent (Ether or Ethanol) Injection Technique: lipids dissolved in ethanol are rapidly injected into a buffer solution where they spontaneously form SUVs, with a diameter of 30 nm (Brunner J et al., 1976). However, the size of liposomes can be increased by

increasing the lipid concentration (Szoka F and Papahadjopoulos D, 1980). This liposome preparation method has the advantage of avoid chemical or physical treatment of lipids. Nevertheless, the concentration of vesicles produced is low and it involves an extra step to remove solvent (Antimisiaris SG et al., 2007). The ether injection method differs from the ethanol injection method since the ether is immiscible in the aqueous phase, which is also heated so that the solvent is removed from the liposomal product. The method involves injection of ether-lipid solutions into warmed aqueous phases above the boiling point of the ether. The ether vaporizes upon contacting the aqueous phase and the dispersed lipid forms primarily unilamellar liposomes (Deamer DW, 1978). An advantage of the ether injection method compared to the ethanol injection method is the removal of the solvent from the product, enabling the process to be run for extended periods forming a concentrated liposomal product with high entrapment efficiencies.

- ✓ Detergent Dialysis: liposomes, in the size range of 40–180 nm, are formed when lipids are solubilized with detergent, yielding defined mixed micelles (Zumbuehl O and Weder HG, 1981). The detergent is subsequently removed by controlled dialysis and phospholipids form homogeneous unilamellar vesicles with usefully large encapsulated volume.

## 2. Aim of the study

The non-receptor tyrosine kinase c-Src plays a fundamental role in the development of various forms of cancer, including neuroblastoma and glioblastoma, and in the formation of metastases. Thereby, the inhibition of c-Src can be a viable strategy to arrest the growth and migration of cancer cells. Pyrazolo [3,4-*d*] pyrimidine compounds constitute a promising class of molecules in cancer therapy, being able to inhibit many oncogenic tyrosine kinases. This class of compounds have been optimized to selectively inhibit the c-Src tyrosine kinase. Unfortunately, during development some of these molecules, while acquiring a good biological activity, reduced their water solubility resulting in non-ideal ADME characteristics.

In recent years, liposomes have been extensively studied as a novel drug delivery system for anticancer chemotherapeutics. The liposomal formulation of anticancer drugs affords enhanced stability, improved targeting to tumoral cells, controllable release rate and more favorite pharmacokinetic and biodistribution with respect to free drugs. Furthermore, liposomes are able to improve solubility of lipophilic compounds.

On these base, the aim of my project has been to improve the solubility and the activity of free pyrazolo [3,4-*d*] pyrimidine compounds by creating a formulation of pyrazolo [3,4-*d*] pyrimidine-entrapped liposomes.

The main intent of my work was to create a liposomes formulation with specific structural characteristics for an optimal drug delivery system. Parameters such as size, zeta (ζ) potential and polydispersity index (PDI) were evaluated by Dynamic Light Scattering analysis and electron microscopy. Moreover, liposomes were analyzed for their encapsulation efficacy (EE). In addition, liposomes biological properties were analyzed to verify the stability in serum (physiologic conditions), the absence of toxic activity for liposomes without encapsulated drug, the ability to recognize the cell membrane and to release the cargo in cellular cytoplasm and the cytotoxic activity against cancer cells that overexpressed c-Src, at least as the activity of free compounds. Liposomes formulation encapsulating pyrazolo [3,4-*d*] pyrimidine compounds was morphological and dimensional characterized and the interaction with cancer cells was investigated by fluorescence analysis. Both free molecules that the related liposomal formulations were tested in vitro on SH-SY5Y neuroblastoma cells and U87 glioblastoma cells to evaluate the cytotoxic activity of the encapsulated compounds compared to free compounds solubilized in dimethyl sulfoxide (DMSO). Finally, a

tissue distribution test in mouse, after 24 hours of treatment, was performed and results were compared with those obtained from free compounds solubilized in DMSO.

## 3. Materials and methods

### 3.1 Preparation of stealth liposomes

The thin layer evaporation method, developed by AD Bangham was used to prepare stealth liposomes. The 1,2-dipalmitoyl-*sn*-glycero-3-phosphocholine (DPPC), cholesterol and 1,2-dipalmitoyl-sn-glycero-3 phosphoethanolamine-N-carbonil-methoxy polyethylene glycol-2000 (sodium salt) (DPPE-$PEG_{2000}$) were used in a 2:1:0,1 molar ratio and solubilized in a mixture of Chloroform/Methanol 3:1 v/v. Fluorescent liposomes were prepared by the same method with the addition of 1,2-Dioleoyl-sn-glycero-3-phosphoethanolamine, 7-nitrobenzofurazan-labeled (DOPE-NBD) with a final molar ratio of 2% of total lipids in the lipid mixture. The mixture was transferred in a round bottom flask and the compound to encapsulate solubilized at a concentration of 1 mM. Solvents were removed by rotary evaporator obtaining a homogeneous lipid film on the flask wall. The lipid film was hydrated with a 0,9% NaCl saline solution, pH 7,4 and mixed for 1 h at a temperature higher than lipids T*c*. Liposomes were mixed with a vortex for 3 minutes obtaining a lattice solution containing multilamellar vesicles (MLV). Liposomes were sonicated for 20 minutes at RT to reduce liposomes average size and lamellarity obtaining a clearer solution containing small unilamellar vesicles (SUV). Finally, the solution was filtered with a 13 mm PTFE filter with 200 nm pores excluding large liposomes and the non-encapsulated or precipitated compound.

### 3.2 Efficiency encapsulation (EE) measurements

Liposomes were treated with ethanol in a 1:1 volume to extract the encapsulated compound. The compound was analysed by liquid chromatography-UV (LC-UV) at 254 and 280 nm using acetonitrile (ACN) and water as mobile phase with a 0,8 ml/min flux and a Varian Microsorb Polaris C18 (150 x 4,6 mm, 5 micron) column at RT. The concentration of the extracted compound was calculated with respect to calibration lines, while the encapsulation in liposomes was measured with respect to the amount of the compound initially loaded, using the following formula:

$$\mathrm{EE} = \frac{\text{Encapsulated drug}}{\text{Total added drug}} \times 100$$

## 3.3 Liposomes morphological and dimensional characterization

*3.3.1 Dynamic light scattering (DLS)*

Liposomes were analysed by a Zetasizer Nano ZS (Malvern) DLS. Measurements were performed after the re-hydration of liposomes with a solution 1 mM NaCl. Three consecutive sessions with a 90° angle, each consisting of 10-100 scans, according to the characteristics of the sample, were performed.

*3.3.2 Field Emission Scanning Electron Microscopy (FESEM)*

Samples were diluted in water and few drops were deposited on a carbon film grid where samples were air-dried until complete evaporation of the solvent and subsequently analyzed. FESEM images were acquired with an acceleration potential to stranded between 10-20 kV at different magnifications.

*3.3.3 Cryo-Trasmission Electron Microscopy (Cryo-TEM)*

Liposomes morphology was also observed by cryo- transmission electron microscopy. 3 μl of sample was applied on a Quantifoil® coal perforated grid (copper Multi A, Quantifoil® Micro Tools GmbH, Jena, Germany) and the excess fluid was buffered with filter paper. The sample was then frozen by immersion in liquid ethane, using an immersion freezer, to obtain vitrification of the sample. Frozen samples were stored in liquid nitrogen until the EM analysis. The vitrified samples were analysed using a CM200 FEG transmission EM (EIF, Eindhoven, the Netherlands) operating at 200 keV and equipped with a CCD camera F224HD 2048x2048 (TVIPS Gauting, Germany). Images were acquired at a 27,500 x magnification (pixel size 0.602 nm) at -12, -18 μm of defocus.

## 3.4 Cellular uptake studies

Fluorescent liposomes, carrying NBD-DOPE in the lipid bilayer, were prepared as described in 2.1. SH-SY5Y and U87 cells were maintained in DMEM medium supplemented with 10% FBS, 2 mM L-glutamine and 10000 U/mL Penicillin/Streptomycin at 37 °C in 5% $CO_2$ atmosphere. SH-SY5Y cells were plated on glass coverslip at a density of $20 \times 10^3$ cells/well in 24-well plates. After 24 h, cells were

incubated with liposome formulation and then fixed in 4% paraformaldehyde in PBS for 20 min. Nuclei and cellular membranes were stained respectively with a 6 μM solution of DAPI and 2 μg/mL WGA Alexa Fluor 647 labelled for 10 min. Samples were visualized on a TSC SP5 confocal microscope (Leica, 5100000750) installed on an inverted LEICA DMI 6000CS (10741320) microscope and equipped with an oil immersion Plan Apo 63 Å~1.4 NA objective. Images were acquired using the LAS AF acquisition software (Leica, 10210).

### 3.5 *In vitro* cytotoxicity assay

Cytotoxicity assay was carried out on human neuroblastoma cell lines SH-SY5Y and U87. Cells were seeded at $10 \times 10^4$ cells/well density in 6-well plate and treated with empty liposomes, liposomes-encapsulating compounds, and free compounds (in DMSO solution) at increasing concentrations (0.1 μM, 1.0 μM, 10 μM and 50 μM). All liposomal formulations have been realized in a 0.9% NaCl solution w/v, pH 7.4. Cultures were maintained at 37 °C in 5% CO2 and then treated for 24, 48 and 72 h. Cell number and viability were evaluated using the Bürker chamber after treatment with Trypan Blue. $IC_{50}$ was calculated by GraphPad Prism 6.0 software.

### 3.6 *In vitro* release

Rates of drug release were studied by dialyzing the liposomes containing Si306 (3.5 mL, 0.4 mM) against PBS (20 mL, pH 7.4, 10 mM) with 50 mg/mL of BSA (physiological plasma concentration). The entire system was stirred at 37 °C and samples (1 mL, from the PBS-BSA) were collected at different time points (0, 1,2, 3, 24, 48, 72 and 96 h) (1 mL of PBS-BSA was added each time to maintain sink condition). Each sample was treated with 1 mL of ACN and centrifuged at 4000 rpm for 20 min. Then, the supernatant was recovered, concentrated under reduced pressure and analyzed to determine the concentration of compound by liquid chromatography–mass spectrometry (LC-UV-MS).

### 3.7 *In vivo* distribution

Male Sprague Dawley rats (Charles River, Milan, Italy) were maintained according to ethical EEC regulations for animal research. The animal protocols used were reviewed and approved by the Animal Care and Ethics Committee of the University of Siena,

Italy. The animals were anesthetized (i.p. xylazine hydrochloride, 10 mg/kg, Xilor, Bayer AG, and ketamine hydrochloride 35 mg/kg, Ketavet, Gellini) and treated by i.v. injection through the tail vein. The experiment was performed in triplicate. The two groups received intravenously liposomes containing Si306 (500 μL, PBS, pH 7.4) or Si306 (50 μL in DMSO), corresponding to a bolus of 10 mg/Kg. After 24 h, animals were sacrificed and blood and tissues were treated for the quantitative analysis. The blood, previously heparinized, was centrifuged at 4000 rpm for 20 min to separate the plasma fraction and then, 500 μ L were collected in a test tube. Tissues were homogenized using a glass/glass Potter-Elvehjem homogenizer. For each sample 1 mL of ACN (in the presence of the internal standard 1-(2-chloro-2-(4-chlorophenyl) ethyl)-N-(3-fluorobenzyl)-1H-pyrazolo[3,4-*d*] pyrimidin-4-amine, 10 μM was added to denature proteins and to extract Si306. Samples were centrifuged at 4000 rpm for 20 min; the supernatant was recovered, evaporated and analysed by LC-UV-MS.

## 4. Results

### 4.1 ADME properties and enzymatic activity of selected compounds

Before liposomes preparation, c-Src inhibitors permeability was evaluated to establish the natural ability of selected compounds to overcome a phospholipid membrane. Molecules encapsulated inside liposomes were chosen on the base of cellular activity data and water solubility: Si13, Si34, Si161, Si163, Si192, Si306, Si307, Si322 and Si323 (Table 1).

| Compound | Src Activity $K_i$ (μM)[a] | Water Solubility (μg/mL) | P. App. ($10^{-6}$ $cm^2$ /sec) [b] MR (%) [c] | Metabolic Stability (%) [d] |
|---|---|---|---|---|
| **Si13** | 3,0 | 0,70 | 11,08(5,9) | 78,3 |
| **Si34** | 3,7 | 0,21 | 3,98(46,8) | 95,8 |
| **Si161** | 0,223 | 0,00022 | ND | ND |
| **Si163** | 0,0093 | 0,098 | 10,00(10,2) | 93,6 |
| **Si192** | 0,209 | 1,72 | 10,16(32,0) | 94,0 |
| **Si306** | 0,13 | 3,71 | 5,27(46,1) | 96.0 |
| **Si307** | 0,4 | 0,22 | 5,51(48,9) | 97,9 |
| **Si322** | 0,03 | 0,0091 | 5,92(17,9) | ND |
| **Si323** | 0,01 | 0,016 | 4,53(49,6) | 93,5 |

**Table 1.** Pyrazolo [3,4-*d*] pyrimidine compounds enzymatic activity against Src and ADME properties. [a] constant of enzyme inhibition; [b] apparent permeability; [c] Membrane Retention (MR) expressed as percentage of compound unable to reach the acceptor compartment; [d] stability expressed as percentage of unmodified drug.

### 4.2 Liposomes Encapsulation Efficiency (EE)

The encapsulation efficiency (EE) is measured by the quantification of the encapsulated compound in comparison to the total amount of the compound introduced. To estimate the EE, liposome suspension was disrupted with ethanol after their filtration to release the entrapped compound. Unfiltered and filtered liposome preparations were analysed by LC-UV at 280 nm and chromatograms are shown in Figure 1. As it can be seen from the difference in area between the two peaks, liposomes filtration decreased the amount of released compound in the filtered sample, probably due to the shrinkage of larger liposomes that can encapsulate more compound. Moreover, the compound-filter

interactions enhanced the loss of the compound because a small part of the compound can be trapped in the filter. Using appropriate calibration lines, the concentration values of the selected encapsulated compounds were obtained.

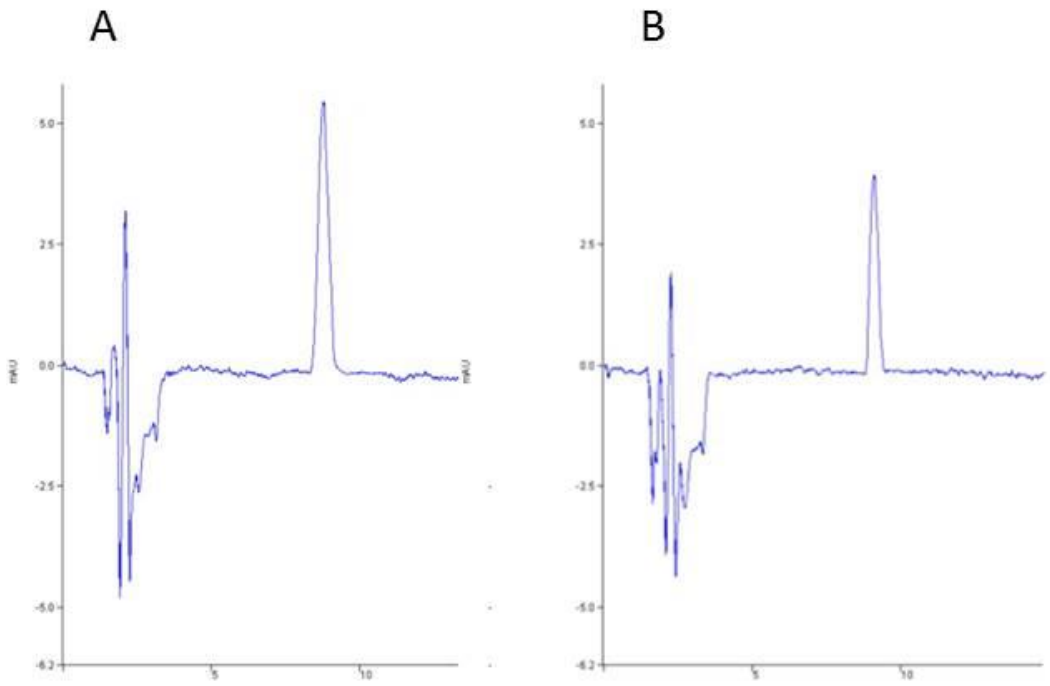


**Figure 1. Unfiltered (A) and filtered (B) liposome chromatogram of liposome preparations, representative of all selected compounds.**

The liposomal suspension undergoes a sonication step during the preparation to obtain a uniform distribution of the liposomal population. To understand the contribute of sonication, the EE before and after sonication was evaluated. Figure 2A reported the Si163-loading differences between sonicated or not sonicated liposomes, showing a higher EE for the sonicated liposomes with respect to the sonicated formulation. In addition, the EE of Si161 and Si163-loading liposomes were analysed after sonication at a temperature lower or higher than the T*c* with respect to room temperature (Figure 2B). A greater load is obtained when the sonication is carried out at room temperature. Higher temperatures than T*c* cause a shift towards the gel status of membranes bilayer, increasing their permeability and probably causing a loss of compound, which leaks from liposomes.

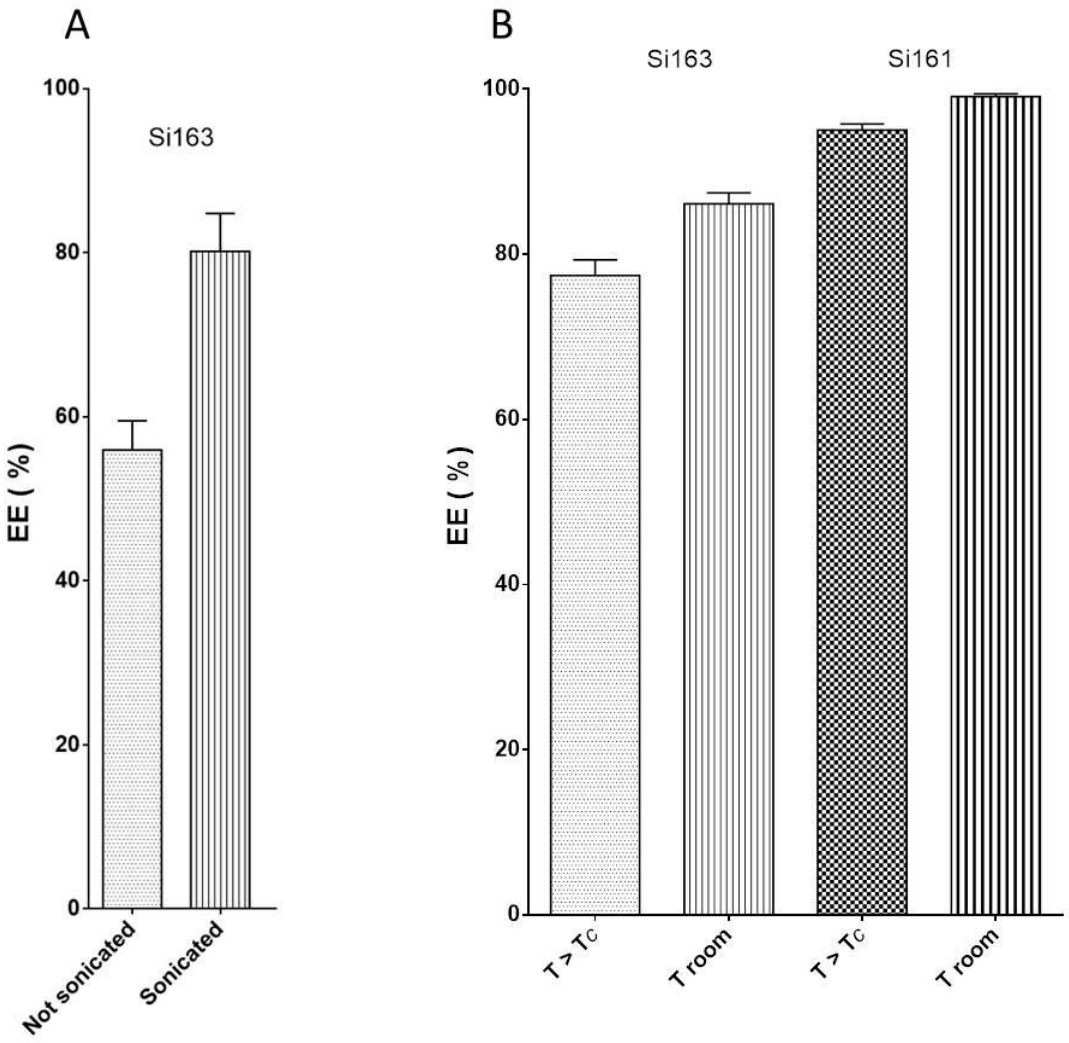


**Figure 2. Contribute of Sonication in the encapsulation process (A); influence of the temperature on the sonication step (B)**

Furthermore, liposomes formulations were optimized to obtain the maximum EE. For this reason, three different drug-to-lipid ratios of 1:6, 1:12 and 1:24 for Si163-loading liposomes, varying the total amount of lipids and preserving the amount of compound and hydration volume, were tested (Figure 3). Results show that the 1:6 drug-to-lipid ratio is not sufficient to obtain a good loading of compound, with an EE value of about 30%. Instead, 1:12 and 1:24 drug-to-lipid ratio ensure both an optimal loading.

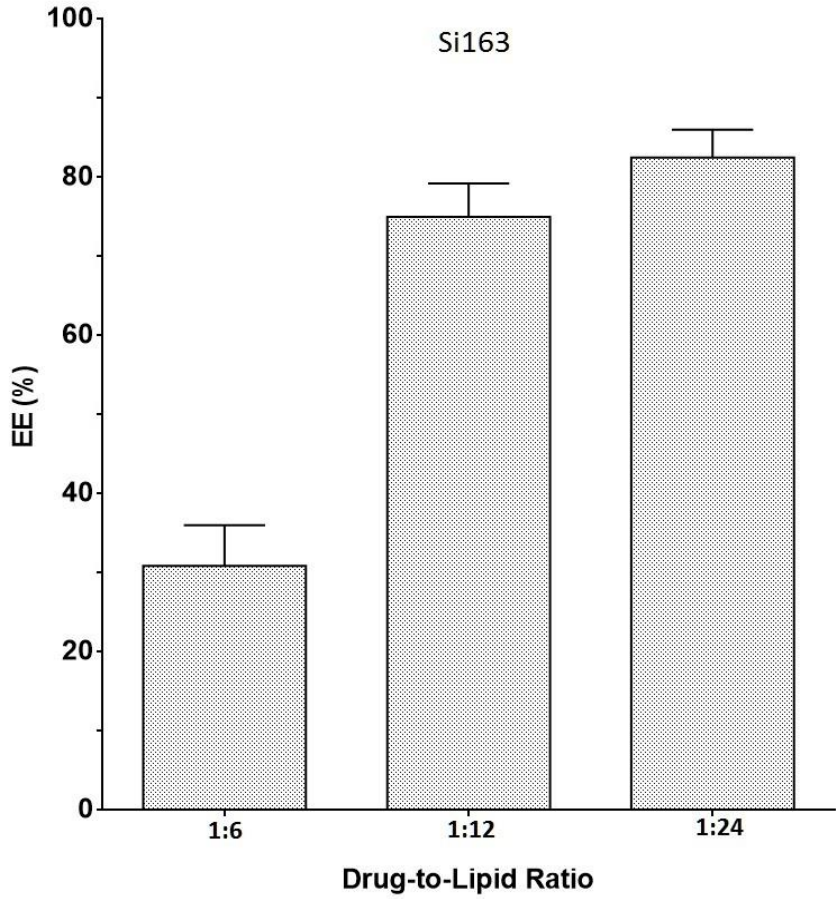


**Figure 3**. **Drug-to-Lipid ratio optimization**

Liposomes with the best drug-to-lipid ratio (1:24) were prepared for each selected compound. The EE of each liposomal formulation was evaluated and compared with the corresponding values of water solubility of the compound. Results showed that a great percentage of loading was obtained, in fact it is greater than 80% for all the selected compounds despite their difference in water solubility (Figure 4).

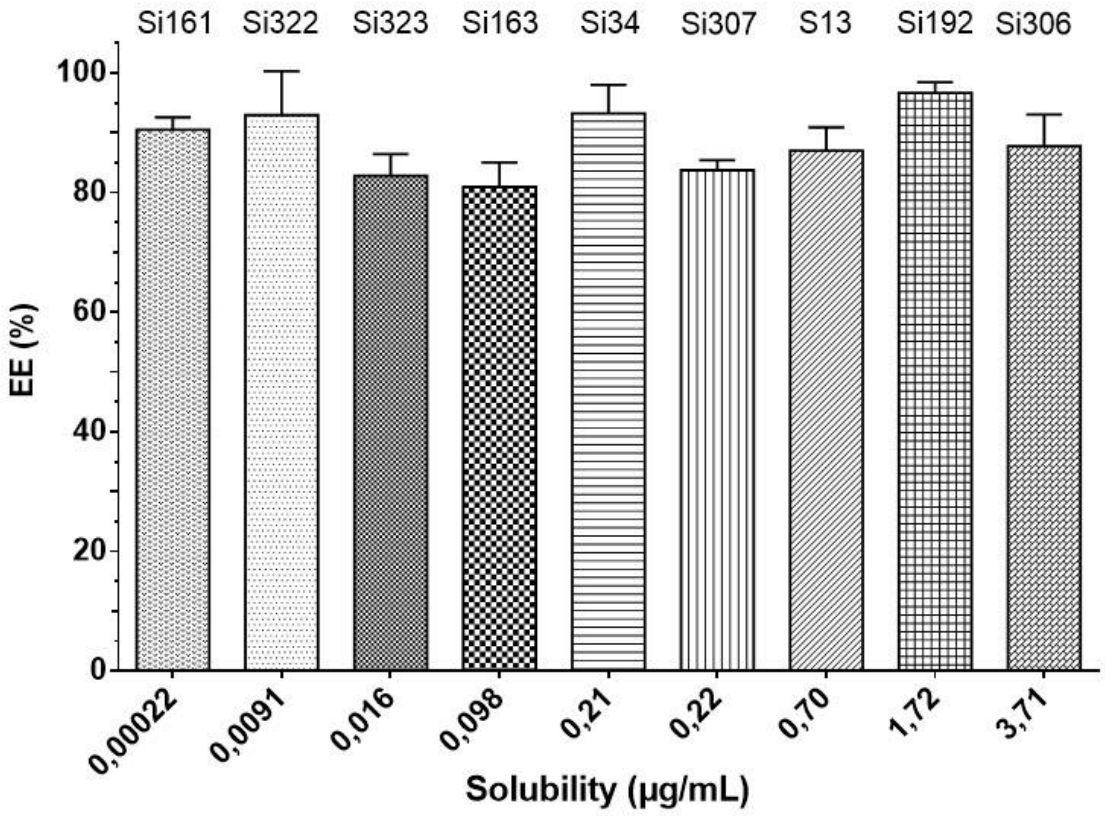


**Figure 4. EE for each selected compound and respective water solubility.**

### 4.3 Morphologic and dimensional characterization of liposomal formulation

Particle size has a significant impact on the circulation and larger is the nanoparticle, faster is the clearance. In addition, particle size affects cellular uptake, influencing phagocytosis and endocytosis.

The morphology and size of liposomes were observed by Field Emission Scanning Electron Microscopy (FESEM) (Figure 5) and subsequently by the most appropriate cryo Transmission Electron Microscopy (cryo-TEM) (Figure 6).

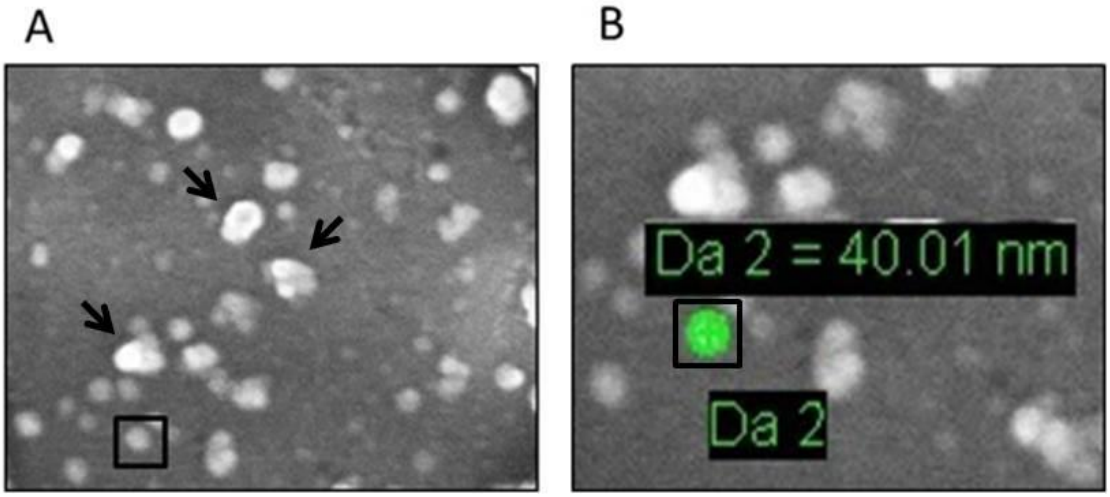


**Figure 5. Morphological analysis by FESEM of Si163-loading dried liposomes (A); Zoom 2x of evidencied area (B)**

Liposomes analized by FESEM showed a diameter smaller than 100 nanometers (Figure 5B). In addittion several aggregates (indicated by the arrows), with higher size and heterogeneous morphology, are visible. The presence of aggregates and of reduced size liposomes can be attributed to the preparation of the sample, which include the complete evaporation of the solvent determining the implosion of liposomes and their aggregation. For this reason, samples were also analysed with cryo-TEM (Figure 6). The result confirmed the presence of a homogeneous population of unilamellar nanoparticles with size around 100 nm. Liposomes were round, smooth and free from drug crystals, while bilamellar, multilamellar or giant-liposomes were not observed in the image from cryo-TEM. The average thickness of the phospholipidic bilayer corresponded to 5.77 ± 1.05 nm (12 measurements performed by Image J Software). Arrows indicate the presence of small phospholipid bilayer fragments (PBF) which are one of the alternative structure that phospholipids can assume during liposomes preparation in particular during the sonication (Tejera-Garcia R et al., 2011).

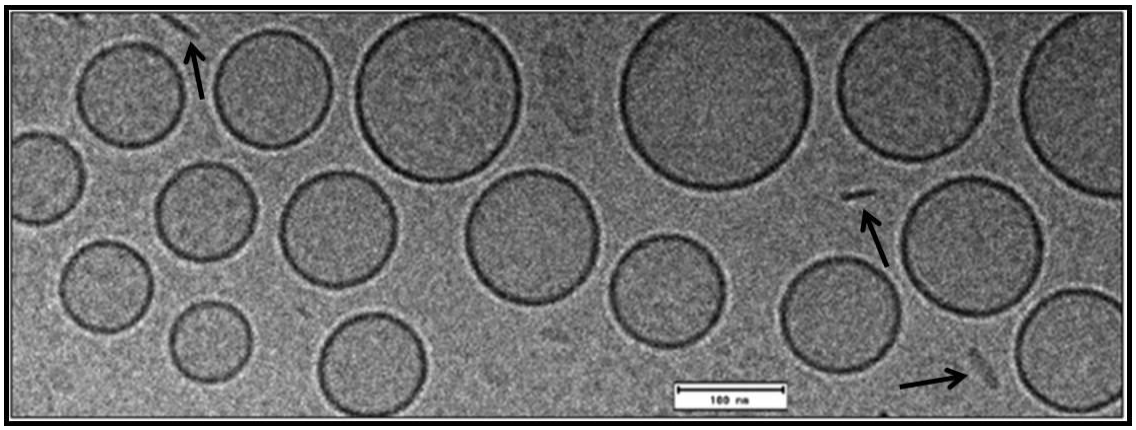

**Figure 6. Morphological analysis by Cryo-EM of Si306-loading liposomes**

In addition, the size and stability of liposomes in physiological solution, expressed as ζ potential and polydispersity index (PDI) value, was also evaluated by the DLS for liposomes encapsulating the Si34, Si306, Si307 and Si323 compounds.

ζ potential is the potential present between the particles surface and the ionic layer which surround them in solution. The value of the ζ potential allows predicting the stability of small or low density nanoparticles. A value of high ζ potential (i.e. < -30mV and > + 30mV) is necessary for nanoparticles to be repelling enough to eliminate the possibility of agglomeration, aggregation and / or flocculation.

Polydispersity is the distribution of individual molecular masses in a batch of polymers and is used to describe the degree of "non-uniformity" of a distribution. A perfectly uniform sample has the PDI value of 0.0. Values greater than 0.7 indicate that the sample has a very broad size distribution and is probably not suitable for the DLS analysis.

Figure 7 shows the comparison between empty (A) and Si306-loading liposomes (B). The presence of the compound did not result in the increase in size of liposomes, which have the same distribution of the population of non-loaded liposomes.

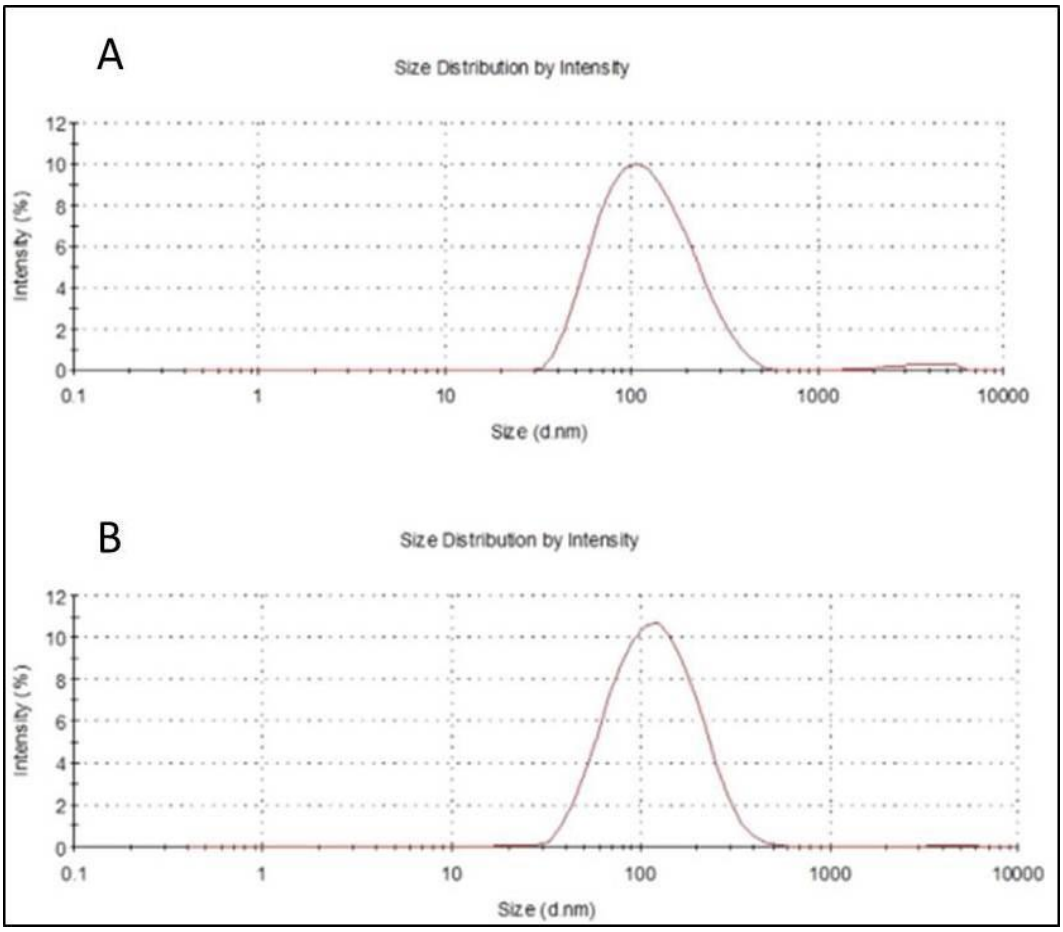


**Figure 7**. **Size distribution by DLS. Empty liposomes (A); Si306-loading liposomes (B).**

The mean diameter, PDI and ζ potential of liposomes encapsulating the selected compounds are shown in Table 2. The size of nanoparticles ranged between 105 nm and 232 nm (Si306 and Si323-loading liposomes), with Si34-loading liposomes and Si307-loading liposomes being around 151 nm and 131 nm, respectively. The whole set of liposomes presented good values of ζ potential (from − 27.4 mV to − 47.6 mV) and PDI (from 0.2 to 0.4). These data suggested that the liposomes suspensions are characterized by optimal value of size, ζ potential and PDI and consequently they are good preparations to investigate their ability as drug delivery system.

| Liposomes | Size (nm) | PDI | ζ potential (mV) |
|---|---|---|---|
| Empty | 135.2 ± 9.45 | 0.23 ± 0.01 | − 27.4 ± 1.79 |
| Si34 | 151.3 ± 2.06 | 0.40 ± 0.04 | −41.9 ± 5.75 |
| Si306 | 105.1 ± 6.39 | 0.21 ± 0.01 | − 39.9 ± 0.55 |
| Si307 | 131.3 ± 5.14 | 0.21 ± 0.03 | − 28.8 ± 0.15 |
| Si323 | 232.4 ± 7.35 | 0.13 ± 0.01 | − 47.6 ± 0.38 |

**Table 2. Properties of liposomes determined by DLS.**

Moreover, fluorescent liposomes used for the internalization studies in cells, were visualized by confocal microscopy (Figure 8). Fluorescent liposomes before (A) and after filtration with a 0.2 µm filter (B) were analysed by confocal microscopy. Non-filtered fluorescent liposomes are well visualized because the confocal microscope resolution focuses structures with a diameter of few micrometers instead of nanometers dimension. Non-filtered fluorescent liposomes have large dimensions and can form structure with more lipid bilayer, such as MLV, indicated by the arrow. After filtration, liposomes reach a size below the micrometer. They are therefore too small to be displayed in focus with confocal microscope and therefore they appear as small dots (B).

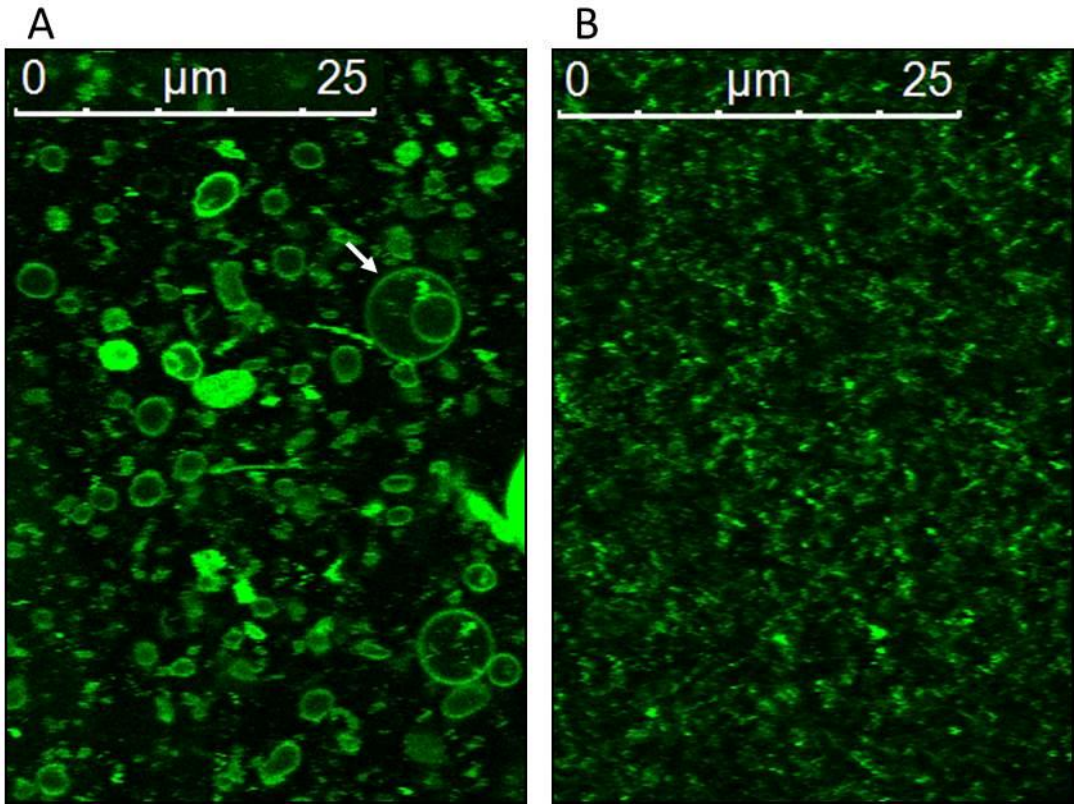


**Figure 8. Fluorescent liposomes before (A) and after filtration (B).**

### 4.4 Liposomes uptake in cancer cells

Neuroblastoma (SH-SY5Y) and Glioblastoma (U87) cells were incubated with non-fluorescent (blank) and fluorescent liposomes to evaluate their possible uptake. After 1, 4 and 8 hours of incubation in U87 cells and of 4h in SH-SY5Y cells, liposomes fluorescent signal was detected inside the cells by confocal microscopy. As shown in Figure 9 (U87) and Figure 10 (SH-SY5Y), liposomes are able to penetrate cells, fusing with the cellular membrane or through endocytosis. In this way, they can release their cargo into the cytoplasm. Liposomes with 300 µM of DOPE-NBD had a more intense signal compared to those with 100 µM of DOPE-NBD in U87 cells, but treatment for 8 hours resulted in the suffering of cells, which show an altered cell membrane. SH-SY5Y cells treated for 4 hours showed a weaker fluorescent signal than the U87, and Z-stack images showed the presence of liposomes (arrows) inside neuroblastoma cells. Blank liposomes showed no fluorescence in either type of cells, suggesting that fluorescence displayed inside cells is given exclusively by the NBD-DOPE when is present in liposomes.

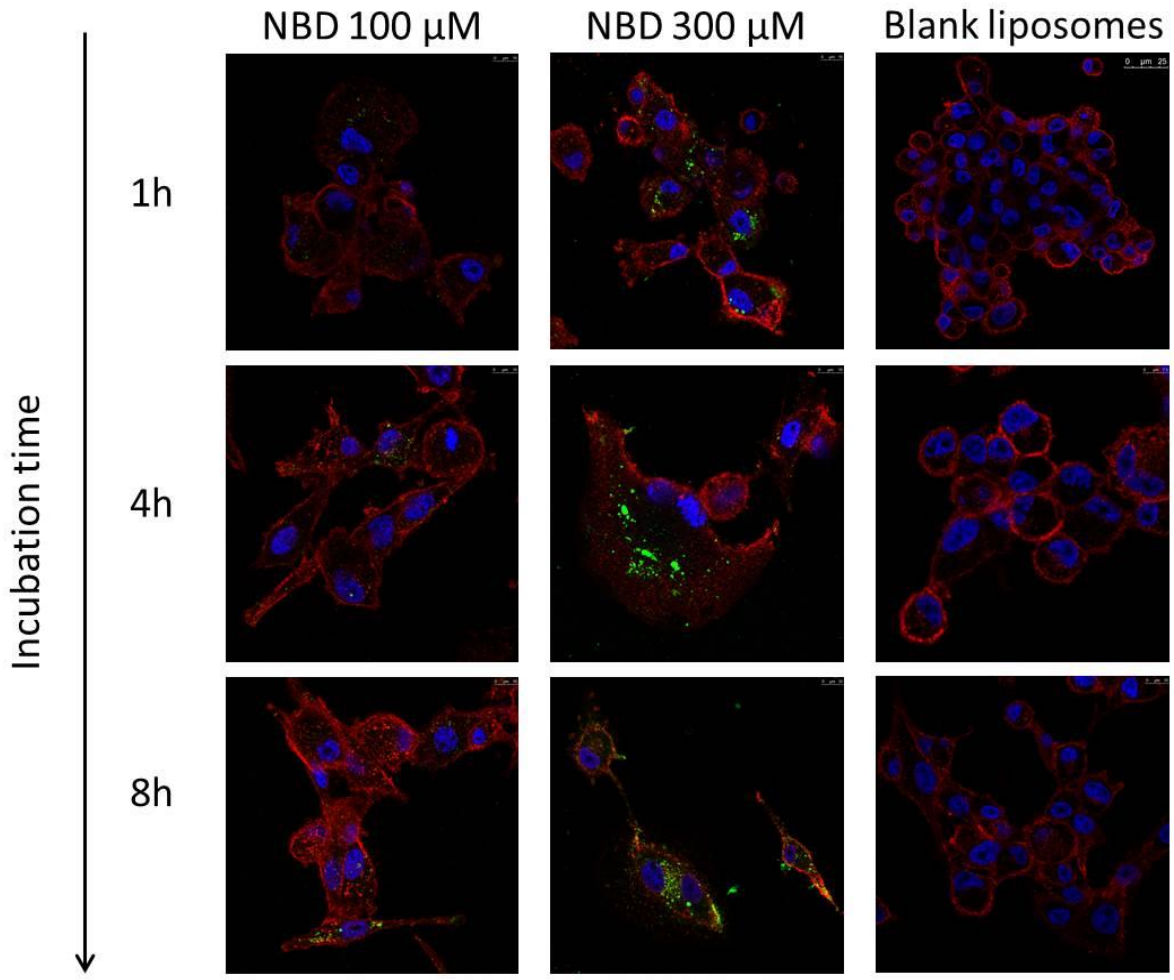


**Figure 9. Liposomes uptake in U87 cells. Fluorescent liposomes are visualized in green, cellular membranes in red and nuclei in blue.**

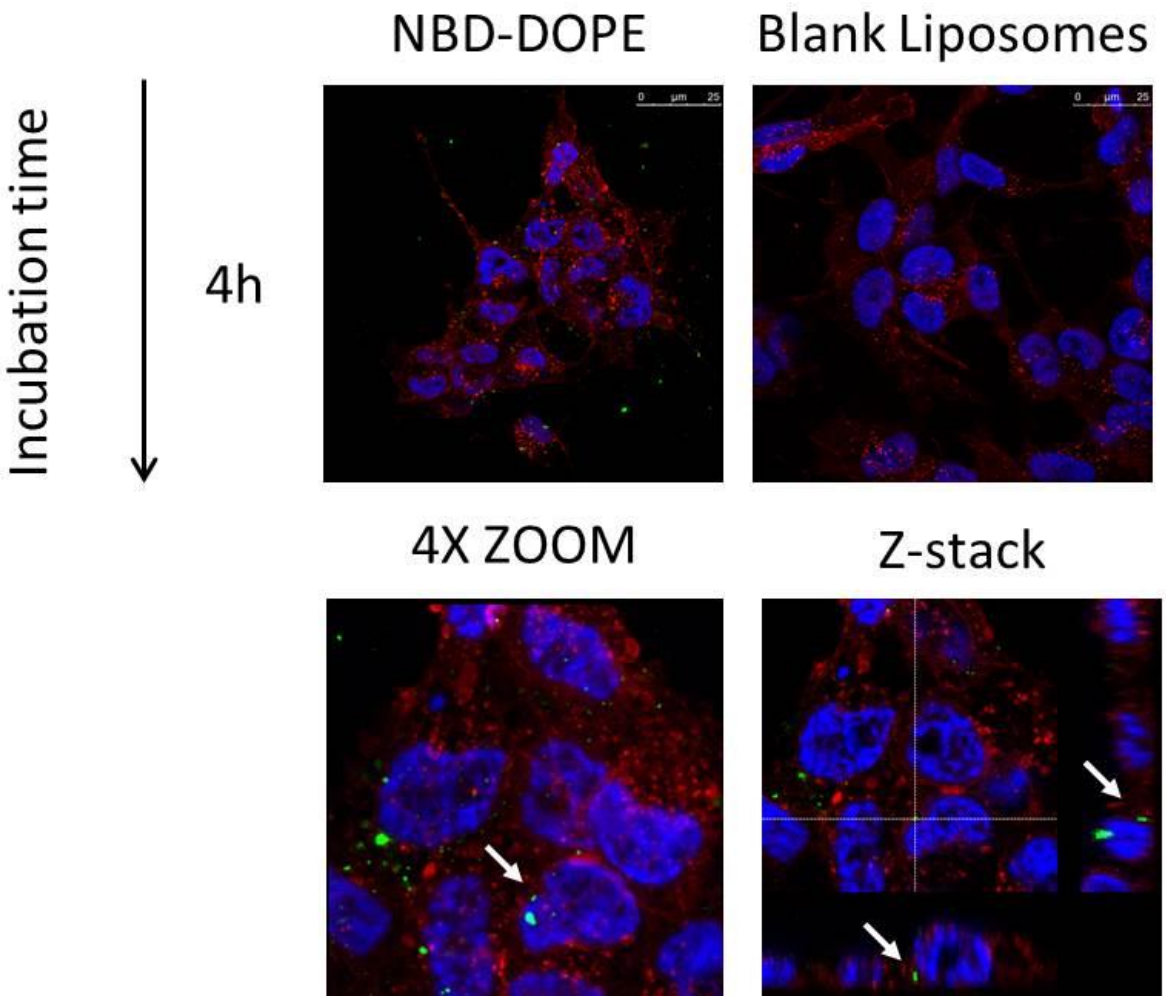


**Figure 10. Liposomes uptake in SH-SY5Y cells. Fluorescent liposomes are visualized in green, cellular membranes in red and nuclei in blue.**

### 4.5 *In vitro* release

To determine the stability of liposomes in physiological settings and to confirm the release of compounds from liposomal formulations, the release kinetics of Si306-loading liposomes was analysed *in vitro* by measuring the concentration of Si306 released from liposomes into a physiological medium (BSA 50 mg/mL) at 37°C (Figure 11). The cumulative percentage of Si306 release was determined over a 96 h-period. The percentage of Si306 released from Si306-loading liposomes resulted below 28% after 24 h and 49% over a 72 h-period. The final percentage of Si306 released was of 50.5%. In addition, the rate of Si306 release was evaluated during the 24 h (0.96 μg/h). These data demonstrated a good stability of liposomes in physiological conditions at 37°C which can thus reach the target site with high concentration of encapsulated compounds and perform their biological activity in cancer cells.

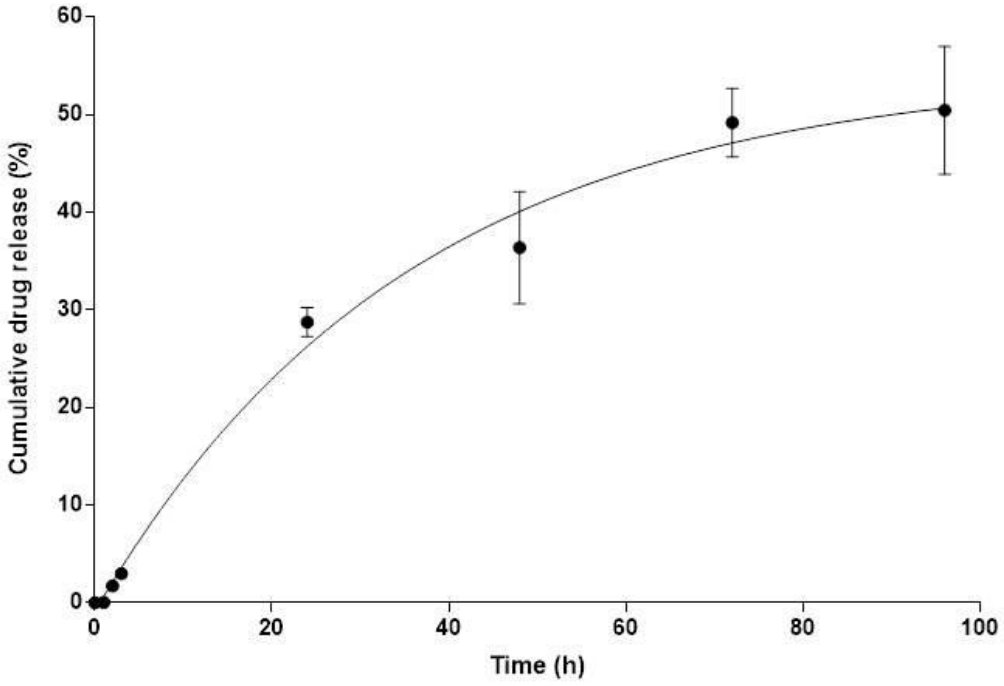


**Figure 11. *In vitro* release. Release of Si306 from Si306-loading liposomes in physiological conditions, with 50 mg/mL of BSA, at 37°C.**

### 4.6 Biodistribution

Biodistribution of Si306-loading liposomes and free Si306 were evaluated in male Sprague-Dawley rats. After 24 hours of treatment with the selected compounds, animals were sacrificed and blood and tissues were treated for the quantitative analysis. The concentration of Si306 was determined in the following tissues: plasma, brain, liver and adipose tissue (Figure 12). The concentration of the active compound was one order of magnitude higher in the plasma of rats treated with Si306-loading liposomes with respect to rats treated with free Si306 compound, validating the use of liposomes to enhance the plasma-exposure of a drug. In fact, the concentration of the free Si306 was 0.11 μg/mL and 2.05 μg/mL in groups of animals treated with Si306 and Si306-loading liposomes, respectively. The concentration of compound recovered in the brain was 0.05 μg/g (group treated with Si306) versus 0.39 μg/g (group treated with Si306-loading liposomes). The increase of Si306 quantity suggested an improved biodistribution of Si306 when liposomes are used as drug delivery systems. Furthermore, due to their lipid

composition, liposomes are easily caught by adipose tissue and for this reason a high concentration of Si306 from liposomes is found in this tissue.

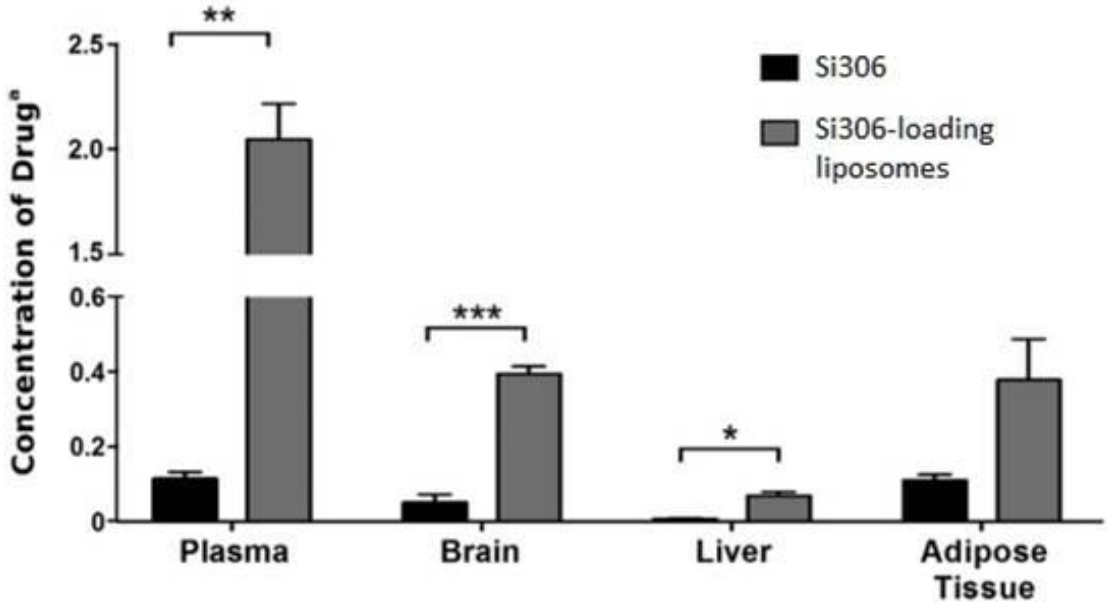


**Figure 12. Biodistribution of free Si306 and Si306-loading liposomes at 24 h. The concentration is expressed as µ g/mL for plasma and as µ g/g for brain, liver and adipose tissue.**

### 4.7 Cytotoxicity activity against U87 and SH-SY5Y cancer cell lines

The pyrazolo[3,4-*d*] pyrimidines family showed a good cytotoxicity profile against several cancer cell lines, as reported in literature (He H et al., 2011). Recently, remarkable results have been obtained in several mouse models of cancer. In order to evaluate the cytotoxic activity of selected compound, antiproliferative activity was detected by cellular assays.

The cytotoxicity of free Si306 and Si306-loading liposomes was evaluated in U87 cell line, while the cytotoxicity of free Si34, Si306, Si307, Si323 and respective liposomes formulation was evaluated in SH-SY5Y cell line. Compounds solubilized in DMSO and empty liposomes hydrated with 0.9% NaCl solution, pH=7.4, were analysed as controls. $IC_{50}$ of these compounds, using different treatment concentrations (0.1, 1.0, 10, 50 µM), were evaluated at 24, 48 and 72h. In SH-SY5Y (Figure 13) cells, a higher 24 h-activity was obtained for liposomal samples in comparison with the corresponding free drugs. The analysis of free Si307 and Si307-loading liposomes revealed a comparable cytotoxicity. Results collected after 48h of treatment showed no significant difference in

cytotoxicity between free Si307 and SI307-loading liposomes, while significant differences were detected between free Si323 and Si323-loading liposomes and free Si34 and Si34-loading liposomes. The antiproliferative activity at 72h was higher for Si34 and Si323 liposomal samples in comparison with the respective free drug. The analysis of free Si306 and Si306-loading liposomes and free Si307 and Si307-loading liposomes showed a comparable $IC_{50}$ value between each drug and the respective liposomal formulation. For U87, no differences in antiproliferative activity were found between the free Si306 and Si306 in liposomes (Figure 14). Probably the higher solubility in water compared to the other selected compounds promote the passage of the compound from the lipophilic portion of the cell membrane to the aqueous core of the cytoplasm encouraging the inhibition of c-Src. In fact, in both SH-SY5Y and U87 cell lines there is no high differences in the cytotoxicity activity between free Si306 and Si306-loading liposomes.

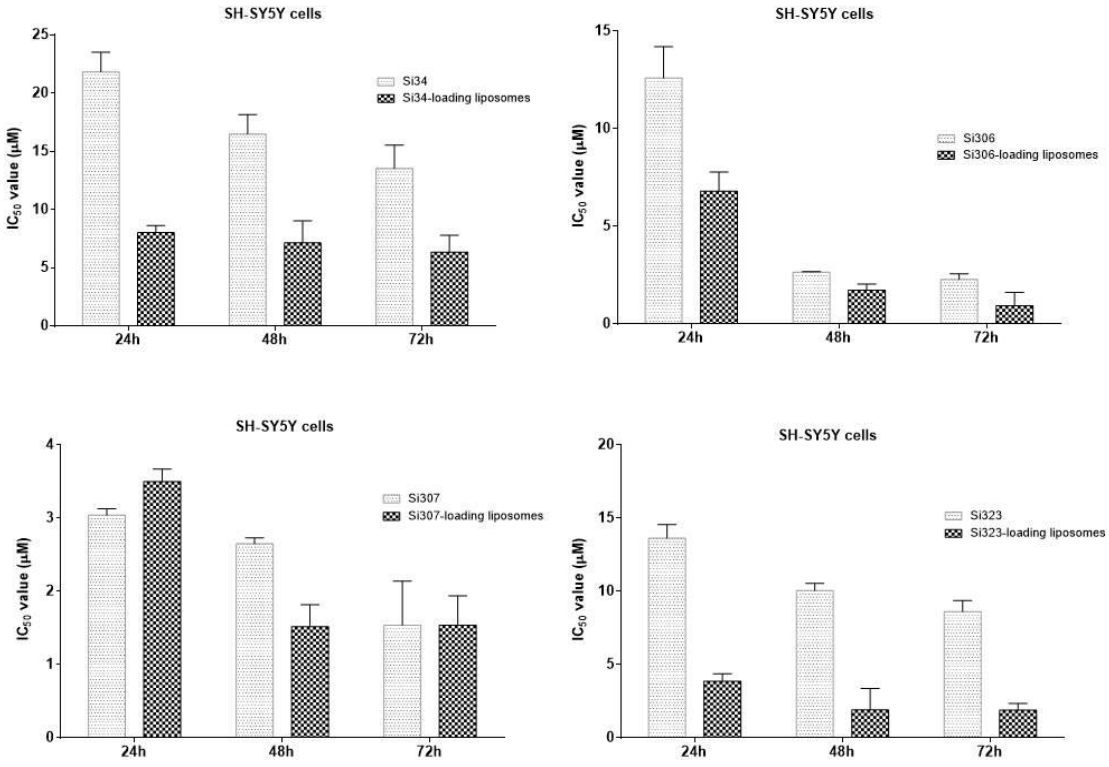


**Figure 13. $IC_{50}$ values after 24, 48 and 72h in SH-SY5Y cell line.**

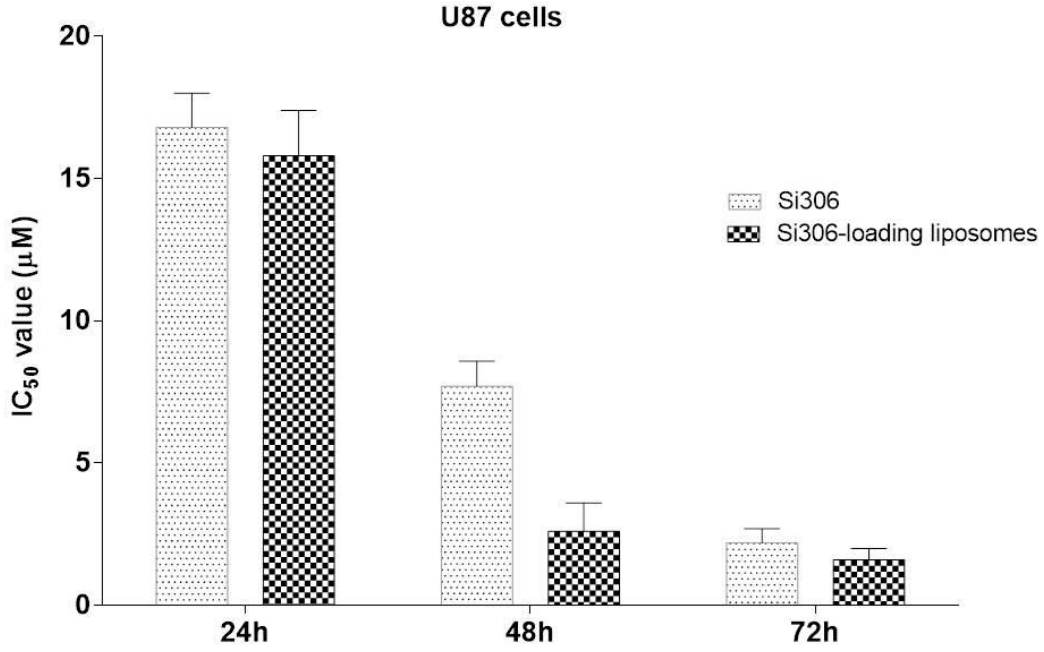


**Figure 14. $IC_{50}$ values after 24, 48 and 72h in U87 cell line.**

Finally, the cytotoxicity of blank liposomes was evaluated to understand whether the phospholipids can yield toxicity. SH-SY5Y and U87 were treated with the same amount of liposomes encapsulating compounds in the cytotoxicity tests and the $IC_{50}$ curves were evaluated.

Figure 15 show that empty liposomes have no toxic activity in both cell line and therefore that the cytotoxic action is performed by the molecules encapsulated in them which are released inside the cells where can inhibit c-Src.

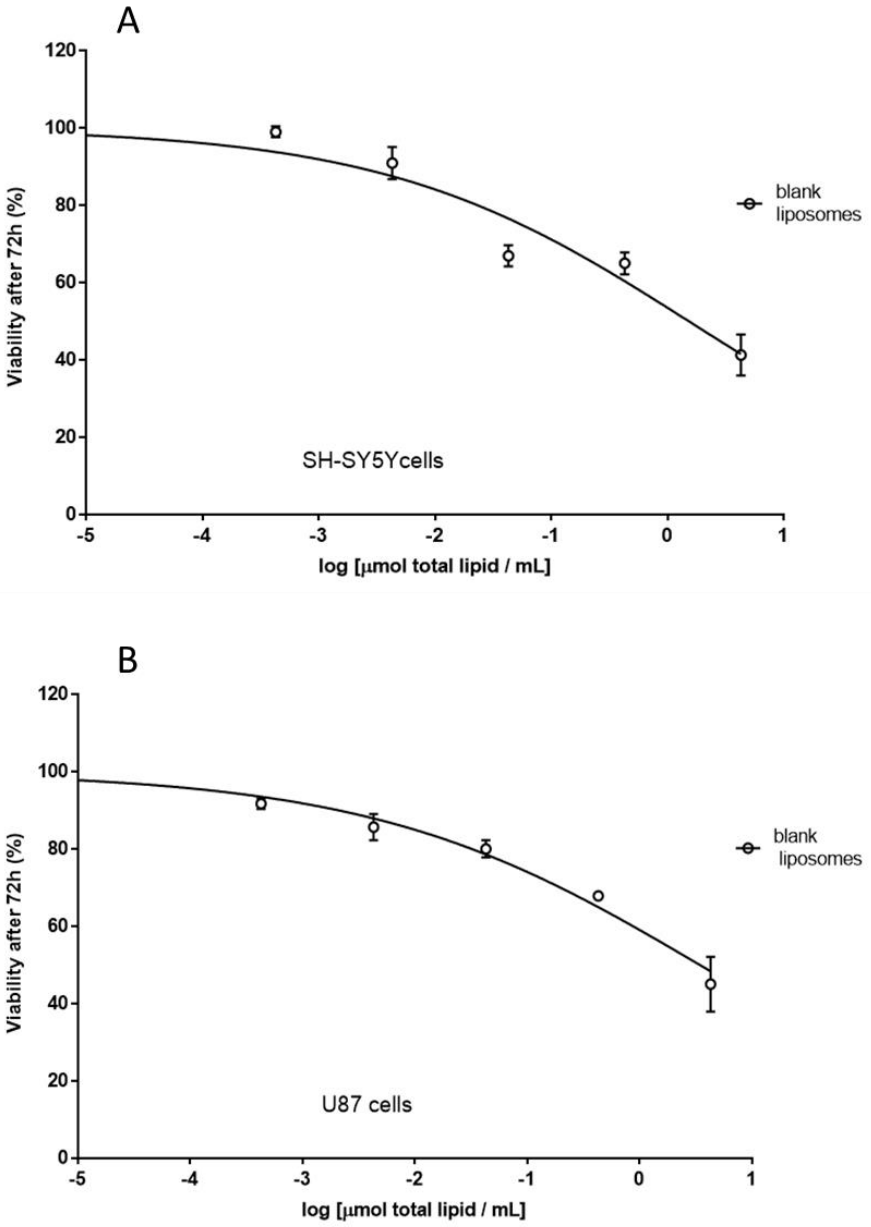


**Figure 15. Cytotoxicity of blank liposomes after incubation for 72h in SH-SY5Y (A) and U87 (B) cell line.**

## 5. Discussion

With the aim determining if the use of the liposomes could represent a possible strategy to improve pharmacokinetic properties of our compounds, a set of pyrazolo [3,4-*d*] pyrimidines, selected from our library of compounds, were encapsulate in these nanosystems. Pyrazolo [3,4-*d*] pyrimidines have demonstrated a high anticancer activity associated to the inhibition of tyrosine kinases c-Src and Bcr-Abl and we have recently demonstrated that pyrazolo [3,4-*d*] pyrimidines were able to reduce tumor growth in NB xenograft mouse model (Tintori C. et al., 2015). Compounds were selected on the base of previously reported data regarding activity and *in vitro* ADME properties (Tintori C. et al., 2015; Navarra M. et al., 2010; Radi M. et al., 2011). Nanoparticles were characterized by DLS regarding their size, polydispersity index and ζ potential. Particle size has a significant impact on the circulation time (Laverman P. et al., 1999). Furthermore, the dimensions of the smallest capillaries need to be considered to avoid a possible obstruction. Particle size also affects cellular uptake, influencing phagocytosis and endocytosis. In general, the larger is the nanoparticle, the faster is the clearance by the MPS. Optimal size to facilitate extravasation is about 150 nm or less, i.e. Doxil© has size between 80–100 nm and Myocet© is around 150 nm. In this context, this study demonstrated that our liposomes are suitable drug-delivery systems with a diameter that ranges from 105 nm to 232 nm. Another important feature for nanoparticle dispersion stability is the ζ potential that indicates the degree of electrostatic repulsion between particles. In detail, nanoparticles with ζ-potential values greater than + 25 mV or less than −25 mV typically have high degrees of stability (Gregoriadis G. et al., 1999). Showing a ζ potential value between −28.65 mV and −48.00 mV, our liposome systems were confirmed to be stable.

Liposomes demonstrated a greater 24 h activity then the corresponding free drug (comparable $IC_{50}$s of Si307 in liposomes and free Si307, represented the only exception). This difference in cytotoxicity might be related to different internalization processes. In fact, while the free drug can enter into cells by passive membrane transport, liposomes need to be taken up by different processes (i.e. endocytosis, fusion). At 48 h and 72 h, pairs Si306-loading liposomes / free Si306 and Si307-loading liposomes / free Si307 showed similar $IC_{50}$s. However, Si34-loading liposomes and Si323-loading liposomes demonstrated higher cytotoxicity than the respective free drug both, in 48 h and 72 h measurements.

Si306-loading liposomes resulted our most promising liposomal candidate because of the following reasons: (I) $IC_{50}$ value of $0.97\,\mu M$ against NB cells, (II) 99% of entrapment efficiency, (III) $\zeta$ potential value of $-39.9 \pm 0.55\,mV$ and (IV) size of $105.1 \pm 6.39\,nm$. Additionally, Si306 was the compound previously tested in NB xenograft mouse model (Tintori C. et al., 2015). Thus, Si306-loading liposomes was further characterized by cryo-EM, confirming the data obtained by DLS analysis. The sample was indeed characterized by a homogenous population of unilamellar liposomes with size around 100 nm. Furthermore, a confocal microscopy-based study was performed to elucidate whether the drug is released from liposomes outside the cells or inside the cytoplasm, after an internalization of the whole liposomal system. The analysis showed the presence of fluorescent liposomes into the cytoplasm of NB cells, suggesting a delivery of the free drug after cellular uptake of liposomes.

The release of Si306 from the liposomal system was evaluated with an *in vitro* assay that allowed the quantification of Si306 likely to be released from liposomes into physiological conditions. The resulting monophasic release curve was a typical feature of unilamellar liposomes, accordingly with DLS and cryo-EM results. A proof of concept in *in vivo* experiments was then performed to evaluate and compare the biodistribution of Si306 and Si306-loading liposomes in several tissues, at 24 h. Additionally, this study was important to determine the *in vivo* stability of our liposomal systems. Data showed a generally improved biodistribution - higher concentration - of the Si306 when liposomes were used as drug-delivery system. Considerably, when Si306-loading liposomes was administered a 20-fold increase in plasma-concentration of Si306 was observed. In addition, the quantity of Si306 recovered from the brain tissue after injection of Si306-loading was significantly higher than the concentration obtained after administration of free Si306.

In conclusion, this study validated the use of stealth liposomes to improve the biodistribution of pyrazolo [3,4-*d*] pyrimidines. Herein we demonstrate that liposomes retain the efficacy of our encapsulated drug against SH-SY5Y cells and that this cytotoxic activity is likely to be exerted by the release of the active compound in the cytoplasm after uptake of the nanoparticles. Importantly, the liposomal system resulted stable and able to release the encapsulated drug in physiological conditions. The biodistribution assay finally proved the beneficial properties of Si306-loading

liposomes. Further preclinical *in vivo* studies will allow the determination of the full pharmacokinetic profile and the therapeutic efficacy of this novel formulation.

## 6. References

Alexis F, Rhee JW, Richieb JP, Radovic-Moreno AF, Langer R, Farokhzad OC. New frontiers in nanotechnology for cancer treatment. 2008, *Urol Oncol* 26:74-85.

Alvarez RH, Kantarjian HM, Cortes JE. The role of Src in solid and hematologic malignancies: development of new-generation Src inhibitors. 2006, *Cancer* 107(8):1918-1929.

Angelucci A, Schenone S, Gravina GL, Muzi P, Festuccia C, Vicentini C, Botta M, Bologna M. Pyrazolo [3,4-*d*] pyrimidines c-Src inhibitors reduce epidermal growth factor-induced migration in prostate cancer cells. 2006, *Eur J Cancer* 42(16):2838-2845.

Antimisiaris SG, Kallinteri P, Fatouros DG. *Liposomes and drug delivery*. 2007, In Pharmaceutical manufacturing handbook (ed. S Cox Gad), pp. 443–533. Hoboken, NJ: John Wiley and Sons, Inc.

Bain J, McLauchlan H, Elliott M, Cohen P. The specificities of protein kinase inhibitors: an update. 2003, *Biochem J* 371:199-204.

Bajda M, Boryczka S, Wietrzyk J, Malawska B. Investigation of lipophilicity of anticancer active thioquinoline derivatives. 2007, *Biomed Chromatogr* 21:123-131.

Bangham AD, Standish MM, Watkins JC. Diffusion of univalent ions across the lamellae of swollen phospholipids. 1965, *J Mol Biol* 13:238-252.

Bawarski WE, Chidlowsky E, Bharali DJ, Mousa SA. Emerging nanopharmaceuticals. 2008, *Nanomedicine* 4:273-282.

Bharali DJ, Khalil M, Gurbuz M, Simone TM, Mousa SA. Nanoparticles and cancer therapy: a concise review with emphasis on dendrimers. 2009, *Int J Nanomedicine* 4:1-7.

Bjorge JD, Pang A, Fujita DJ. Identification of protein-tyrosine phosphatase 1B as the major tyrosine phosphatase activity capable of de-phosphorylating and activating c-Src in several human breast cancer cell lines. 2000, *J Biol Chem* 275:41439-41446.

Boggon TJ and Eck MJ. Structure and regulation of Src family kinases. 2004, *Oncogene* 23:7918-7927.

Bozzuto G and Molinari A. Liposomes as nanomedical devices. 2015, *Int J Nanomedicine* 10:975-999.

Brigger I, Dubernet C, Couvreur P. Nanoparticles in cancer therapy and diagnosis. 2002, *Adv Drug Deliv Rev* 54:631-651.

Brunner J, Skrabal P, Hauser H. Single bilayer vesicles prepared without sonication physicochemical properties. 1976, *Biochim Biophys Acta* 455:322–331.

Carraro F, Naldini A, Pucci A, Locatelli GA, Maga G, Schenone S, Bruno O, Ranise A, Bondavalli F, Brullo C, Fossa P, Menozzi G, Mosti L, Modugno M, Tintori C, Manetti F, Botta M. Pyrazolo [3,4-*d*] pyrimidines as potent antiproliferative and proapoptotic agents toward A431 and 8701-BC cells in culture via inhibition of c-Src phosphorylation. 2006, *J Med Chem* 49(5):1549-1561.

Carraro F, Pucci A, Naldini A, Schenone S, Bruno O, Ranise A, Bondavalli F, Brullo C, Fossa P, Menozzi G, Mosti L, Manetti F, Botta M. Pyrazolo [3,4-*d*] pyrimidines endowed with antiproliferative activity on ductal infiltrating carcinoma cells. 2004, *J Med Chem* 47(7):1595-1598.

Castilla LH, Couch FJ, Erdos MR, Hoskins KF, Calzone K, Garber JE, Boyd J, Lubin MB, Deshano ML, Brody LC, Collins FS, Weber BL. Mutations in the *BRCA1* gene in families with early-onset breast and ovarian cancer. 1994, *Nat Genet* 8(4):387-391.

Chong YP, Mulhern TD, Cheng HC. C-terminal Src kinase (CSK) and CSK-homologous kinase (CHK) endogenous negative regulators of Src-family protein kinases. 2005, *Growth Factors* 23:233-244.

Chu B and Lin FL. Laser light-scattering study of a ternary liquid-mixture—ethanol water chloroform. 1974, *J Chem Phys* 61:5132–5146.

Covelli I and Veneziani BM. *Principi di Patologia Generale, 5th edition*. 2000, Florio.

Creedon H and Brunton VG. Src kinase inhibitors: promising cancer therapeutics? 2012, *Crit Rev Oncog* 17(2):145–159.

Davis ME, Chen Z, Shin DM. Nanoparticle therapeutics: an emerging treatment modality for cancer. 2008, *Nat Rev Drug Discov* 7:771-782.

Deamer DW. Preparation and properties of ether-injection liposomes. 1978, *Ann NY Acad Sci* 308:250.

Dehm SM and Bonham K. SRC gene expression in human cancer: the role of transcriptional activation.2004, *Biochem Cell Biol* 82(2):263-274.

Dietel M and Sers C. Personalized medicine and development of targeted therapies: The upcoming challenge for diagnostic molecular pathology. A review. 2006, *Virchows Arch* 448(6):744-755.

Drummond DC, Meyer O, Hong K, Kirpotin DB, Papahadjopoulos D. Optimizing liposomes for delivery of chemotherapeutic agents to solid tumors. 1999, *Pharmacol Rev* 51(1):691-743.

Eibl H and Kaufmann-Kolle P. Medical application of synthetic phospholipids as liposomes and drugs. 1995, *J. Liposome Res* 5:131–148.

Fanciullino R and Ciccolini J. Liposome-encapsulated anticancer drugs: still waiting for the magic bullet? 2009, *Curr Med Chem* 16:4361–4373.

Finn RS. Targeting Src in breast cancer. 2008, *Annals of Oncology* 19:1379-1386.

Frolov VA, Shnyrova AV, Zimmerberg J. Lipid polymorphisms and membrane shape. 2011, *Cold Spring Harb Perspect Biol* 3: a004747.

Gabizon A, Shmeeda H, Barenholz Y. Pharmacokinetics of pegylated liposomal Doxorubicin: review of animal and human studies. 2003, *Clin Pharmacokinet* 42(5):419-436.

Ganta S, Devalapally H, Shahiwala A, Amiji M. A review of stimuli responsive nanocarriers for drug and gene delivery. 2008, *J Control Release* 126(3):187-204.

Geahlen RL, Handley MD, Harrison ML. Molecular interdiction of Src-family kinase signaling in hematopoietic cells. 2004, *Oncogene* 23:8024-8032.

Gerber DE. Targeted therapies: a new generation of cancer treatments. 2008, *Am Fam Physician* 77(3):311-319.

Goren D, Horowitz AT, Tzemach D, Tarshish M, Zalipsky S, Gabizon A.Nuclear delivery of doxorubicin via folate-targeted liposomes with bypass of multidrug-resistance efflux pump. 2000, *Clin Cancer Res* 6(5):1949-1957.

Gullotti E and Yeo Y. Extracellularly activated nanocarriers: a new paradigm of tumor targeted drug delivery. 2009, *Mol Pharm* 6(4):1041-1051.

Hanke JH, Gardner JP, Dow RL, Changelian PS, Brissette WH, Weringer EJ, Pollock BA, Connelly PA. Discovery of a novel, potent, and Src family selective tyrosine kinase inhibitor. Study of Lck and Fyn T-dependent cell activation. 1996, *J Biol Chem* 271:695-701.

He H, Zhao J, Jia R, Zhao Y, Yang S, Yu L and Yang L. Novel Pyrazolo[3,4-d]pyrimidine Derivatives as Potential Antitumor Agents: Exploratory Synthesis, Preliminary Structure-Activity Relationships, and in Vitro Biological Evaluation. 2011, *Molecules* 16:10685-10694.

Hobbs SK, Monsky WL, Yuan F, Roberts WG, Griffith L, Torchilin VP, Jain RK. Regulation of transport pathways in tumor vessels: role of tumor type and microenvironment. 1998, *Proc Natl Acad Sci USA* 95:4607-4612.

Hofheinz RD, Gnad-Vogt SU, Beyer U, Hochhaus A. Liposomal encapsulated anti-cancer drugs. 2005, *Anticancer Drugs* 16:691–707.

Irby RB and Yeatman TJ. Role of Src expression and activation in human cancer. 2000, *Oncogene* 19:5636-5642.

Israelachvili J, Marcelja S, Horn R. Physical principles of membrane organization. 1980, *Rev Biophys* 13:121.

Jin Y, Ren X, Wang W, Ke L, Ning E, Du L, Bradshaw J. A 5-fluorouracil-loaded pH-responsive dendrimer nanocarrier for tumor targeting. 2011, *Int J Pharm* 420(2):378-384.

Johnston MJ, Semple SC, Klimuk SK, Ansell S, Maurer N, Cullis PR. Characterization of the drug retention and pharmacokinetic properties of liposomal nanoparticles containing dihydrosphingomyelin. 2007, *Biochim Biophys Acta* 1768:1121–1127.

Kaplan KB, Bibbins KB, Swedlow JR, Arnaud M, Morgan DO, Varmus HE. Association of the amino-terminal half of c-Src with focal adhesions alters their properties and its regulated by phosphorylation of tyrosine 527. 1994, *EMBO J* 13:4745-4756.

Kerns EH and Di L. *Drug-like Properties: Concepts, Structure Design and Methods: from ADME to Toxicity Optimization*. 2008, Elsevier Inc.

Kim B, Han G, Toley BJ, Kim CK, Rotello VM, Forbes NS. Tuning payload delivery in tumour cylindroids using gold nanoparticles. 2010, *Nat Nanotechnol* 5(6):465-472.

Kim KY. Nanotechnology platforms and physiological challenges for cancer therapeutics. 2007, *Nanomedicine* 3:103-110.

Klein, CA. Parallel progression of primary tumours and metastases. 2009, *Nat Rev Cancer* 9(4):302-312.

Kmiecik TE and Shalloway D. Activation and suppression of pp60 c-src transforming ability by mutation of its primary sites of tyrosine phosphorylation. 1987, *Cell* 49:65-73.

Kumar A, Wang Y, Lin X, Sun G, Parang K. Synthesis and evaluation of 3-phenylpyrazolo [3,4-*d*] pyrimidine-peptide conjugates as Src kinase inhibitors. 2007, *Chem Med Chem* 2(9):1346-1360.

Kumar V, Abbas AK, Aster J. *Robbins Basic Pathology, 8th edition*. 2007, Saunders/Elsevier.

Kwiatkowska K, Frey J, Sobota A. Phosphorylation of Fc gammaRIIA is required for the receptor-induced actin rearrangement and capping: the role of membrane rafts. 2003, *J Cell Sci* 116:537-550.

Laouini A, Jaafar-Maalej C, Limayem-Blouza I, Sfar S, Charcosset C, Fessi H. Preparation, Characterization and Applications of Liposomes: State of the Art. 2012, *Journal of Colloid Science and Biotechnology* 1:147–168.

Lasic DD and Papahadjopoulos D. Liposomes revisited. 1995, *Science* 276(5202):1275-1276.

Lasic DD. Novel applications of liposomes. 1998, *Trends Biotechnol* 16(7):301-321.

Lawrence DS. Signaling protein inhibitors via the combinatorial modification of peptide scaffolds. 2005, *Biochim Biophys Acta* 1754:50-57.

Li SD and Huang L. Pharmacokinetics and Biodistribution of Nanoparticles. 2008, *Mol Pharm* 5(4):496-504.

Liang X, Lu Y, Wilkes M, Neubert TA, Resh MD. The N-terminal SH4 region of the Src family kinase Fyn is modified by methylation and heterogeneous fatty acylation:

role in membrane targeting, cell adhesion and spreading. 2004, *J Biol Chem* 279:8133-8139.

Liu Y, Bishop A, Witucki L, Kraybill B, Shimizu E, Tsien J, Ubersax J, Blethrow J, Morgan DO, Shokat KM. Structural basis for selective inhibition of Src family kinases by PP1. 1999, *Chem Biol* 6(9):671-678.

Ma P, Dong X, Swadley CL, Gupte A, Leggas M, Ledebur HC, Mumper RJ. Development of Idarubicin and Doxorubicin Solid Lipid Nanoparticles to overcome Pgp–mediated Multiple Drug Resistance in Leukemia. 2009, *J Biomed Nanotechnol* 5(2):151-161.

Maeda H. The enhanced permeability and retention (EPR) effect in tumor vasculature: the key role of tumor-selective macromolecular. 2001, *Advan Enzyme Regul* 41:189-207.

Malinowsky K, Wolff C, Gundisch S, Berg D, Becker K. Targeted therapies in cancer - challenges and chances offered by newly developed techniques for protein analysis in clinical tissues. 2010, *J Cancer* 2:26-35.

Manetti F, Santucci A, Locatelli GA, Maga G, Spreafico A, Serchi T, Orlandini M, Bernardini G, Caradonna NP, Spallarossa A, Brullo C, Schenone S, Bruno O, Ranise A, Bondavalli F, Hoffmann O, Bologna M, Angelucci A, Botta M. Identification of a novel pyrazolo [3,4-*d*] pyrimidine able to inhibit cell proliferation of a human osteogenic sarcoma in vitro and in a xenograft model in mice. 2007, *J Med Chem* 50(23):5579-5588.

Maria Laura I, Franco D, Cattel L. Stealth liposomes: review of the basic science, rationale, and clinical applications, existing and potential. 2006, *Int J Nanomedicine* 1(3):297–315.

Matsunaga T, Shirasawa H, Tanabe M, Ohnuma N, Kawamura K, Etoh, T, Takahashi H, Simizu B. Expression of neuronal Src mRNA as a favorable marker and inverse

correlation to N-myc gene amplification in human neuroblastomas. 1994, *Int J Cancer* 58:793-798.

Matsunaga T, Shirasawa H, Tanabe M, Ohnuma N, Takahashi H, Simizu B. Expression of alternatively spliced src messenger RNAs related to neuronal differentiation in human neuroblastomas. 1993, *Cancer Res* 53:3179-3185.

Miller WT. Determinants of Substrate Recognition in Nonreceptor Tyrosine Kinases.2003, *Acc Chem Res* 36:393-400.

Mills JK and Needham D. The Materials Engineering of Temperature-Sensitive Liposomes. 2004, *Methods in Enzymology* 387:82-113.

Minko T, Pakunlu RI, Wang Y, Khandare JJ, Saad M. New Generation of Liposomal Drugs for Cancer. 2006, *Anticancer Agents Med Chem* 6:537-552.

Moghassemi S and Hadjizadeh A. Nano-niosomes as nanoscale drug delivery systems: An illustrated review. 2014, *Journal of Controlled Release* 185:22-36.

Moghimi SM and Szebeni J. Stealth liposomes and long circulating nanoparticles: critical issues in pharmacokinetics, opsonization and protein-binding properties. 2003, *Progress in Lipid Research* 42:463-78.

Monteiro N, Martins A, Reis RL, Neves NM. Liposomes in tissue engineering and regenerative medicine. 2014, *J R Soc Interface* 11:20140459.

Navarra M, Celano M, Maiuolo J, Schenone S, Botta M, Angelucci A, Bramanti P, Russo D. Antiproliferative and pro-apoptotic effects afforded by novel Src-kinase inhibitors in human neuroblastoma cells. 2010, *BMC Cancer* 10:602.

Newton HB. Advances in strategies to improve drug delivery to brain tumors. 2006, *Expert Rev Neurother* 6(10):1495-1509.

Noble GT, Stefanick JF, Ashley JD, Kiziltepe T, Bilgicer B. Ligand-targeted liposome design: challenges and fundamental considerations. 2014, *Trends in Biotechnology* 32(1):32–45.

Ogawara K, Un K, Tanaka K, Higaki K, Kimura T.In vivo anti-tumor effect of PEG liposomal doxorubicin (DOX) in DOX-resistant tumor-bearing mice: Involvement of cytotoxic effect on vascular endothelial cells. 2009, *Journal of Controlled Release* 133:4-10.

Omri A, Suntres ZE, Shek PN. Enhanced activity of liposomal polymyxin B against Pseudomonas aeruginosa in a rat model of lung infection. 2002, *Biochem Pharmacol* 64:1407–1413.

Papahadjopoulos D and Kimelberg HK. Phospholipid vesicles (liposomes) as models for biological membranes: their properties and interactions with cholesterol and proteins. 1974, *Progress in Surface Science* 1973:141–149.

Park JW, Benz CC, Martin FJ. Future directions of liposome- and immunoliposome-based cancer therapeutics. 2004, *Seminars in Oncology* 31:196-205.

Parsons SJ and Parsons JT. Src family kinases, key regulators of signal transduction. 2004, *Oncogene* 23:7906-7909.

Peer D, Karp JM, Seungpyo H, Farokhzad OC, Margalit R, Langer R. Nanocarriers as an emerging platform for cancer therapy. 2007, *Nat Nanotechnol* 2(12):751-760.

Poole AW and Jones ML. A SHPing tale: perspectives on the regulation of SHP-1 and SHP-2 tyrosine phosphatases by the C-terminal tail. 2005, *Cell Signal* 17:1323-1332.

Radi M, Brullo C, Crespan E, Tintori C, Musumeci F, Biava M, Schenone S, Dreassi E, Zamperini C, Maga G, Pagano D, Angelucci A, Bologna M, Botta M. Identification of potent c-Src inhibitors strongly affecting the proliferation of human neuroblastoma cells. 2011, *Bio Med Chem Lett 21:*5928-5933.

Rangel L. *Cancer Treatment - Conventional and Innovative Approaches*. 2013, InTech.

Remauta K, Lucasa B, Braeckmansa K, Demeestera J, De Smedt SC. Pegylation of liposomes favours the endosomal degradation of the delivered phosphodiester oligonucleotides. 2007, *J Control Release* 117(2):256-266.

Reynolds AB, Kanner SB, Bouton AH, Shaller MD, Wed SA, Flynn DC, Parsons JT. SRChing for the substrates of Src. 2014, *Oncogene* 33:4537-4547.

Roskoski R. Src kinase regulation by phosphorylation and dephosphorylation. 2005, *Biochem Biophys Res Comm* 331:1-14.

Roskoski RJ. Src protein tyrosine kinase structure and regulation. 2004, *Biochem Biophys Res Comm* 324:1155-1164.

Ruozi B, Belletti D, Tombesi A, Tosi G, Bondioli L, Forni F, Vandelli MA. AFM, ESEM, TEM, and CLSM in liposomal characterization: a comparative study. 2011, *Int J Nanomed* 6:557–563.

Sapra P and Allen TM. Internalizing antibodies are necessary for improved therapeutic efficacy of antibody-targeted liposomal drugs. 2002, *Cancer Res* 62(24):7190-7194.

Schiffelers RM, Storm G, Bakker-Woudenberg IA. Host factors influencing the preferential localization of sterically stabilized liposomes in Klebsiella pneumoniae-infected rat lung tissue.2001, *Pharm Res* 18:780–787.

Schindler T, Sicheri F, Pico A, Gazit A, Levitzki A, Kuriyan J. Crystal structure of Hck in complex with a Src family selective tyrosine kinase inhibitor. 1999, *Mol Cell* 3:639-648.

Schornack PA and Gillies RJ. Contributions of cell metabolism and H+ diffusion to the acidic pH of tumors. 2003, *Neoplasia* 5(2):135-145.

Sen B and Johnson FM. Regulation of Src Family Kinases in Human Cancers. 2011, *J Signal Transduc* 2011:865819.
Sicheri F, Moarefi I, Kuriyan J. Crystal structure of the Src family tyrosine kinase Hck. 1997, *Nature* 385:602-609.

Sigal CT, Zhou W, Buser CA, McLaughlin S, Resh MD. Amino-terminal basic residues of Src mediate membrane binding through electrostatic interaction with acidic phospholipids. 1994, *Proc Natl Acad Sci U.S.A.* 91:12253-12257.

Smallbonea K, Gavaghanb DJ, Gatenbyc RA,Maini PK. The role of acidity in solid tumour growth and invasion. 2005, *J Theor Biol* 235:476-484.

Smith DA, Jones BC, Walker DK. Design of drugs involving the concepts and theories of drug metabolism and pharmacokinetics. 1996, *Med Res Rev* 16:243-266.

Spandidos DA, Anderson ML. Oncogenes and onco-suppressor genes: their involvement in cancer. 1989, *J Pathol* 157(1):1-10.

Stano P, Bufali S, Pisano C, Bucci F, Barbarino M, Santaniello M, Carminati P, Luisi PL. Novel camptothecin analogue (gimatecan)-containing liposomes prepared by the ethanol injection method. 2004, *J Liposome Res* 14:87–109.

Stehelin D, Fujita DJ, Padgett T, Varmus HE, Bishop JM. Detection and enumeration of transformation-defective strains of avian sarcoma virus with molecular hybridization. 1977, *Virology* 76(2):675-684.

Surendiran A, Sandhiya S, Pradhan SC, Adithan C. Novel applications of nanotechnology in medicine. 2009, *Indian J Med Res* 130:689-701.

Suri SS, Fenniri H, Singh B. Nanotechnology-based drug delivery systems. 2007, *J Occup Med Toxicol* 2:16.

Szakács G, Paterson JK, Ludwig JA, Booth-Genthe C, Gottesman MM. Targeting multidrug resistance in cancer. 2006, *Nat Rev Drug Discov* 5:219-234.

Szoka F and Papahadjopoulos D. Comparative properties and methods of preparation of lipid vesicles (liposomes). 1980, *Annu Rev Biophys Bioeng* 9:467–508.
Tarbit MH and Berman J. High-throughput approaches for evaluating absorption, distribution, metabolism and excretion properties of lead compounds. 1998, *Curr Opin Chem Biol* 2:411-416.

Tatton L, Morley GM, Chopra R, Khwaja A. The Src-selective kinase inhibitor PP1 also inhibits Kit and Bcr-Abl tyrosine kinases. 2003, *J Biol Chem* 278(7):4847-4853.

Tejera-Garcia R, Ranjan S, Zamotin V, Sood R, and Kinnunen PKJ. Making Unilamellar Liposomes Using Focused Ultrasound. 2011, *Langmuir* 27(16):10088–10097.

Tihanyi K and Vastag M. *Solubility, Delivery and ADME Problems of Drugs and Drug-Candidates*. 2011, Bentham Science Publishers.

Vemuri S and Rhodes CT. Preparation and characterization of liposomes as therapeutic delivery systems: a review. 1995, *Pharm Acta Helv* 70:95–111.

Wang D, Esselman WJ, Cole PA. Substrate conformational restriction and CD45-catalyzed dephosphorylation of tail tyrosine phosphorylated Src protein. 2002, *J Biol Chem* 277:40428-40433.

Williams NK, Lucet IS, Klinken SP, Ingley E, Rossjohn J. Crystal structures of the Lyn protein tyrosine kinase domain in its Apo- and inhibitor-bound state. 2009, *J Biol Chem* 284(1):284-291.

Xu W, Harrison SC, Eck MJ. Three-dimensional structure of the tyrosine kinase c-Src. 1997, *Nature* 385:595-602.

Yan E, Barnes TJ, Fornasiero D, Prestidge CA. The encapsulation and release of guanosine from PEGylated liposomes. 2009, *J Liposome Res* 19(1):29-36.

Zhang S and Yu D. Targeting Src family kinases in anti-cancer therapies: turning promise into triumph. 2012, *Trends Pharmacol Sci* 33(3):122-128.

Zhu X, Kim JL, Newcomb JR, Rose PE, Stover DR, Toledo LM, Zhao H, Morgenstern KA. Structural analysis of the lymphocyte-specific kinase Lck in complex with non-selective and Src family selective kinase inhibitors. 1999, *Struct Fold Des* 7:651-661.

Zumbuehl O, Weder HG. Liposomes of controllable size in the range of 40 to 180 nm by defined dialysis of lipid/detergent mixed micelles. 1981, *Biochim Biophys Acta* 640:252.

# Chapter 2

## Functionalization of stealth liposomes encapsulating pyrazolo [3,4-*d*] pyrimidine to target tumor areas overexpressing plasmin.

## 1. Introduction

Tumors manifest as an uncontrolled proliferation of a tissue as result of mutations in the genomic sequences that control cell growth. The biochemical alterations that result can confer to cells the ability to degrade the constituents of the cellular basal lamina (collagen, proteoglycans and glycosaminoglycan) to avoid the control of the immune system and to ignore the contact signals with surrounding tissue cells. In these circumstances occur the characteristics of invasiveness into surrounding tissues and spread far from the site of origin, which outline the tumor malignancy. Cancer cells can invade other districts degrading the cellular basal lamina, primarily by proteases, enzymes deputed to protein catabolism as well as the disintegration of cell membranes. Proteases are produced by cancer cells and can promote cancer cell invasion and intravasation in several ways. Proteases can cleave cell adhesion molecules, leading to the disruption of cell contacts. Next, degradation or turnover of proteins in the extracellular matrix (ECM) facilitate invasion of cells into surrounding tissue and vasculature. All these steps require complex interactions between cancer and host cells. The ECM, as a part of the tumor microenvironment, plays an important role in cell adhesion, proliferation, and motility. The degradation of the ECM within the tumor stroma by proteases results in the disaggregation of stromal barriers basal lamina facilitating tumor cell movements (Figure 1) (Kleinman HK et al., 2001; Rao JS, 2003). A correlation between the aggressiveness of tumor and the secretion of proteases from tumor cells was reported in several studies (DeClerck YA et al., 2004). In addition, some tumor cells can induce the expression of proteolytic enzymes in the neighbouring non-malignant cells, diverting their activity to invade tissue (Zucker S et al., 2000). During all steps of tumorigenesis, from initiation to progression and metastasis, five classes of proteases have been reported to be involved: serine, cysteine, aspartic, threonine and metalloproteases (Koblinski JE et al., 2000). One of the best-studied serine proteases involved in cancer cells progression is plasmin (PLA). PLA is the final product of the plasminogen (PLG) activation system.

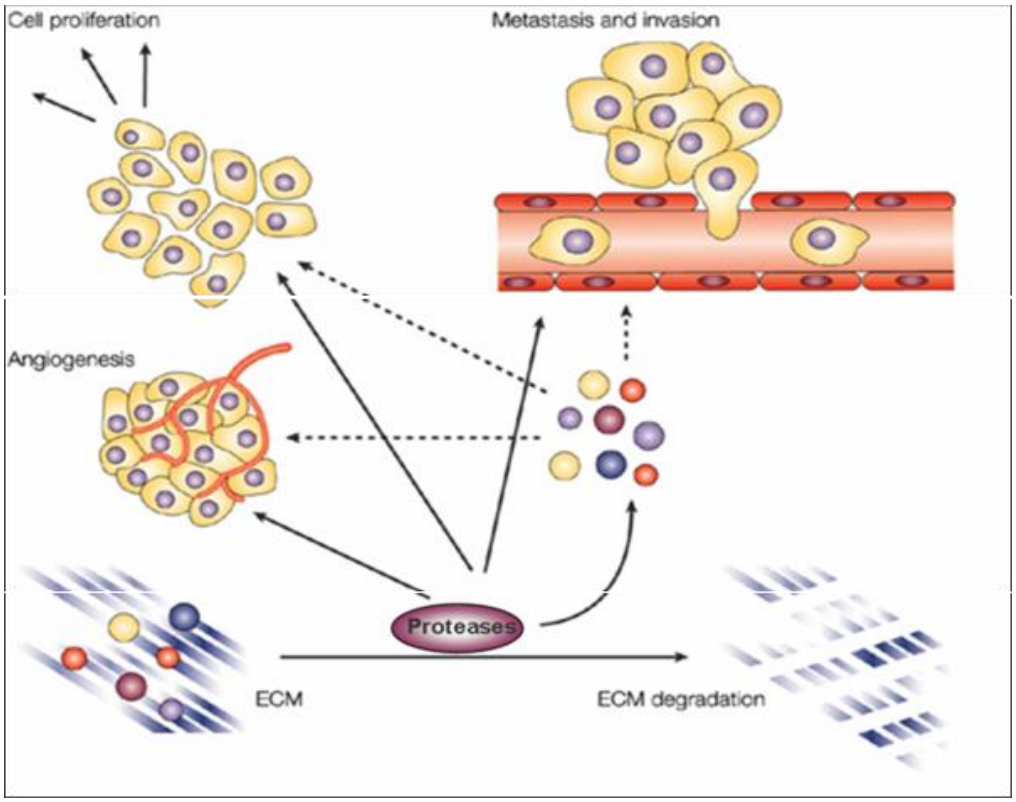


**Figure 1. The role of proteases in cancer progression** (modified from Rao JS, 2003).

### 1.1 Plasminogen/plasmin activation system components

Plasminogen/plasmin (PLG/PLA) activation system plays an important role in numerous biological and pathological events. In addition to its function in fibrinolysis (Nicoloso G et al., 1988), PLG/PLA system is involved in processes such as tissue remodelling (Collen D et al., 2001), ovulation (Ogiwara K et al., 2012), embryogenesis (Papanikolaou T et al., 2008), angiogenesis (Pepper MS, 2001) and tumor invasion (Kwaan HC and McMahon B, 2009). PLG is the precursor of PLA, mainly found in the human circulation and in association to the ECM (Li WY et al., 2003). PLA is the final product of the PLG activation system, which involves a precursor, cellular receptors and PLG activators (Figure 2) (Didiasova M et al., 2014).

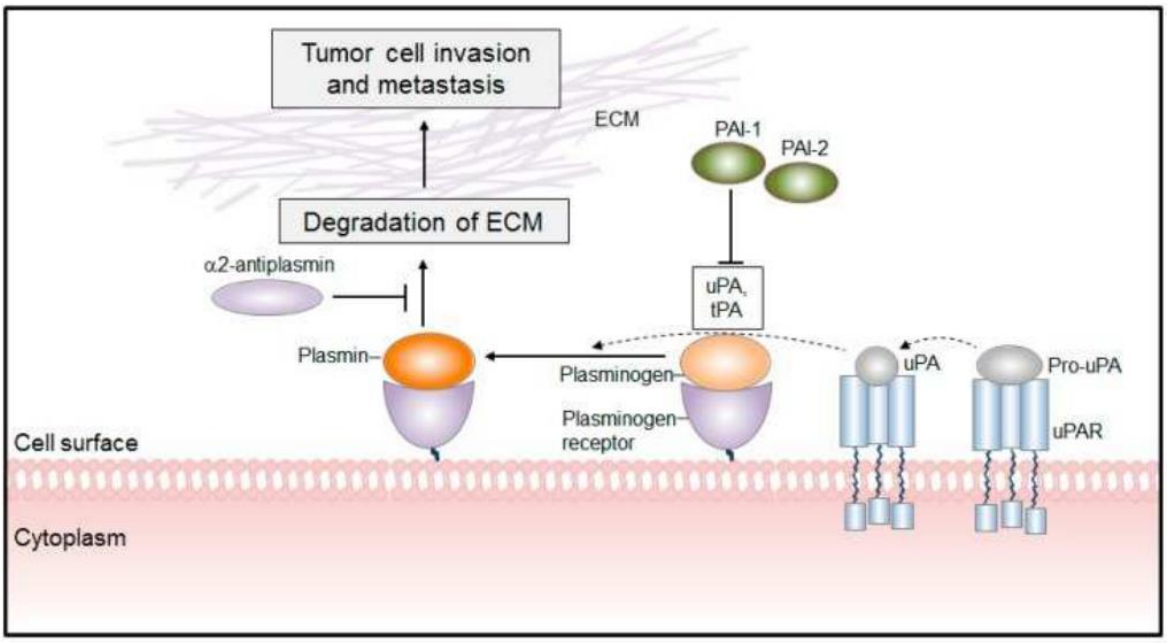


**Figure 2. PLG/PLA system components in tumor cell invasion (Didiasova et al., 2014).**

The zymogen PLG is mainly produced by the liver and is present in the plasma as well as in extravascular interstitial fluids. Plasma concentration of the plasminogen is about 100-150 mg/L and the half-life in circulation is about 2.8 days (Collen D et al., 1972). PLG is secreted as a 93 kDa single chain glycoprotein by the liver and circulates in blood in an activation-resistant form (Sinniger V et al., 1999). The glycoprotein contains an N-terminal peptide (NTP), five similar kringle domains (K1-K5) and the domain with protease activity (PD) (Figure 3).

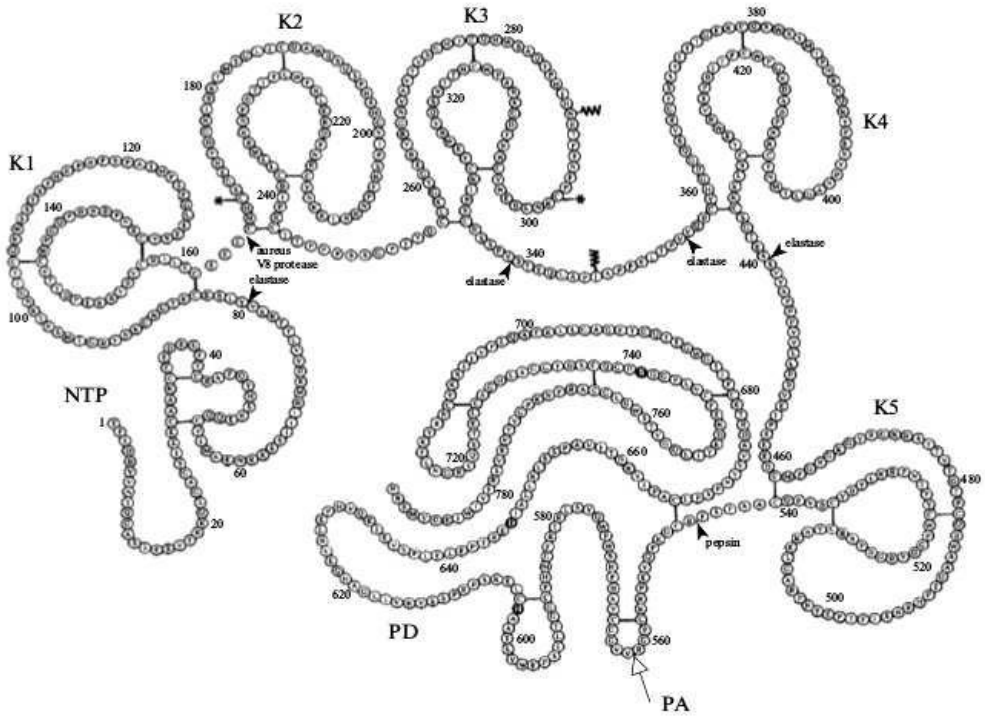


**Figure 3. Plasminogen structure.** PD: protease domain (Val562-Asn791); K1-K5: kringle domains; NTP: N-terminal peptide; ⋀⋁: glycosylation site; PA: cleavage site by activators.

The binding of PLG to the cellular receptors alters the conformation of PLG and enables its activation. Receptor bound PLG is subsequently cleaved by the urokinase plasminogen activator (uPA) or the tissue plasminogen activator (tPA) to PLA (Robbins KC et al., 1967). Even though both uPA and tPA share a common plasminogen converting function they have structural and functional differences. uPA acts as a fibrin-independent activation enzyme and controls pericellular proteolysis, while tPA mainly acts as a fibrin-dependent and intravascular activation enzyme involved in clot dissolution (Andreasen PA et al., 1997). Active PLA remains associated to the cell surface, where it is protected from inhibitors. Although PLG binding to the cell surface is necessary for PLA production, the presence of PLG activators is critical for successful PLG activation (Stillfried GE et al., 2007). PLG is activated in the two-chain proteolytically active plasmin by tPA or uPA by the cleavage of the single peptide bond between $Arg^{560}$ and $Val^{561}$ (Robbins KC et al., 1967). The heavy (A) chain (60 kDa) and the light (B) chain (25 kDa) are held together by two disulphide bonds (Figure 4). The light chain contains the serine protease catalytic triad, while the heavy chain contains

five kringle domains and mediates the interactions of plasminogen with fibrinogen, inhibitors and cell-surface receptors.

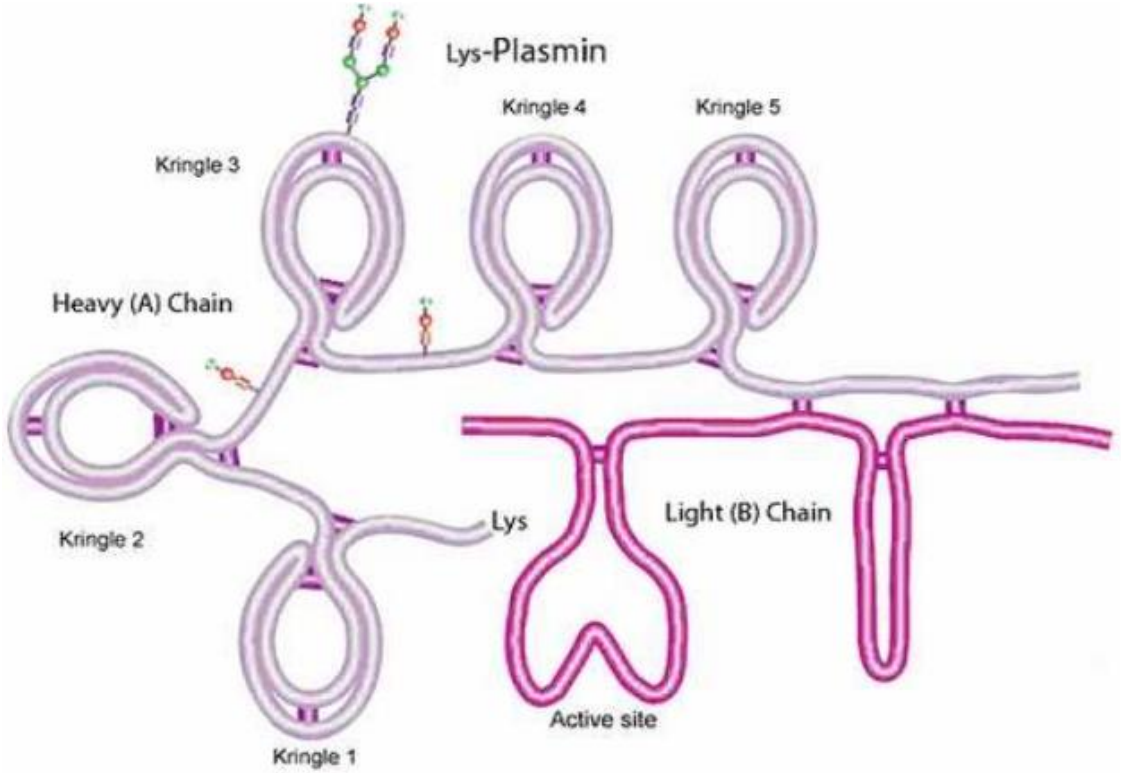


**Figure 4. Plasmin structures.**

### 1.2 Plasminogen/plasmin receptors

Plasminogen receptors (PLG-R) are a heterogenous group of cell surface proteins, which binds PLG as well as PLA. PLG-R are expressed on various eukaryotic cells including monocytes, monocytoid cells, macrophages, endothelial cells, fibroblasts, platelets and carcinoma cells (Kumari S and Malla R, 2015). The heterogeneity of PLG-R and their different cell surface expression can explain how the regulation of different biological processes, including fibrinolysis, inflammation, wound healing and angiogenesis takes place at the same time. PLG-R can be grouped into four classes. The first class includes proteins possessing pre-existing C-terminal lysine residue, such as α-enolase (ENO-1) on monocytes (Redlitz A et al., 1995), neurons (Nakajima K et al., 1994), carcinoma cells, lymphoid cells, myoblasts (Lopez-Alemany R et al., 1994; 2003a; 2003b) and pathogenic bacteria (Pancholi V and Fischetti VA, 1998); cytokeratin 8 on carcinoma cells (Hembrough TA et al., 1995); p11 on endothelial cells

(Kassam G et al., 1998) and glyceraldehyde-3-phosphate dehydrogenase on bacteria (Winram SB and Lottenberg R, 1996). The second class of PLG-R requires to be cleaved to expose lysine residue and includes annexin A2 on endothelial cells (Hajjar KA et al., 1994) and actin on endothelial and carcinoma cells (Andronicos NM and Ranson M, 2001; Dudani AK and Ganz PR, 1996). The third class includes proteins synthetized without a C-terminal lysine residue. αIIbβ3 integrin on platelets (Miles LA et al., 1986), activated αMβ2 integrin on PMA-stimulated neutrophils (Pluskota,E et al., 2004), amphoterin on cancer cells (Parkkinen J et al., 1993) and GP330 in kidney cells (Kanalas JJ and Makker SP, 1991) belong to this class. The fourth group of receptors binds PLG, but does not promote its activation. Tissue factor and gangliosides are members of this group (Fan Z et al., 1998; Miles LA et al., 1989). Most of PLG-R belongs to the so called "moonlighting proteins", which exhibit multiple functions at distinct cellular and extracellular sites (Jeffery CJ, 1999). Indeed, most proteins that bind PLG, are well characterized cytosolic or nuclear proteins with established functions in metabolism, DNA packaging or cytoskeleton organization. These proteins do not contain a signalling sequence that direct them to the cell surface and do not possess hydrophobic region to be simply inserted into the membrane, with exception of annexin A2 (Gerke V et al., 2005). Thus, "non-classical" proteins release independent of the endoplasmic reticulum (ER) -Golgi pathway has been proposed to explain their cell surface localization (Danielsen EM et al., 2003).

### 1.3 Plasminogen/plasmin system in tumorigenesis

Degradation of the ECM is one of the most important requirements for tumor development and progression. PLA destroys components of tumor stroma, acts on components of the ECM such as laminin and activates latent MMPs such as collagenase IV, facilitating tissue invasion and contributing to metastasis (Kleinman HK et al., 2001). The PLG/PLA system promotes tumor spreading also controlling tumor angiogenesis, a process that is essential for tumor nutrition and oxygen supply (Folkman J, 2002). The first step in angiogenesis is the disassembly of vessel wall, basal lamina degradation and cell migration. All these processes are regulated by extracellular proteolysis and the PLG/PLA system. In addition, PLA can directly activate the vascular endothelial growth factor (VEGF), which is a key mediator of angiogenesis (Roskoski R Jr, 2007). Furthermore, the PLG/PLA system affects cell adhesion,

proliferation, migration (Jo M et al., 2005; Planus E et al., 1997) and apoptosis (Kwaan HC et al., 2000), cellular events that are dysregulated upon tumorigenesis. The imbalance between PLG activators and PLA in tumor microenvironment is responsible for the excessive production of PLA. A prerequisite for PLA formation is the binding of its precursor PLG to the cell surface. One of these PLG-R, ENO-1, was found to be overexpressed in more than 20 types of human cancer (Altenberg B and Greulich KO, 2004). Furthermore, high levels of uPA were found in gastric cancer and were significantly associated with decreased survival (Nekarda H et al., 1994). In addition, tPA is overexpressed in several cancers, including melanoma (Stack MS et al., 1993), hepatocellular carcinoma (De Petro G et al., 1998), ovarian (Fishman DA et al., 1997), uterine (Saito K et al., 1990) and pancreatic ductal adenocarcinoma (Ryu B et al., 2002).

### 1.4 Plasmin activity

Plasmin system enzymes (plasmin, urokinase and tissue plasminogen activator) belong to the trypsin-like serine protease family (Polgár L, 2005). Serine proteases contain the nucleophilic serine residue (the serine hydroxyl group is an essential catalytic group) at the active site (Hedstrom L, 2002). The active site serine residue is assisted by a histidine and an aspartate residue (His57, Asp102 and Ser195), known as the 'catalytic triad' system, with an essential role in proteolysis (Di Cera E, 2009; Perona JJ and Craik CS, 1995; Polgár L, 2005). Any change in the catalytic triad residues or in the spatial relationship markedly changes the enzyme specificity and the hydrolysis rate (Craik CS et al., 1987; Mhashilkar AM et al., 1993; Polgár L, 2005). Serine proteases, including plasmin, are characterized by the presence of a S1 pocket. The S1 site is a pocket adjacent to Ser195 in serine proteases and the specificity of the serine protease depends on the residue located at the bottom of the protease S1 pocket (Perona JJ and Craik CS, 1995). The pocket S1 is a substrate-binding site of the protease. (Hedstrom L, 2002).

Another important feature of plasmin is the ability of the domain S3 to bind selectively an endogenous substrate thanks to a D-amino acid residue on the P3 domain (Xue F et al., 2005). This evidence suggested different molecular models of plasmin substrates. The sequence D-Ile-Phe-Lys forms a complex with plasmin in which each amino acid is recognized by a domain of plasmin (Gohda K et al., 2012). In particular, the plasmin S2 and S3 domains are occupied by the hydrophobic residues D-Ile and Phe, while Lys is the substrate of S1 domain, as shown in Figure 5.

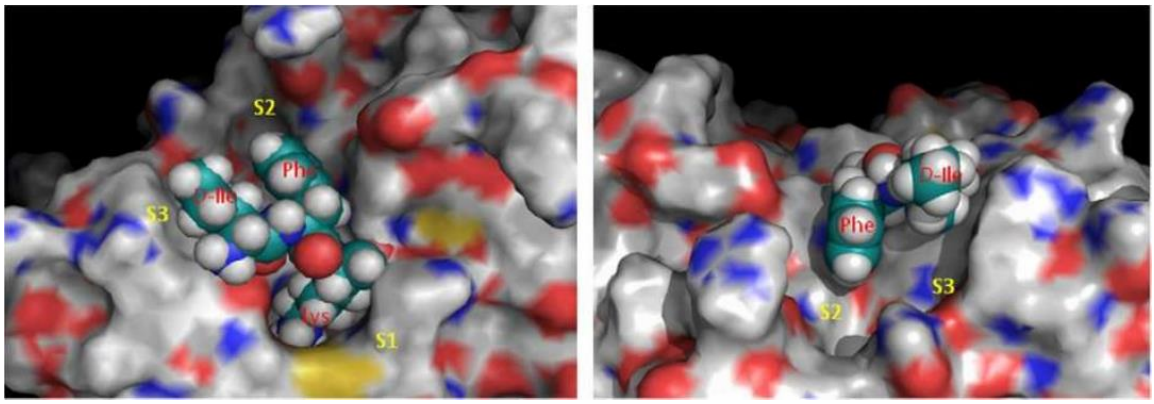


**Figure 5. Molecular modelling of substrate D-Ile-Phe-Lys bound to the active site of plasmin.**

To assess the structure of the sites of plasmin binding the substrates L-Ile-Phe-Lys and D-Ile-Phe-Lys were used in computational docking protocols. The affinity of the two substrates for the plasmin is very different. The D- and L- form have Km (Michaelis-Menten constant) values of 20 micromolar and 330 micromolar, respectively. For this reason, new peptide sequences as possible substrates of plasmin containing the higher enzyme-affinity D-form have been developed.

## 2. Aim of the study

The plasminogen / plasmin system plays a key role in tumor development and in particular in progression and metastatization. For this reason, the aim of my project was to functionalize the surface of stealth liposomes encapsulating pyrazolo [3,4-*d*] pyrimidines with a peptide able to bind plasmin. Since the plasmin is overexpressed in tumor areas, the bond between plasmin and peptide in liposomes surface would lead to a destabilization of the liposomes and consequently to a greater drug release in the tumor site. Many are the substrates of plasmin, especially peptide sequences that have a D-terminal amino acid and a lysine as cleavage site. For this purpose, a peptide that has all the requirements mentioned above, whose structure is not shown to preserve confidentiality, has been chosen.

To functionalize liposomes, the peptide modified with a terminal sulfhydryl group and phospholipids conjugated with a molecule of maleimide were used. Thioethers were generated by reaction of terminal sulfhydryl group of the peptide with the maleimide in liposomes phospholipids combining the peptide to the liposomes surface. The selected compounds S29, Si113 and Si163 with pyrazolo [3,4-*d*] pyrimidine structure were loaded in liposomes.

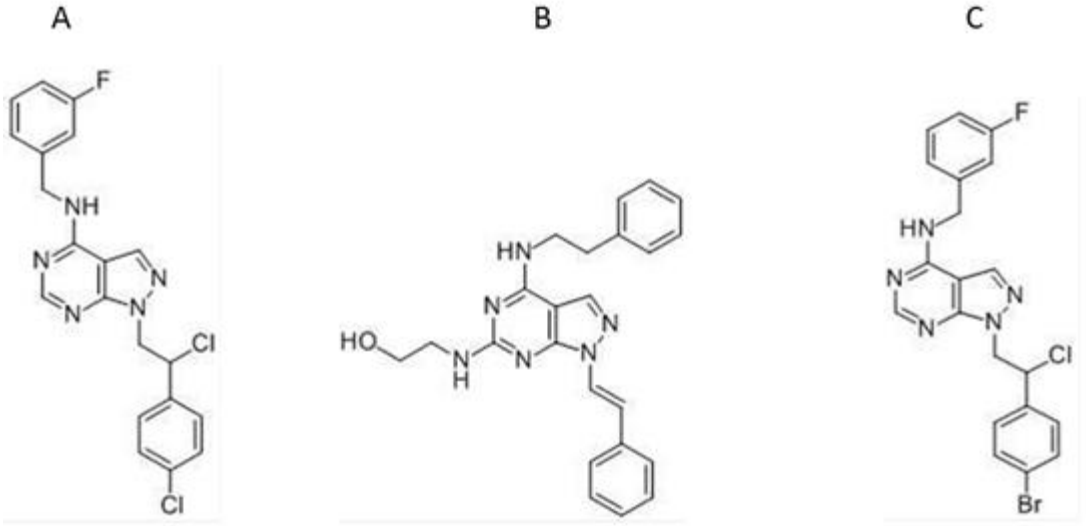


**Selected compound with pyrazolo [3,4-*d*] pyrimidine.** (A) S29. (B) Si113. (C) Si163.

These compounds are c-Src inhibitors with an effective activity previously studied with enzyme assays and cytotoxicity assays on different cell lines of chronic myelogenous leukemia, neuroblastoma, glioblastoma, osteosarcoma and hepatocellular carcinoma (Vignaroli G, Calandro P et al., 2016). As shown in the Table, these molecules have poor solubility in water and thus a non-ideal pharmaceutical profile.

| Compound | c-Src activity $K_i$ (μM)[a] | Water solubility (μg/mL) | P. App. ($10^{-6}$ $cm^2$ /sec) [b] [MR] (%) [c] | Metabolic stability (%) [d] |
|---|---|---|---|---|
| S29 | 0.8 | <0.04 | 16.6 [63.9] | 94.0 |
| Si113 | 2.4 | 0.4 | 2.6 [86.2] | 84.0 |
| Si163 | 0.0093 | 0.098 | 10 [10.2] | 93.6 |

**Table.** Enzymatic activity against c-Src and ADME properties of compounds.
[a] constant of enzyme inhibition; [b] apparent permeability; [c] Membrane Retention (MR) expressed as percentage of compound unable to reach the acceptor compartment; [d] stability expressed as percentage of unmodified drug.

Therefore, S29, Si113 and Si163 compounds were encapsulated within stealth liposomes functionalized with the peptide to obtain a dual effect of improve the apparent solubility of compounds and target them against the tumor.
The obtained liposomes were characterized after purification evaluating the size, the ζ potential, the polydispersity index (PDI) and the encapsulation efficiency (EE). Furthermore, several tests to quantify the peptide bound to liposomes were performed unfortunately with poor results. Moreover, peptide-bearing fluorescent liposomes were also prepared and tested on hepatocarcinoma cell line HepG2 to investigate any change in the cellular uptake. Finally, cytotoxicity assays on HepG2 cells were performed to test the efficacy of liposomes conjugate with the peptide with respect to non-conjugated liposomes both encapsulating the selected compounds.

## 3. Materials and Methods

### 3.1 Liposomes formulation

1,2-dipalmitoyl-sn-glycero-3-phosphocholine (DPPC), cholesterol, 1,2-distearoyl-sn-glycero-3-phosphoethanolamine-N-[amino(polyethylene glycol)-2000] (ammonium salt) ($DSPEmPEG_{2000}$) and 1,2-distearoyl-sn-glycero-3-phosphoethanolamine-N-[maleimide(polyethylene glycol)-2000] (ammonium salt) (DSPE-$mPEG_{2000}$-Mal) in molar ratio of 2: 1: 0.1: 0,02 were used to formulate stealth liposomes for functionalization, after solubilisation in a $CHCl_3$/MeOH mixture 3:1 v/v.

DSPE-$mPEG_{2000}$-Mal was add only in the liposomes formulation for the functionalization.

Similarly, fluorescent liposomes using as fluorophore the fluorescent phospholipid 1,2-distearoyl-sn-glycero-3-phosphoethanolamine-N-[poly(ethyleneglycol)2000-N'-carboxyfluorescein] (ammonium salt) (PE-CF) in a concentration of 20 μg/mL, were formulated. Liposomes formulations were prepared according to the thin layer film method, previously described in chapter 1, 2.1.

The encapsulation efficacy (EE), the morphological and dimensional characterization were performed as describer in chapter 1, 3.2 and 3.3.

### 3.2 Functionalization of stealth liposomes with L-Cysteine and modified peptide

Stealth liposomes were prepared as in chapter 1, 3.1.

Liposomes were incubated with 0.1 mM L-cysteine solution phosphate buffer, pH 7.4 in molar ratio L-cysteine maleimide 1:4. The reaction was conducted in ice and has been monitored by quantification of free thiols with Ellman assay. Similarly, liposomes have been functionalized with the modified peptide and monitored by Ellman assay.

### 3.3 Ellman assay for the quantification of free thiols

The Ellman assay involves the use of 5,5'-dithio-bis-(2-nitrobenzoic acid), known as DTNB, a compound soluble in water for the specific quantification of free thiols in solution.

The DTNB reacts with a free sulfhydryl group to give a mixed disulphide and 2-nitro-5-thiobenzoic acid (TNB). The DTNB target is the conjugate base $R\text{-}S^-$, as shown in Figure.

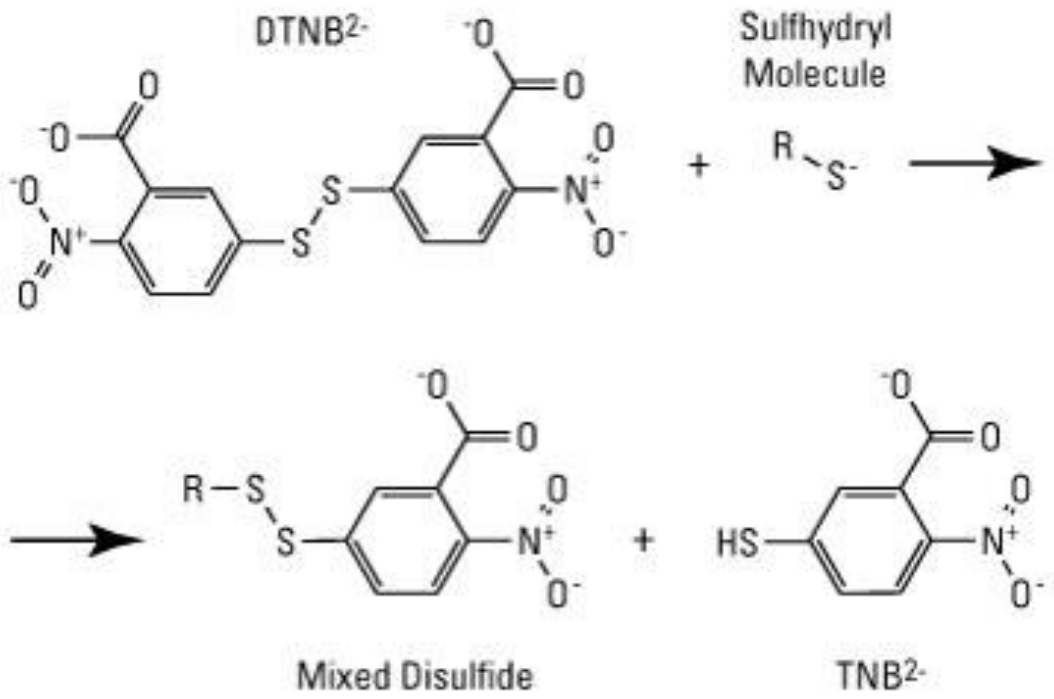


**Reaction of $DTNB^{2-}$ with conjugate bases of free thiols in aqueous solutions.**

The yield of the reaction depends on three factors: the reaction pH, the sulfhydryl pKa and on steric and electrostatic effects. The produced colored specie is the TNB that absorbs at 412 nm.

50 µL of Ellman's reagent 4mg/mL and 2.5 mL of 0.1mM phosphate buffer, pH 7.4 were added to 250 µL of each sample in a quartz cuvette with 1 cm optical path., The absorbance was read at 412 nm after 15 minutes of incubation. Free sulfhydryl groups were estimated by comparison with a calibration line of cysteine in known concentration and with the modified peptide for L-Cysteine-functionalized stealth liposomes and modified peptide- functionalized stealth liposomes.

### 3.4 Purification of liposomal suspension

The liposomal suspension underwent dialysis to eliminate the cysteine and the peptide in excess. The dialysis process is carried out through a cellulose semipermeable membrane (60 mL/ft, cut-off 14,000 Da, diameter 16 mm, width 25 mm) starting from 3 mL of liposomal suspension against 40 mL of saline solution 0.9% NaCl at RT for 2 hours, changing the external medium every 30 minutes.

### 3.5 In vitro cytotoxicity assay

Cytotoxicity assay was carried out on human liver hepatocellular cells HepG2. Cells were cultured in DMEM/F12 medium supplemented with 10% FBS, 2 mM L-glutamine and 10000 units/mL Penicillin/Streptomycin at 37 °C in 5% CO2 atmosphere. HepG2 cells were seeded at $10^5$cells/well density and treated with empty liposomes, liposomes-encapsulating compounds, empty liposomes functionalized with peptide, liposomes functionalized with peptide encapsulating compounds and free compounds (in DMSO solution) at increasing concentrations (0.1 μM, 1.0 μM, 10 μM and 50 μ M). All liposomal formulations have been realized in a 0.9% NaCl solution w/v, pH 7.4.

Cultures were maintained at 37 °C in 5% CO2 for 24 h and then treated for 48h. Cell number and viability were evaluated using the Bürker chamber, after treatment with Trypan Blue. $IC_{50}$ was calculated by GraphPad Prism 6.0 software.

### 3.6 Confocal microscopy studies on the cellular uptake

Fluorescent liposomes functionalized with cysteine or peptide or non-functionalized, prepared as described in 3.1, were tested on HepG2 cells to evaluate liposomes cellular uptake. HepG2 cells were incubated with fluorescent liposomes and non-fluorescent liposomes as control for 1h.

HepG2 cells were maintained in DMEM/F12 medium supplemented with 10% FBS, 2 mM L-glutamine and 10000 units/mL Penicillin/Streptomycin at 37 °C in 5% CO2 atmosphere. HepG2 cells were plated on glass coverslip at a density of $20^5$cells/well in a 24-wellplates. After 24 h, cells were incubated with liposome formulations for 1h, fixed in 4% paraformaldehyde in PBS for 20 min. Nuclei and cellular membranes were stained respectively with a 6 μ M solution of DAPI and 2 μg/mL WGA Alexa Fluor 647 labelled for 10 min. Samples were visualized on a TSC SP5 confocal microscope (Leica, 5100000750) installed on an inverted LEICA DMI 6000CS (10741320) microscope and equipped with an oil immersion Plan Apo 63 Å~ 1.4 NA objective. Images were acquired using the LASAF acquisition software (Leica, 10210).

## 4. Results

### 4.1 Liposomes functionalization with the peptide

Liposomes that include maleimide on their surfaces were used for direct conjugation with sulfhydryl group-containing peptide (Figure 1).


**Figure 1. Reaction of conjugation of the peptide (in green) on liposomes surface (Mi Kyung Yu et al., 2012).**

A first attempt was carried out to optimize the conjugation method using the cysteine instead of the peptide. Cysteine is an amino acid possessing a free sulfhydryl group. Therefore, it was possible to use it as a substitute of the peptide. The functionalization reaction was carried out in ice for 4 h, in 0.1 mM phosphate buffer testing the maleimide-to-cysteine molar ratios 1:1, 1:2 and 1:4. The 1:4 molar ratio was found to be better and was used for the experiments. The Ellman assay allowed the quantification of free sulfhydryl groups after the functionalization reaction using appropriate calibration lines. Data in Table 1 show a reduction of free sulfhydryl groups after the functionalization reaction with cysteine of 24%, which represent the amount of cysteine bound to liposomes.

| | Phosphate buffer | |
|---|---|---|
| Ice, 4h | Cysteine (µg/mL) | Cysteine (µg/mL) after functionalization |
| | 54.9 | 41.7 |

**Table 1. Quantification of free sulfhydryl groups after functionalization of liposomes with cysteine.**

Unfortunately, Ellman assay did not allow the quantification of the peptide bound to liposomes probably for the low sensibility of the technique in the detection of free sulfhydryl groups in the peptide as showed from data of the calibration lines (Figure 2). To analytically evaluate the binding of the peptide with liposomes an ion trap mass spectrometer was used.

A

| Peptide-SH (µg/mL) | Absorbance (412 nm) |
|---|---|
| 20 | 0,0069 |
| 40 | 0,0117 |
| 210 | 0,0472 |
| 420 | 0,0928 |
| 630 | 0,1395 |

B

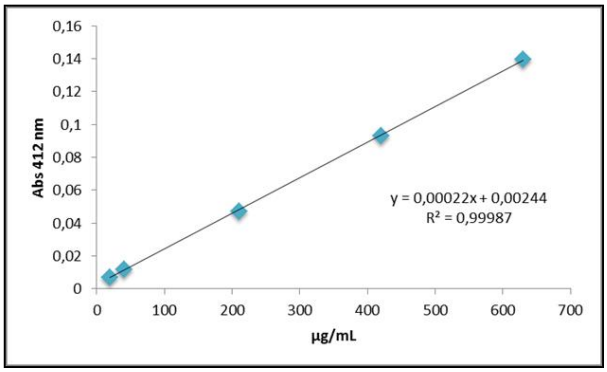


**Figure 2. (A) Absorbance values for known concentrations of peptide with free sulfhydryl group. (B) calibration lines with $R^2$ value.**

## 4.2 Encapsulation efficiency (EE)

The analysis of loading of each compound (S29, S163 and Si113) in peptide-bearing liposomes after purification was performed with the procedure described in chapter 1, 3.2 As shown in Figure 3, the EE was greater than 90% for all the three liposome-encapsulating compound formulations.

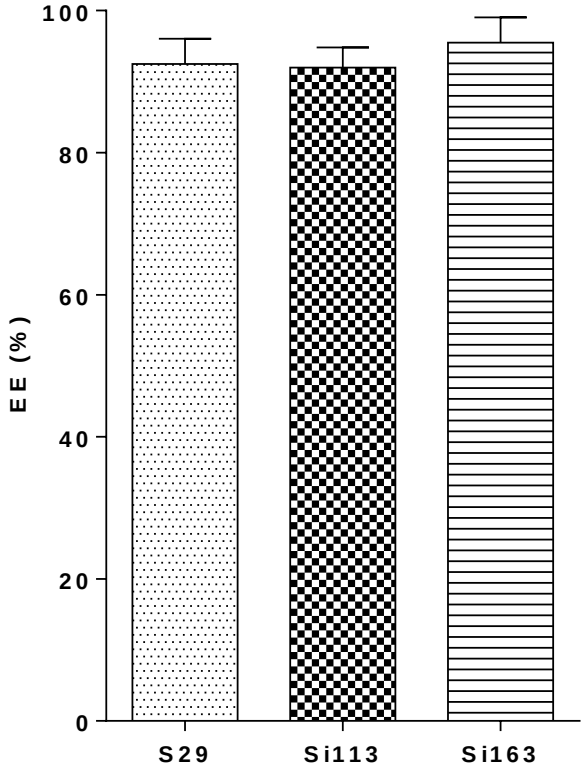


**Figure 3. Encapsulation efficacy (EE) in peptide-bearing liposomes.**

The high loading capacities showed that the functionalization process of liposomes with the peptide did not result in a destabilization of the phospholipid bilayer and therefore in a loss of the encapsulated compound during the reaction.

### 4.3 Morphologic and dimensional characterization

The morphology and the size of empty liposomes after functionalization with the peptide were observed through Cryo Transmission Electron Microscopy (cryo-TEM). Instead, to determine liposomes size and stability, expressed as ζ potential and polydispersity index (PDI), Dynamic Light Scattering (DLS) technique was used.

The result obtained from the analysis by cryo-TEM confirmed the presence of a homogeneous population of unilamellar liposomal particles with size around 100 nm. Liposomes were spherical, with uniform surface. There were no bi-lamellar, multilamellar or giants liposomes. The average thickness of the double phospholipidic layer corresponded to 5.8 ± 1.2 nm (12 measurements performed by Image J Software).

In the formulation, small phospholipid bilayer fragments (PBF) were also present, as indicated by arrows (Figure 4).

DLS analysis were initially carried out on not filtered empty liposomes functionalized with the cysteine or the peptide and not filtered and non-functionalized empty liposomes having phospholipids conjugated with maleimide in the bilayer. Results of analysis are shown in Table 2.

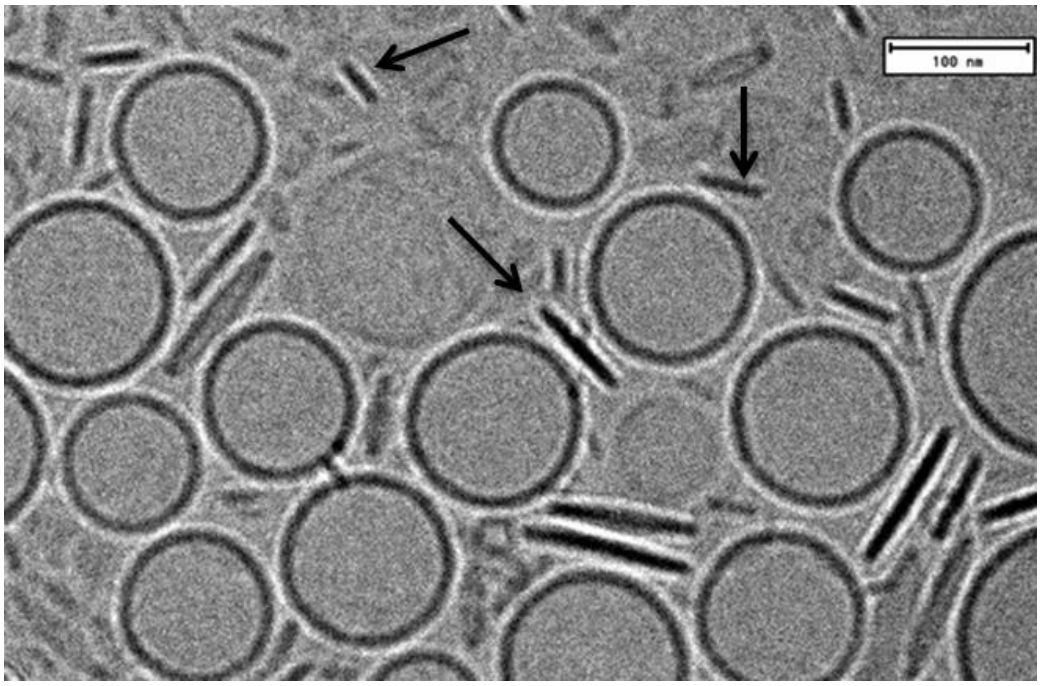


**Figure 4. Morphological analysis of peptide-bearing liposomes by Cryo-TEM.**

Although all the formulations were not filtered, the non-functionalized liposomes having the maleimide expressed on the surface formed aggregates with dimensions of approximately 600 nm. In contrast, liposomes functionalized with the cysteine were smaller, about 100 times lower than the non-functionalized liposomes. Moreover, the 89% of the population had dimensions of about 62 nm, indicating that the liposomal suspension was homogeneous. The 92.7% of the population of liposomes functionalized with the peptide had an average size of 232.5 nm. Therefore, the peptide caused an increase in the size of liposomes compared to liposomes functionalized with cysteine, but at the same time increased the stability of the liposomes which showed the ζ potential moving to a threshold of -42.8 to a value of -40.2 of liposomes functionalized with the cysteine. Moreover, PDI values confirmed the homogeneity and uniformity of the liposomal formulation functionalized with cysteine or peptide and the polydispersity

and then the poor stability of non-functionalized liposomes. Despite the lack of an analytical method to quantify the peptide-functionalized liposomes, the marked differences in the size of the liposomes and, in particular, in the zeta potential and PDI values suggested that the functionalization occurred in accordance with data reported in the literature.

| **Sample** | **Size (nm)** | **Population (%)** | **PDL** | **ζ potential (mV)** |
|---|---|---|---|---|
| Non-functionalized liposomes | 608.7 | 60.7 | 0.794 | -25.7 ± 4.15 |
| Liposomes functionalized with cysteine | 61.97 | 89.6 | 0.256 | -40.2 ± 4.73 |
| Liposomes functionalized with peptide | 232.5 | 92.7 | 0.476 | -42.8 ± 6.37 |

**Table 2. DLS analysis of liposomes.**

Subsequently, DLS analysis was carried out on non-filtered liposomal formulations containing compounds S29, Si113 and Si163 in comparison to the respectively non-filtered formulations containing the compounds and functionalized with the peptide. Liposomes functionalized with peptide showed lower sizes than non-functionalized liposomes and better values of ζ potential and PDI (Table 3) resulting in a more uniform system with a greater stability.

| | **S29 loaded liposomes** | | **Si113 loaded liposomes** | | **Si163 loaded liposomes** | |
|---|---|---|---|---|---|---|
| | **Without peptide** | **With peptide** | **Without peptide** | **With peptide** | **Without peptide** | **With peptide** |
| **Size (nm)** | 299.5 | 103.4 | 465.6 | 118.3 | 239.3 | 93.95 |
| **Pop. (%)** | 63.2 | 100 | 59.4 | 97.1 | 78.3 | 98.4 |
| **PDI** | 0.679 | 0.083 | 0.864 | 0.228 | 1 | 0.317 |
| **ζ potential (mV)** | -9.58 ± 4.28 | -20.1 ± 4.36 | -6.74 ± 4.79 | -36.3 ± 5.25 | -9.73 ± 3.48 | -15.4 ± 6.12 |

**Table 3. DLS analysis of liposomes functionalized with or without peptide encapsulating pyrazolo [3,4-*d*] pyrimidine compounds.**

### 4.4 Liposomes uptake in epatocarcinoma cells (HepG2).

Fluorescent liposomes (in green) functionalized with the peptide (LP-peptide) were analysed for the cellular uptake capacity in hepatocarcinoma cell line (HepG2) with respect to liposomes functionalized with cysteine (LP-cysteine) and non-functionalized liposomes (LP-fluo) to assess any differences in cellular uptake. Figure 5 show results after 1h treatment with fluorescent liposomes (LP-fluo, LP-peptide and LP-cysteine), non-fluorescent liposomes (LP-blank) as control and non-treated cells. Cells treated with the LP-peptide displayed a higher green fluorescence in HepG2 cells than cells treated with LP-cysteine after 1h of treatment. This result suggested that the peptide allowed a better internalisation and in a shorter time of the liposomes in comparison to the cysteine, as indicated by arrows. Unexpectedly, LP-fluo were not able to be internalized, in fact no green fluorescence in cells after 1h hours of treatment was observed. Cells treated with LP-blank and non-treated cells showed no fluorescence, as expected.

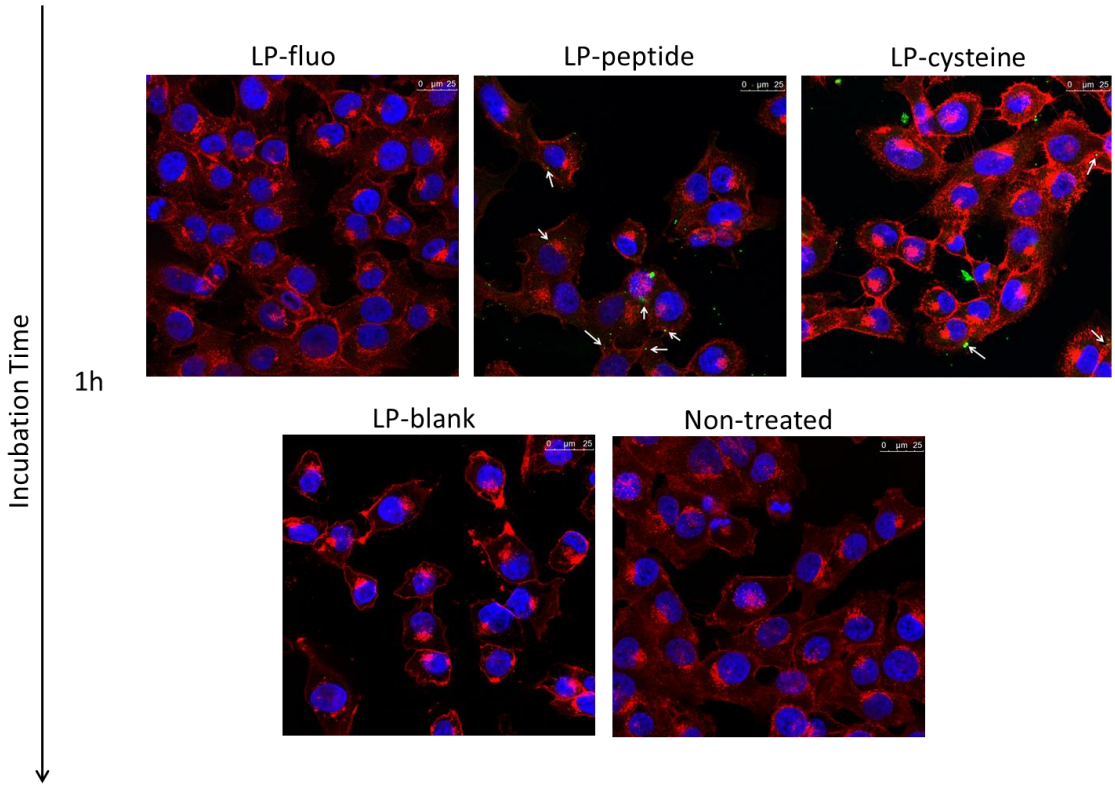


**Figure 5. Liposomes uptake in HepG2 cells.** LP-fluo: non-functionalized liposomes; LP-peptide: liposomes functionalized with peptide; LP-cysteine: liposomes functionalized with cysteine; LP-blank: non-functionalized liposomes; Non-treated: non-treated cells.

### 4.5 Cytotoxicity effects of liposomes on HepG2 cells.

The cytotoxicity tests were conducted on HepG2 hepatocarcinoma cells to assess any differences in the activity of the selected compounds (the pyrazolo [3,4-*d*] pyrimidine S29, Si113 and Si163) encapsulated in non-functionalized liposomes and liposomes functionalized with the peptide.

Cells were treated with different concentrations (0.1, 1,10 and 100 µM) of compounds in dimethyl sulfoxide (DMSO) or non-functionalized or peptide-functionalized liposomes-encapsulating compounds for 48h.

Results in Figure 6 indicate that S29 activity is not altered by the drug delivery system, while Si113 and Si163 both in non-functionalized liposomes and liposomes functionalized with peptide show a higher cytotoxic activity than to the free compound. Moreover, the presence of the peptide increases the activity of the compound indeed functionalized liposomes result more active of about 3 times for the Si113 and of almost 2 times for the Si163.

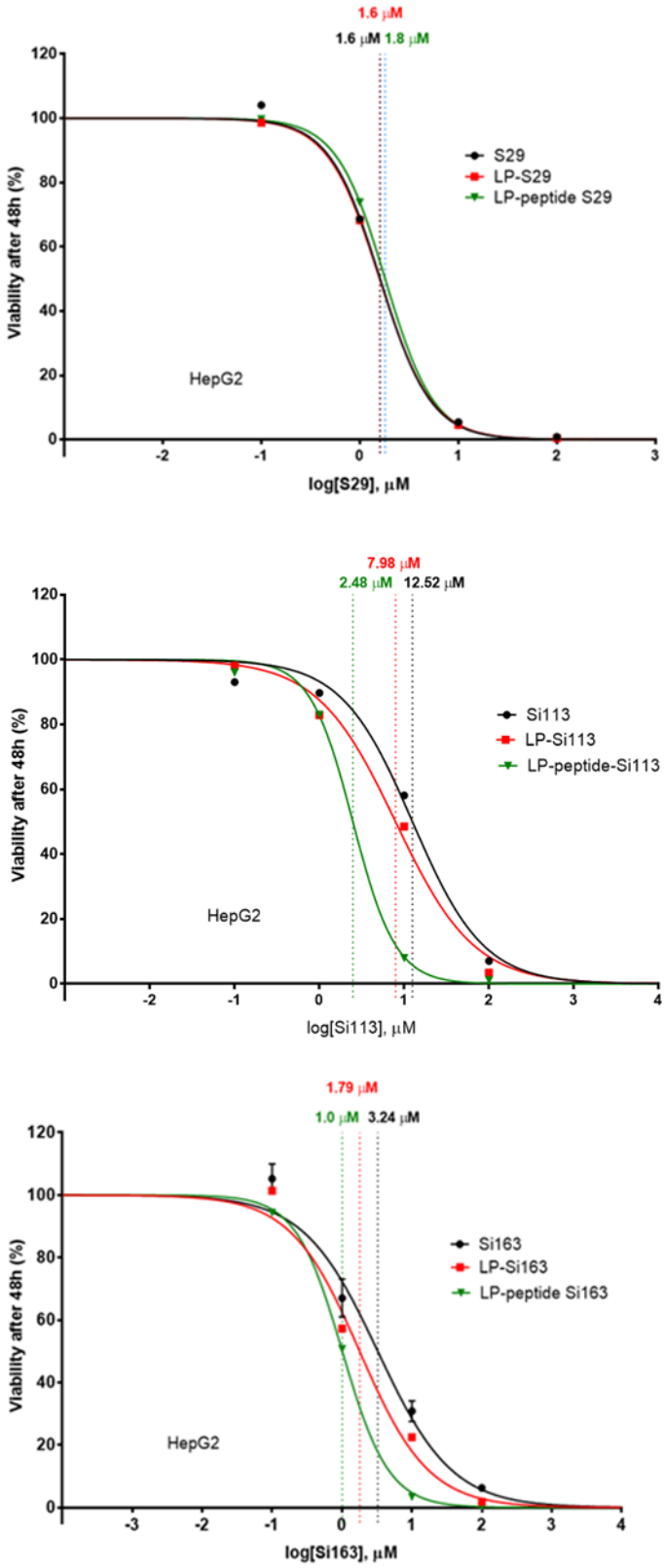


**Figure 6. $IC_{50}$ values after 48h of cells treatment with free compounds in DMSO (in black) or liposomal formulation with (in green) or without (in red) peptide.**

Furthermore, cytotoxicity of empty liposomes functionalized with the peptide (blank) was evaluated. Blank liposomes were safe and became toxic for cells only at high concentrations as shown in Figure 7.

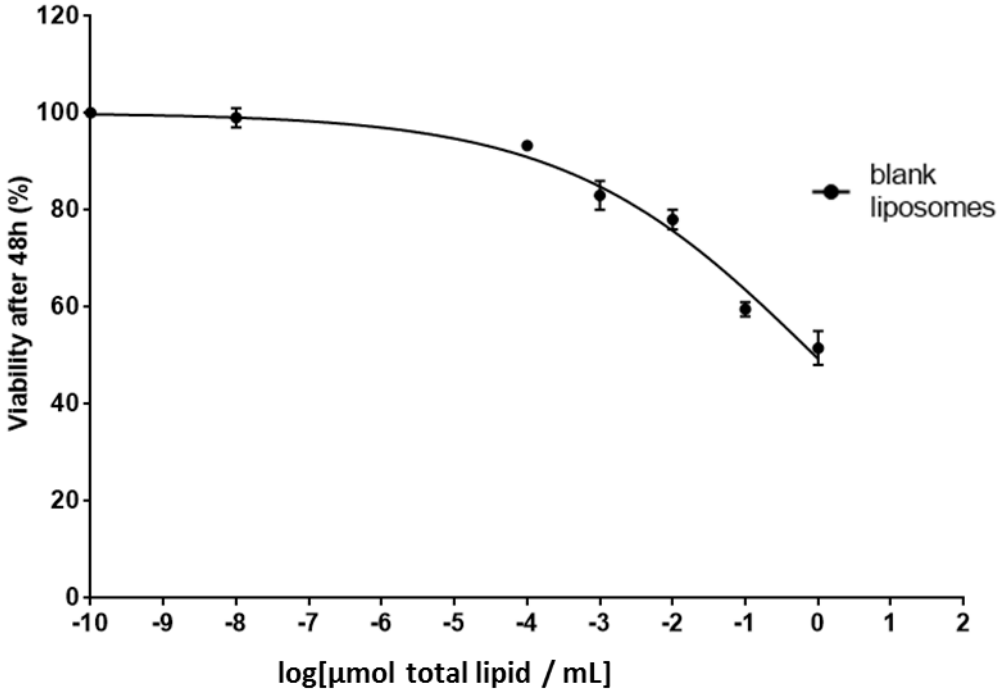


**Figure 7. Cytotoxicity of blank liposomes in HepG2 after 48h of treatment.**

## 5. Discussion

To enhance the ability of liposomes of reaching tumor areas overexpressing plasmin, a peptide selectively recognized by plasmin was linked to a liposomal system by a reaction between a maleimide group (on liposomes) and a sulfhydryl group (on the peptide). The Ellman's test, assay that allows the quantification of free sulfhydryl groups after the functionalization with the peptide, failures the quantification of the peptide conjugated to the liposomes; nevertheless, DLS data confirm the effective bond of the peptide on the liposomes surface, changing the size, the ζ potential and PDI properties of liposomes. Three pyrazolo [3,4-*d*] pyrimidine compounds (S29, Si113, Si163) were selected, according to their ADME properties, to be encapsulated in the peptide-functionalized liposomes. The presence of the peptide stabilizes the liposomal formulations allowing the reduction of liposomes size compared to non-functionalized liposomes. In particular, peptide-functionalized liposomes encapsulating the S29 and Si113 compounds have size slightly greater than 100 nm (103.4 nm and 118.3 nm, respectively), while the sizes of those encapsulating the Si163 compound are below 100 nm (93.95 nm). Moreover, the presence of the peptide increases the percentage of liposomal population with the reported sizes compared to non-functionalized liposomes. In fact, the 100% of the liposomal formulation with compound S29 have sizes of 103.4 nm, while the liposomal formulation with compound Si113 have the 97.1% of the population with the size of 118.3 nm and the liposomal formulation with compound Si163 have the 98.4% of the population with the size of 93.95 nm. In addition, the presence of only 60.7% of non-functionalized blank liposomes with large size (608.7 nm) indicates a non-homogeneous population, highlighting the ability of the peptide to compact liposomes, to assume an appropriate size for the drug delivery and to stabilize the formulations as evidenced by the PDI and ζ potential values. Non-functionalized liposomes encapsulating the selected compounds show PDI values close to 1, highlighting the non-uniform composition of the liposomal formulation. Instead the presence of the peptide in the same liposomes allows the stabilization of the system and the uniformity of the formulation with a PDI value closer to 0. Consequently, the stability of liposomal formulations, expressed as ζ potential, is also enhanced when peptide is introduced in liposomes surface. ζ potential values increase of 2 times when peptide is added in liposomes encapsulating S29, more than 5 times for the liposomes encapsulating Si113 and more than once time in the case of liposomes encapsulating

Si163. Thus, the presence of the peptide on the liposomes surface reduces the possibility of liposomes aggregation or flocculation allowing the use of liposomes also *in vivo.*

Moreover, fluorescent liposomes functionalized with the peptide were prepared to evaluate the peptide ability to improve or decrease the uptake of the liposomal formulation in HepG2 cancer cell line. After 1h incubation, no signal by liposomes is captured in cells incubated with non-functionalized fluorescent liposomes, tested as control. On the contrary, cells treated with fluorescent liposomes functionalized with peptide show several green spots indicating that the peptide promotes the uptake of liposomes probably interacting with a receptor on the cell surface.

In addition, liposomes functionalized with the peptide encapsulating the selected compounds were tested on the HepG2 cell line to evaluate the ability of these liposomes to release their cargo inside cells. Data show that liposomes with the peptide have lower $IC_{50}$ values than to non-functionalized liposomes, except for liposomes encapsulating S29. Liposomes encapsulating S29 compound show an $IC_{50}$ value comparable with non-functionalized liposomes values, suggesting that the peptide do not influence the cytotoxicity activity, while liposomes encapsulating Si113 and Si163 show an improved cytotoxicity activity of 5 and 3 times, respectively.

In future, tests will be carried out on xenograft mice to evaluate the efficacy and stability of liposomal system functionalized with the peptide *in vivo*.

## 6. References

Altenberg B and Greulich KO. Genes of glycolysis are ubiquitously overexpressed in 24 cancer classes. 2004, *Genomics* 84(6):1014-20.

Andreasen PA, Kiøller L, Christensen L, Duffy MJ. The urokinase-type plasminogen activator system in cancer metastasis: a review. 1997, *Int J Cancer* 72(1):1-22.

Andronicos NM and Ranson M. The topology of plasminogen binding and activation on the surface of human breast cancer cells. 2001, *Br J Cancer* 85(6):909-916.

Collen D, Tytgat G, Claeys H, Verstraete M, Wallén P. Metabolism of plasminogen in healthy subjects: effect of tranexamic acid. 1972, *J Clin Invest* 51(6):1310-8.

Collen D. Ham-Wasserman lecture: role of the plasminogen system in fibrin-homeostasis and tissue remodeling. 2001, *Hematology Am Soc Hematol Educ Program* 2001:1-9.

Craik CS, Roczniak S, Largman C, Rutter WJ. The catalytic role of the active site aspartic acid in serine proteases. 1987, *Science* 237(4817):909-913.

Danielsen EM, van Deurs B, Hansen GH. "Nonclassical" secretion of annexin A2 to the lumenal side of the enterocyte brush border membrane. 2003, *Biochemistry* 42(49):14670-14676.

De Petro G, Tavian D, Copeta A, Portolani, Giulini SM, Barlati S. Expression of urokinase-type plasminogen activator (u-PA), u-PA receptor, and tissue-type PA messenger RNAs in human hepatocellular carcinoma. 1998, *Cancer Res* 58(10):2234-2239.

DeClerck YA, Mercurio AM, Stack MS, Chapman HA, Zutter MM, Muschel RJ, Raz A, Matrisian LM, Sloane BF, Noel A, Hendrix MJ, Coussens L, Padarathsingh M. Proteases, extracellular matrix, and cancer: a workshop of the path B study section. 2004, *Am J Pathol* 164(4):1131-1139.

Di Cera E. Serine proteases. 2009, *IUBMB Life* 61(5):510-515.

Didiasova M, Wujak L, Wygrecka M, Zakrzewicz D. From plasminogen to plasmin: role of plasminogen receptors in human cancer. 2014, *Int J Mol Sci* 15(11):21229-21252.

Dudani AK and Ganz PR. Endothelial cell surface actin serves as a binding site for plasminogen, tissue plasminogen activator and lipoprotein(a). 1996, *Br J Haematol* 95(1):168-178.

Fan Z, Larson PJ, Bognacki J, Raghunath PN, Tomaszewski JE, Kuo A, Canziani G, Chaiken I, Cines DB, Higazi AA. Tissue factor regulates plasminogen binding and activation. 1998, *Blood* 91(6):1987-1998.

Fishman DA, Bafetti LM, Banionis S, Kearns AS, Chilukuri K, Stack MS. Production of extracellular matrix-degrading proteinases by primary cultures of human epithelial ovarian carcinoma cells. 1997, *Cancer* 80(8):1457-1463.

Folkman J. Role of angiogenesis in tumor growth and metastasis. 2002, *Semin Oncol* 29(6 Suppl 16):15-8.

Gerke V, Creutz CE, Moss SE. Annexins: linking Ca2+ signalling to membrane dynamics. 2005, *Nat Rev Mol Cell Biol* 6(6):449-461.

Gohda K, Teno N, Wanaka K, Tsuda Y. Predicting subsite interactions of plasmin with substrates and inhibitors through computational docking analysis. 2012, *J Enzyme Inhib Med Chem* 27(4):571-577.

Hajjar KA, Jacovina AT, Chacko J. An endothelial cell receptor for plasminogen/tissue plasminogen activator. I. Identity with annexin II. 1994, *J Biol Chem* 269(33):21191-21197.

Hedstrom L. Serine protease mechanism and specificity. 2002, *Chem Rev* 102(12):4501-4524.

Hembrough TA, Vasudevan J, Allietta MM, Glass WF 2nd, Gonias SL. A cytokeratin 8-like protein with plasminogen-binding activity is present on the external surfaces of hepatocytes, HepG2 cells and breast carcinoma cell lines. 1995, *J Cell Sci* 108(Pt 3):1071-1082.

Jeffery CJ. Moonlighting proteins. 1999, *Trends Biochem Sci* 24(1):8-11.

Jo M, Thomas KS, Marozkina N, Amin TJ, Silva CM, Parsons SJ, Gonias SL. Dynamic assembly of the urokinase-type plasminogen activator signaling receptor complex determines the mitogenic activity of urokinase-type plasminogen activator. 2005, *J Biol Chem* 280(17):17449-17457.

Kanalas JJ and Makker SP. Identification of the rat Heymann nephritis autoantigen (GP330) as a receptor site for plasminogen. 1991, *J Biol Chem* 266(17):10825-10829.

Kassam G, Choi KS, Ghuman J, Kang HM, Fitzpatrick SL, Zackson T, Zackson S, Toba M, Shinomiva A, Waisman DM. The role of annexin II tetramer in the activation of plasminogen. 1998, *J Biol Chem* 273(8):4790-4799.

Kleinman HK, Koblinski J, Lee S, Engbring J. Role of basement membrane in tumor growth and metastasis. 2001, *Surg Oncol Clin N Am* 10(2):329-338, ix.

Koblinski JE, Ahram M, Sloane BF. Unraveling the role of proteases in cancer. 2000, *Clin Chim Acta* 291(2):113-135.

Kumari S and Malla R. New Insight on the Role of Plasminogen Receptor in Cancer Progression. 2015, *Cancer Growth Metastasis* 8:35–42.

Kwaan HC and McMahon B. The role of plasminogen-plasmin system in cancer. 2009, *Cancer Treat Res* 148:43-66.

Kwaan HC, Wang J, Svoboda K, Declerck PJ. Plasminogen activator inhibitor 1 may promote tumour growth through inhibition of apoptosis. 2000, *Br J Cancer* 82(10):1702-1708.

Li WY, Chong SS, Huang EY, Tuan TL. Plasminogen activator/plasmin system: a major player in wound healing? 2003, *Wound Repair Regen* 11(4):239-247.

Lopez-Alemany R, Longstaff C, Hawley S, Mirshahi M, Fábregas P, Jardí M, Merton E, Miles LA, Félez J. Inhibition of cell surface mediated plasminogen activation by a monoclonal antibody against alpha-Enolase. 2003, *Am J Hematol* 72(4):234-242.

Lopez-Alemany R, Correc P, Camoin L, Burtin P. Purification of the plasmin receptor from human carcinoma cells and comparison to alpha-enolase. 1994, *Thromb Res* 75(4):371-381.

Lopez-Alemany R, Suelves M, Munoz-Canoves P. Plasmin generation dependent on alpha-enolase-type plasminogen receptor is required for myogenesis. 2003, *Thromb Haemost* 90(4):724-733.

Mhashilkar AM, Viswanatha T, Chibber BA, Castellino FJ. Breaching the conformational integrity of the catalytic triad of the serine protease plasmin: localized disruption of a side chain of His-603 strongly inhibits the amidolytic activity of human plasmin. 1993, *Proc Natl Acad Sci U S A* 90(11):5374-5377.

Miles LA, Dahlberg CM, Levin EG, Plow EF. Gangliosides interact directly with plasminogen and urokinase and may mediate binding of these fibrinolytic components to cells. 1989, *Biochemistry* 28(24):9337-9343.

Miles LA, Ginsberg MH, White JG, Plow EF. Plasminogen interacts with human platelets through two distinct mechanisms. 1986, *J Clin Invest* 77(6):2001-2009.

Nakajima K, Hamanoue M, Takemoto N, Hattori T, Kato K, Kohsaka S. Plasminogen binds specifically to alpha-enolase on rat neuronal plasma membrane. 1994, *J Neurochem* 63(6):2048-2057.

Nekarda H, Schmitt M, Ulm K, Wenninger A, Vogelsang H, Becker K, Roder JD, Fink U, Siewert JR. Prognostic impact of urokinase-type plasminogen activator and its inhibitor PAI-1 in completely resected gastric cancer. 1994, *Cancer Res* 54(11):2900-2907.

Nicoloso G, Hauert J, Kruithof EK, Van Melle G, Bachmann F. Fibrinolysis in normal subjects-comparison between plasminogen activator inhibitor and other components of the fibrinolytic system. 1988, *Thromb Haemost* 59(2):299-303.

Ogiwara K, Minagawa K, Takano N, Kageyama T, Takahashi T. Apparent involvement of plasmin in early-stage follicle rupture during ovulation in medaka. 2012, *Biol Reprod* 86(4):113.

Pancholi V and Fischetti VA. alpha-enolase, a novel strong plasmin(ogen) binding protein on the surface of pathogenic streptococci. 1998, *J Biol Chem* 273(23):14503-14515.

Papanikolaou T, Amiridis GS, Dimitriadis I, Vainas E, Rekkas CA. Effect of plasmin, plasminogen activators and a plasmin inhibitor on bovine in vitro embryo production. 2008, *Reprod Fertil Dev* 20(2):320-327.

Parkkinen J, Raulo E, Merenmies J, Nolo R, Kajander EO, Baumann M, Rauvala H. Amphoterin, the 30-kDa protein in a family of HMG1-type polypeptides. Enhanced expression in transformed cells, leading edge localization, and interactions with plasminogen activation. 1993, *J Biol Chem* 268(26):19726-19738.

Pepper MS. Role of the matrix metalloproteinase and plasminogen activator-plasmin systems in angiogenesis. 2001, *Arterioscler Thromb Vasc Biol* 21(7):1104-1117.

Perona JJ and Craik CS. Structural basis of substrate specificity in the serine proteases. 1995, *Protein Sci* 4(3): 337–360.

Planus E, Barlovatz-Meimon G, Rogers RA, Bonavaud S, Ingber DE, Wang N. Binding of urokinase to plasminogen activator inhibitor type-1 mediates cell adhesion and spreading. 1997, *J Cell Sci* 110(Pt 9):1091-1098.

Pluskota E, Soloviev DA, Bdeir K, Cines DB, Plow EF. Integrin alphaMbeta2 orchestrates and accelerates plasminogen activation and fibrinolysis by neutrophils. 2004, *J Biol Chem* 279(17):18063-18072.

Polgár L. The catalytic triad of serine peptidases. 2005, *Cell Mol Life Sci* 62(19-20):2161-2172.

Rao JS. Molecular mechanisms of glioma invasiveness: the role of proteases. 2003, *Nat Rev Cancer* 3(7):489-501.

Redlitz A, Fowler BJ, Plow EF, Miles LA. The role of an enolase-related molecule in plasminogen binding to cells. 1995, *Eur J Biochem* 227(1-2):407-415.

Robbins KC, Summaria L, Hsieh B, Shah RJ. The peptide chains of human plasmin. Mechanism of activation of human plasminogen to plasmin. 1967, *J Biol Chem* 242(10):2333-2342.

Roskoski R Jr. Vascular endothelial growth factor (VEGF) signaling in tumor progression. 2007, *Crit Rev Oncol Hematol* 62(3):179-213.

Ryu B, Jones J, Blades NJ, Parmigiani G, Hollingsworth MA, Hruban RH, Kern SE. Relationships and differentially expressed genes among pancreatic cancers examined by large-scale serial analysis of gene expression. 2002, *Cancer Res* 62(3):819-826.

Saito K, Nagashima M, Iwata M, Hamada H, Sumiyoshi K, Takada Y, Takada A. The concentration of tissue plasminogen activator and urokinase in plasma and tissues of patients with ovarian and uterine tumors. 1990, *Thromb Res* 58(4):355-366.

Sinniger V, Merton RE, Fabregas P, Felez J, Longstaff C. Regulation of tissue plasminogen activator activity by cells. Domains responsible for binding and mechanism of stimulation. 1999, *J Biol Chem* 274(18):12414-12422.

Stack MS, Gray RD, Pizzo SV. Modulation of murine B16F10 melanoma plasminogen activator production by a synthetic peptide derived from the laminin A chain. 1993, *Cancer Res* 53(9):1998-2004.

Stillfried GE, Saunders DN, Ranson M. Plasminogen binding and activation at the breast cancer cell surface: the integral role of urokinase activity. 2007, *Breast Cancer Res* 9(1):R14.

Vignaroli G, Calandro P, Zamperini C, Coniglio F, Iovenitti G, Tavanti M, Colecchia D, Dreassi E, Valoti M, Schenone S, Chiariello M, Botta M. Improvement of pyrazolo [3,4-*d*] pyrimidines pharmacokinetic properties: nanosystem approaches for drug delivery. 2016, *Nature Scientific Reports* 6:21509.

Winram SB and Lottenberg R. The plasmin-binding protein Plr of group A streptococci is identified as glyceraldehyde-3-phosphate dehydrogenase. 1996, *Microbiology* 142(Pt 8):2311-2320.

Xue F, Seto CT. Selective inhibitors of the serine protease plasmin: probing the S3 and S3' subsites using a combinatorial library. 2005, *J Med Chem* 48:6908-6917.

Zucker S, Cao J, Chen WT. Critical appraisal of the use of matrix metalloproteinase inhibitors in cancer treatment. 2000, *Oncogene* 19(56):6642-6650.